University of Louisville
ThinkIR: The University of Louisville's Institutional Repository

Electronic Theses and Dissertations

12-2021

Visualizing Anhydrobiosis: Liquid-liquid phase separation, membraneless organelles, and cellular reorganization.

Clinton J. Belott
University of Louisville

Follow this and additional works at: https://ir.library.louisville.edu/etd

Part of the Cell Biology Commons

Recommended Citation

Belott, Clinton J., "Visualizing Anhydrobiosis: Liquid-liquid phase separation, membraneless organelles, and cellular reorganization." (2021). *Electronic Theses and Dissertations.* Paper 3778.
https://doi.org/10.18297/etd/3778

This Doctoral Dissertation is brought to you for free and open access by ThinkIR: The University of Louisville's Institutional Repository. It has been accepted for inclusion in Electronic Theses and Dissertations by an authorized administrator of ThinkIR: The University of Louisville's Institutional Repository. This title appears here courtesy of the author, who has retained all other copyrights. For more information, please contact thinkir@louisville.edu.

VISUALIZING ANHYDROBIOSIS: LIQUID-LIQUID PHASE SEPARATION, MEMBRANELESS ORGANELLES, AND CELLULAR REORGANIZATION

By
Clinton J. Belott
B.S., Eastern Illinois University 2015

A Dissertation
Submitted to the Faculty of the
College of Arts and Sciences of the University of Louisville
in Partial Fulfillment of the Requirements
for the Degree of

Doctor of Philosophy
in Biology

Department of Biology
University of Louisville
Louisville, Kentucky

December 2021

VISUALIZING ANHYDROBIOSIS: LIQUID-LIQUID PHASE SEPARATION, MEMBRANELESS ORGANELLES, AND CELLULAR REORGANIZATION

By
Clinton J. Belott
B.S., Eastern Illinois University 2015

A Dissertation Approved on

November 24, 2021

By the following Dissertation Committee:

_____
Dissertation Director
Michael A. Menze

_____
David J. Schultz

_____
Michael H. Perlin

_____
Steven C. Hand

_____
Oleg A. Gusev

DEDICATION

This dissertation is dedicated first and foremost to my mother, Charlotte D. Belott, who spent countless hours helping me overcome my severe dyslexia as a child. With absolute certainty, I know that I would not be writing this dissertation if it was not for her love and compassion. I also dedicate this dissertation to my father, Frank R. Belott, my brother, Joseph R. Belott, and my sister, Jennifer J. (Belott) Therrien. They raised me when I was little and have remained my dear friends as an adult – I would not have become me without them.

I would like to further dedicate this dissertation to Evelyn M. Dorsey, my high school science teacher. While I always had a strong interest in science, Evelyn was the one who spent much more of her time than I deserved to cultivate that interest into a true passion.

In addition, I dedicate this dissertation to my closest friend and dear colleague, Brett R. Janis. He always challenged me intellectually, but more importantly he taught me how to be a much kinder person and how to be happy in life. I would also like to dedicated this dissertation to my dearest friends, Noah D. Featherstone, Daniel A. Webster, Robert A. Skolik, and David F. Grimm. Each of them greatly impacted my life in their own way, leading me to become the person who I am today.

ACKNOWLEDGEMENTS

I would firstly like to thank my mentor, Dr. Michael A. Menze for his mentorship throughout both my undergraduate and graduate career. I am also thankful to all of the incredible people that I had the honor of working with in Dr. Menze's laboratory.

I would like to thank my undergraduate student, Tryphena S. Sithu for all of her academic support and friendship throughout these several years.

I thank Dr. Oleg A. Gusev and Dr. Takahiro Kikawada for inviting me into their laboratories, as well as for their friendship and kindness while I was living and working in Japan.

I sincerely thank Dr. Mohamed (Mido) Z. Rashed and Dr. Stuart J. Williams for collaborating with me on all cellular dielectrophoresis experiments.

I would like to thank Dr. Paul DeMarco, Associate Dean of the Graduate School, for all of his kind help and support in organizing funds associated with the NSF Graduate Research Fellowship (NSF-GRFP).

I sincerely thank the National Science Foundation (NSF) and the Japan Society for the Promotion of Science (JSPS) for their financial support:

NSF Graduate Research Opportunities Worldwide (GROW) / JSPS Postdoctoral Fellowship for Overseas Researchers (Strategic Program), "Characterization of Mitochondrial Morphology and Membrane Potential During Anhydrobiosis: A Comparison Between Desiccation Sensitivity and Tolerance" (2019). Mentor: Dr. Michael Menze; Sponsor in Japan: Dr. Oleg Gusev, Unit Leader, KFU-RIKEN, Yokohama, Kanagawa Prefecture, Japan.

NSF Graduate Research Fellowship (GRFP), "Importance of Protein-based Desiccation Tolerance in the Anhydrobiotic Brine Shrimp, Artemia franciscana, and the Potential to Achieve Dry-state Storage of Insect Cells" (2017). Mentor: Dr. Michael Menze.

NSF Research Grant "Collaborative Research: Mechanisms of Tolerance to Severe Water Stress in Animals" (05/2015 - 04/2020; Michael A. Menze; PI, IOS-1659970, Steven Hand, PI, IOS-1457061.

ABSTRACT

VISUALIZING ANHYDROBIOSIS: LIQUID-LIQUID PHASE SEPARATION, MEMBRANELESS ORGANELLES, AND CELLULAR REORGANIZATION

Clinton J. Belott

November 24, 2021

Water is an integral and necessary component of life. It is then, exceedingly remarkable that some species are capable of surviving virtually complete water loss for extended periods of time. Several decades of intense research into anhydrobiosis, or life without water, have given significant insights into the molecular mechanisms governing this phenomenon. Anhydrobiosis-related intrinsically disordered (ARID) proteins have been demonstrated to be critically important for desiccation tolerance in many anhydrobiotic species and exhibit a considerably wide range of protective properties that include membrane stabilization, reinforcing bioglass formation, and protein stabilization.

This dissertation begins with cellular dielectrophoresis suggesting that two ARID proteins, *Afr*LEA3m and *Afr*LEA6, were undergoing significant folding *in vivo* due to moderate intracellular water loss. This was hypothesized to result in these ARID proteins changing from an untangled state to a tangled one, thereby increasing intracellular viscosity. This dissertation then proceeds to further explore *Afr*LEA6 *in vivo*, finding it able to undergo a domain-dependent liquid-liquid phase separation to form a selective, stress granule-like membraneless organelle (MLO). Furthermore, the dilute fraction of *Afr*LEA6 was found to rapidly increase intracellular viscosity at moderate levels of

intracellular water loss, supporting the hypothesis that *Afr*LEA6 was entering a tangled state. Lastly, this dissertation explores cellular reorganization in the anhydrobiotic *Polypedilum vanderplanki* Pv11 cell line as it undergoes preconditioning, desiccation, and rehydration. The nucleus, mitochondria, ER, Golgi apparatus, nucleolus, F-actin network, and plasma membrane all demonstrated significant morphological and/or physiological changes in response to preconditioning, desiccation and/or rehydration. Surprisingly, the nucleolus still appeared assembled immediately after rehydration, while an identified stress-induced MLO required 1 h to reassemble, suggesting that these two MLOs were protected by different mechanisms. Altogether, this dissertation describes how an ARID protein could protect a wide variety of targets without necessarily requiring a high ratio of protective protein to targets. Furthermore, this dissertation describes the complex cellular reorganization that occurs in Pv11 during preconditioning, desiccation, and rehydration, which may help guide future experiments in the animal model to further our understanding of anhydrobiosis.

TABLE OF CONTENTS

Page
DEDICATION……..……..iii
ACKNOWLEDGEMENTS……iv
ABSTRACT……..….....vi
LIST OF TABLES……..….....xi
LIST OF FIGURES…….……..xii

CHAPTER I: INTRODUCTION……...……..1

FIGURES…….....9

CHAPTER II: NEW INSIGHTS INTO ANHYDROBIOSIS USING CELLULAR DIELECTROPHORESIS-BASED CHARACTERIZATION

SUMMARY……...…11

INTRODUCTION…….12

METHODS……14

RESULTS AND DISCUSSION……16

CONCLUSIONS……...25

TABLES……27

FIGURES……...29

CHAPTER III: LIQUID-LIQUID PHASE SEPARATION PROMOTES ANIMAL DESICCATION TOLERANCE

SUMMARY……...34

INTRODUCTION…….35

METHODS……38

RESULTS AND DISCUSSION……41

CONCLUSIONS……..…48

FIGURES……...49

CHAPTER IV: CELLULAR REORGANIZATION IN DESICCATION TOLERANT PV11 CELLS

SUMMARY……...60

INTRODUCTION…….61

METHODS……62

RESULTS AND DISCUSSION……64

CONCLUSIONS……...72

FIGURES……..….73

CHAPTER V: SUMMARY AND CONCLUSIONS……86

REFERENCES.....……..……..…90

APPENDICES

I. PERMISSION FROM WILEY AND SONS……..……..…100

II. PERMISSION FROM AIP PUBLISHING……...……..…….…..…109

III. PERMISSION FROM *PNAS*..……..……113

CURRICULUM VITAE…….…….115

LIST OF TABLES

TABLE PAGE

Table 1. *Afr*LEA3m and *Afr*LEA6 Cellular Dielectrophoresis…..……..27

LIST OF FIGURES

FIGURE PAGE

Figure 1. Strategies of Anhydrobiotic Animals…....……10

Figure 2. Immunoblot of *Afr*LEA3m and *Afr*LEA6..……31

Figure 3. Osmotic Tolerance of Kc167 Cells Expressing *Afr*LEA3m and *Afr*LEA6..…..32

Figure 4. SEM of Cells Expressing *Afr*LEA3m…….……33

Figure 5. *Afr*LEA6 LLPS Confirmation…….…….…….……...52

Figure 6. Functions of *Afr*LEA6 Domains….……53

Figure 7. Intracellular Viscosity of Cells Expressing *Afr*LEA6…….…...54

Figure 8. Desiccation Tolerance of Cells Expressing *Afr*LEA6……55

Figure 9. Osmotic Tolerance of Cells Expressing *Afr*LEA6…….……56

Figure 10. *Afr*LEA6 LLPS…….……57

Figure 11. Hexanediol Recovery...…….……...58

Figure 12. Viability at Different Rates of Desiccation……..59

Figure 13. Preconditioning in Pv11 Cells...…….……..76

Figure 14. Mitochondria Membrane Potential Recovery……...……..77

Figure 15. Mitochondrial Respiration…….……..78

Figure 16. Nucleolus Recovery……..…….……..79

Figure 17. The ER, Golgi, and Nucleus During Preconditioning……..80

Figure 18. The ER, Golgi, and Nucleus During Desiccation and Rehydration….……81

Figure 19. F-actin Networks During Preconditioning……...……82

Figure 20. SEM of Pv11 Cells…..…….……83

Figure 21. Neuron-like Morphology of Pv11 Cells...……84

Figure 22. Intracellular Viscosity During Desiccation in Pv11 Cells…...…….85

CHAPTER I

INTRODUCTION

Unfavorable conditions for life can arise from changes in abiotic factors, including the availability of water. Some animals have evolved remarkable strategies to tolerate virtually complete water loss for prolonged periods of time, despite the cellular damage associated with desiccation, such as membrane destabilization, protein and nucleic acid denaturation, oxidative stress, and metabolic dysregulation (*1-5*). This transient state of life in the desiccated state has been an enigma since 1702 when Van Leeuwenhoek first noted anhydrobiosis in rotifers or 'wheel animals' (*6, 7*). Since then, desiccation tolerance has been confirmed to occur in several other animal phyla including Arthropoda, Tardigrada, and Nematoda (*8, 9*). Remarkably, many desiccation-tolerant species can survive in an anhydrobiotic state for years, or even decades, with limited impacts on viability (*10*). Understanding the mechanisms that govern desiccation tolerance has significant biotechnological applications, particularly in crop-drought resistance and stabilization of clinically relevant cells and tissues at ambient temperatures (*11*). To translate insights from anhydrobiotic animals into clinical applications, however, it is imperative to compare and contrast the molecular principles among these organisms to distinguish between fundamental and unique strategies.

Janis et al. 2018. *Proteomics*

The term ‘anhydrobiosis-related intrinsically disordered (ARID) proteins’ is an umbrella term for late embryogenesis abundant (LEA) proteins, tardigrade-specific intrinsically disordered proteins (TDPs), and other intrinsically disordered proteins with confirmed or strongly suggested roles in animal desiccation tolerance (*12*). However, this grouping should not imply that all ARID proteins are functionally similar but distinguishes them from more ordered proteins, such as enzymes involved in ROS detoxification, small HSPs, and aquaporins. This term does also not apply to ordered proteins even if they share homology with one or more ARID proteins, such as the Lea-Island-Located proteins in *Polypedilum vanderplanki* (*13*). The term ARID is similar to the term ‘anhydrobiosis-related gene island clusters (ARIds)’ presented by Gusev and colleagues to describe the grouping of anhydrobiosis-related genes in *P. vanderplanki*, where all genes in a given cluster were upregulated during desiccation (*14*). Indeed, it would be highly instructive to know whether similar patterns of ARId regulation are observed in other anhydrobiotic animals. We anticipate that proteins employed in anhydrobiotic organisms from other kingdoms such as plants, eubacteria, archaebacteria, and fungi display physicochemical similarities to ARID proteins found in animals. However, some divergence is to be expected and warrants a closer investigation of ARID proteins from theses kingdoms in the future. Furthermore, several excellent broader reviews covering anhydrobiosis are available (*1, 15-18*). For a comparative review of desiccation tolerance between plants and animals, please see Leprince and Buitnik (*1*).

Molecular strategies in anhydrobiotic animals

The requirements to successfully enter and exit anhydrobiosis remain undefined. In general, animals that rely only on the expression of protective proteins can be distinguished from animals that combine proteins with non-proteinaceous compounds. The expression of ARID proteins to survive desiccation and rehydration is a common strategy in all known anhydrobiotic invertebrates (Fig. 1). In addition to the expression of ARID proteins, a wide variety of stress-response proteins can be upregulated in preparation or response to desiccation (*5, 14, 19-22*).

Antioxidant Enzymes, Heat Shock Proteins (HSPs) and Aquaporins

Antioxidant system upregulation to scavenge ROS is a common strategy among anhydrobiotic animals (*3, 14, 15, 20, 23-29*). Enzyme dysfunction and unregulated metabolic activities in a cell experiencing water loss leads to peroxidation of membrane lipids, carbonylation of proteins, and damage to nucleic acids (*30*). Intuitively, the predominant source of ROS production during desiccation is the mitochondrion, and detoxification at the organelle level might be necessary to prevent excessive intracellular damage. Indirect evidence from *Polypedilum vanderplanki* supports this hypothesis, given that the most strongly upregulated gene in response to desiccation was mitochondrial thioredoxin (*26*). However, it is important to note that several anhydrobiotic animals enter a state of metabolic arrest (e.g., diapause or quiescence) in preparation or response to desiccation stress and thus limit excessive ROS production from dysregulated metabolic activities (*3, 27*).

Small HSPs, characterized by their α-crystallin domain, are also associated with anhydrobiosis and have been found to be upregulated in several animals during water stress (*26, 31-34*). However, only minor changes in the expression levels of small HSPs and their encoding mRNAs was observed in tardigrades during desiccation compared to fully hydrated controls (*19, 35*). Most small HSPs, unlike their larger counterparts, do not require ATP to prevent protein aggregation or aid in refolding (*36*). Since the adenylate energy charge of the cell will likely be dramatically lowered during desiccation, small HSPs might offer a substantial advantage over ATP-dependent HSPs considering the limited metabolic ATP regeneration.

Aquaporins have been suggested to play some role in animal anhydrobiosis, particularly in *P. vanderplanki* and tardigrades (*37-39*). However, no current evidence suggests a role in species like *Artemia franciscana* and nematodes, and relatively low expression levels were found in resting eggs of rotifers (*40*). An attractive hypothesis on the role of aquaporins includes the regulation of water loss to fine tune desiccation kinetics (*16*). While aquaporins may offer applications for engineering water-loss kinetics for cell and tissue preservation, more data will be required before any firm conclusions can be made about their role in anhydrobiotic animal.

Trehalose and Polyamines

The accumulation, or absence, of trehalose, a non-reducing disaccharide, in anhydrobiotic animals has been well studied (*41-43*). In brief, trehalose is hypothesized to confer protection during desiccation by three distinct mechanisms: 1) by replacing water with its hydroxyl groups, 2) by undergoing vitrification at lower water contents to prevent

molecular movement, and 3) by stabilizing globular proteins in solution, where trehalose exhibits a lower preferential interaction with the unfolded protein than the native form (*44, 45*). It is important to point out that these hypotheses are not mutually exclusive, and each mechanism may contribute to the protective properties of trehalose especially at different hydration levels and temperatures that the animal may encounter during desiccation. Early works on anhydrobiotic animals, including *Artemia salina* (*46*) and *Aphelenchus avenae* (*47*), suggested that trehalose may be required for anhydrobiosis. However, later evidence demonstrated that this is not the case since some species of rotifers and tardigrades do not accumulate trehalose prior to desiccation (*41, 48, 49*).

Polyamines are another group of compounds that was more recently associated with protection during desiccation. In the anhydrobiotic dauer larvae of *Caenorhabditis elegans*, mutants unable to synthesize polyamines (particularly spermidine) were rendered extremely sensitive to desiccation (*15*), but the role of these compounds in other anhydrobiotic animals has not been confirmed. Furthermore, it is unclear if spermidine production by spermidine synthase (SPDS-1) has direct protective properties during desiccation or if it affects other processes that modulate desiccation sensitivity. However, it was found for the brine shrimp *A. franciscana* that polyamine concentrations further increased as the organism developed past its anhydrobiotic stage of life (*50*). This may imply a limited role of polyamines for this organism, or that the concentrations present prior to desiccation are sufficient for protection.

ARID Proteins

Animal ARID proteins can currently be divided into two different subgroups that contain little to no homology: late embryogenesis abundant (LEA) proteins and tardigrade-specific intrinsically disordered proteins (TDPs) (*51-54*). It is important to clarify, however, that tardigrades do express some LEA proteins in conjunction to TDPs (*55, 56*). While TDPs are a relatively recent discovery, LEA proteins were discovered by Dure et al. in the late embryogenic stage of cotton (*Gossypium hirsutum*) seeds over 40 years ago (*57, 58*). Plant LEA proteins were initially grouped based on the presence of specific sequence motifs (*59*). Since then, a myriad of LEA proteins has been discovered in anhydrobiotic animals, and several nomenclatures were proposed to accommodate the growing number of known LEA proteins (*8, 60-62*). For the purposes of this dissertation, I will be following the classification scheme proposed by Tunnacliffe and Wise (*17*).

Group 1 LEA proteins contain one or more repeats of a hydrophilic 20 amino acid motif, while group 2 LEA proteins, termed 'dehydrins', contain two or more specific motifs denoted as Y, S, and K. Group 3 contains the largest number of LEA proteins and are characterized by a specific 11 amino acid motif (*17, 63*). While most LEA proteins in plants fall into groups 1-3, other minor groups have been described. Group 4 LEA proteins lack any consensus sequence, and group 5 LEA proteins are characterized by an unusually high content of hydrophobic residues (*64*). Finally, group 6 LEA proteins are characterized by the presence of at least one seed maturation protein motif and have recently been associated with the longevity of orthodox seeds in the desiccated state (*65*). Interestingly, only group 3 LEA proteins have been identified in anhydrobiotic animals, except for

Artemia, which expresses LEA proteins from groups 1, 3, and 6 in their desiccation tolerant encysted embryos.

The reasons why different groups of anhydrobiotic animals rely on different types of ARID proteins remains unresolved. One hypothesis may be that the lack of trehalose or presence of other protective compounds encourages different evolutionary trajectories for proteins involved in desiccation tolerance. Data presented on three *Triops* species demonstrated that the cysts undergo vitrification in absence of trehalose (*66*). These data are strikingly like those presented for tardigrades (*52*). Using blast analysis of LEA protein sequence data from *Artemia* against EST libraries for *Triops* yielded no significant results, while searches against EST libraries derived from tardigrades yielded low-identity hits (*data not shown*). This supports the hypothesis that the absence of trehalose requires proteins with a different set of physicochemical properties compared to animals that accumulate substantial levels of trehalose (e.g. <0.5% dry weight in *Triops longicaudatus, Triops cancriformis, and Triops australiensis vs.* 13-18% dry weight in *A. franciscana* and *P. vanderplanki* (*66*)). However, bdelloid rotifers indeed express LEA proteins and successfully enter anhydrobiosis without the need to accumulate trehalose (*6*).

Proposed molecular functions for ARID proteins include: 1) acting as a molecular shield to prevent protein aggregation, 2) membrane stabilization, 3) acting as a hydration buffer, 4) reinforcing sugar glasses, 5) protein vitrification, and 6) ion sequestration (*67-81*). More recently, however, bioinformatic insights have suggested that some LEA protein from *A. franciscana* may be able to undergo liquid-liquid phase separation (LLPS) to form membraneless organelles (MLOs) (*12, 82*). This dissertation begins with the use of cellular dielectrophoresis cells ectopically expressing of *Afr*LEA3m and *Afr*LEA6 from *A.*

franciscana to gain insights into protein folding and potential membrane interactions. It then proceeds to describe the use of confocal microscopy to identify and characterize the LLPS of *Afr*LEA6. Lastly, this dissertation explores the cellular reorganization that occurs in desiccation tolerant Pv11 cells from the anhydrobiotic midge, *P. vanderplanki*, during preconditioning, desiccation, and rehydration.

Figure Legends

Figure 1. Common and phyla-specific molecular strategies found in anhydrobiotic animals. IDPs, such as LEA proteins and TDPs, are found in all phyla. The role of small HSPs in tardigrades is currently unresolved (small HSPs may contain extended intrinsically disordered regions with functional relevance). Ferritin homologues, hemoglobin, and polyubiquitin may play a role in animal desiccation tolerance, but current data suggests that these are phyla-specific strategies. Non-proteinaceous strategies include trehalose and polyamines, such as spermidine produced by spermidine synthase (SPDS-1) in *C. elegans*. Please refer to text for more information.

Figures

Figure 1

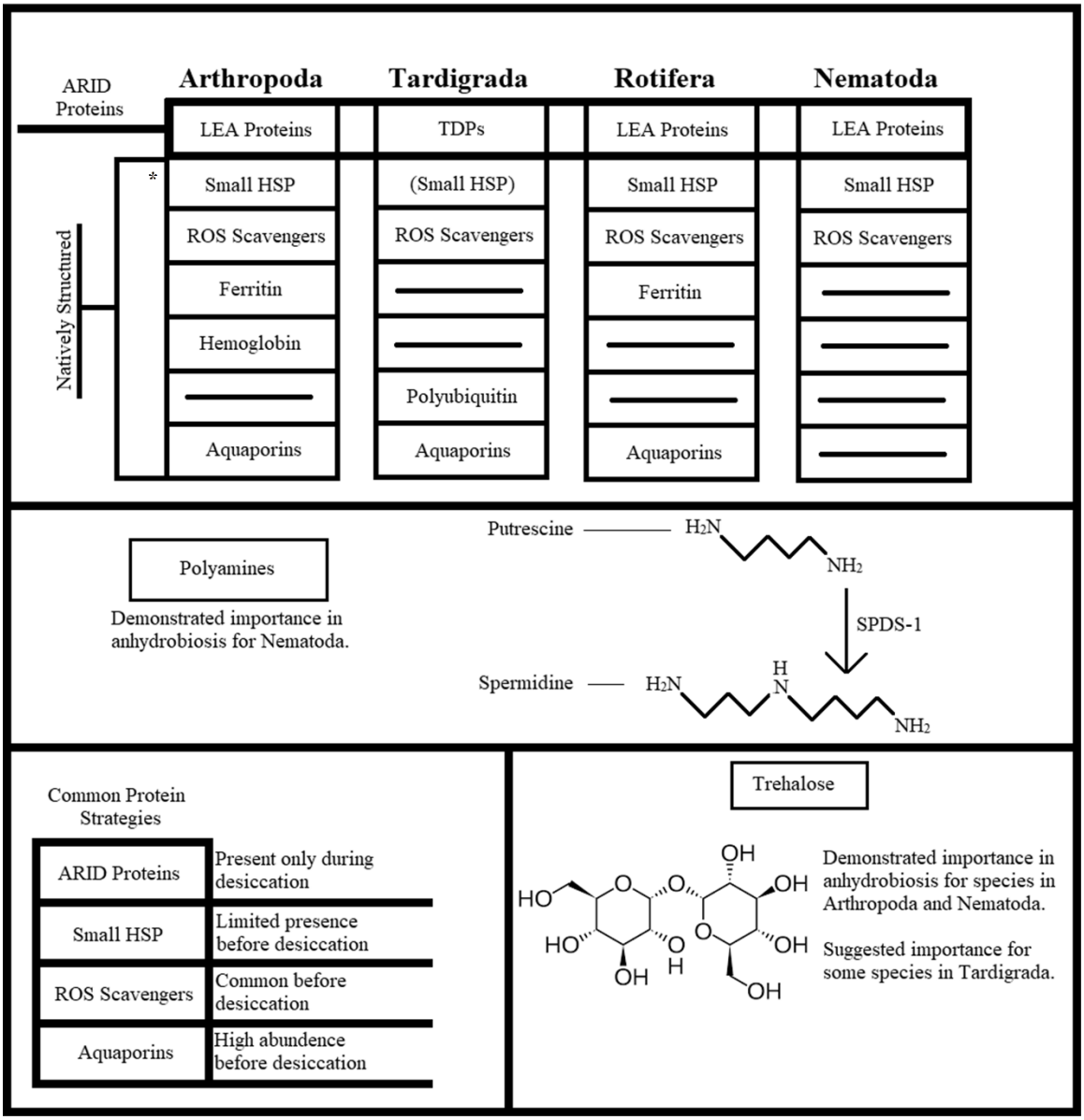

Janis et al. 2018. *Proteomics*

CHAPTER II

NEW INSIGHTS INTO ANHYDROBIOSIS USING CELLULAR DIELECTROPHORESIS-BASED CHARACTERIZATION

SUMMARY

Late embryogenesis abundant (LEA) proteins are found in desiccation-tolerant species from all domains of life. Despite several decades of investigation, the molecular mechanisms by which LEA proteins confer desiccation tolerance is still unclear. In this study, dielectrophoresis (DEP) was used to determine the electrical properties of *Drosophila melanogaster* (Kc167) cells ectopically expressing LEA proteins from the anhydrobiotic brine shrimp, *Artemia franciscana*. Dielectrophoresis-based characterization data demonstrates that single expression of two different LEA proteins, *Afr*LEA3m and *Afr*LEA6, both increases cytoplasmic conductivity of Kc167 cells to a similar extent above control values. The impact on cytoplasmic conductivity was surprising, given that the concentration of cytoplasmic ions is much higher than the concentrations of ectopically expressed proteins. The DEP data also supported previously reported data suggesting that *Afr*LEA3m can interact directly with membranes during water stress. This hypothesis was strengthened using scanning electron microscopy, where cells expressing *Afr*LEA3m were found to retain more circular morphology during desiccation, while control cells exhibited a larger variety of shapes in the desiccated state.

Rashed et al. 2019. *Biomicrofluidics*

These data demonstrate that DEP can be a powerful tool to investigate the role of LEA proteins in desiccation tolerance and may allow characterization of protein-membrane interactions *in vivo* when direct observations are challenging.

INTRODUCTION

Anhydrobiosis, or "life without water," is a remarkable state of life where an organism has lost virtually all cellular water but is able to resume its life cycle upon rehydration. Understanding the molecular mechanism governing anhydrobiosis may lead to profound advances in engineering crop-desiccation tolerance and the ability to store biomedical relevant cell and tissue samples in the desiccated state as an alternative to cryopreservation. Anhydrobiosis-related intrinsically disordered (ARID) proteins are found in all known anhydrobiotic species, spanning all domains of life, and have been linked to the successful entry and exit from anhydrobiosis, but the molecular mechanisms underlying this phenomenon remain enigmatic.

The ability to enter and exit anhydrobiosis relies on an array of molecular mechanisms designed to repair and protect various cellular structures and macromolecules (e.g., DNA, RNA, proteins, membranes, etc.). Common anhydrobiotic strategies observed in animals include the accumulation of protective osmolytes, particularly trehalose, as well as the expression of a variety of ARID proteins including late embryogenesis abundant (LEA) proteins (*4, 12*) and tardigrade-specific intrinsically disordered proteins (TDPs). LEA proteins were originally discovered in plants and predominantly occur in the late embryogenesis stage of orthodox seeds but were later also found in other plant tissues and in anhydrobiotic animals (*62*). Several sequence-based grouping methods for LEA proteins

have been described, and this work will adapt the grouping scheme proposed by Tunnacliffe and Wise as a means to classify and organize groups of LEA proteins (*60*).

This study focuses on two different LEA proteins from *A. franciscana*, *Afr*LEA3m and *Afr*LEA6, group 3 and 6 LEA proteins, respectively. While *Afr*LEA3m is a mitochondrial-targeted protein, it was shown to protect artificial membranes with a composition similar to the inner leaflet (i.e., inner side) of the plasma membrane with the same efficacy as it protected artificial membranes with lipid composition mimicking the inner mitochondrial membrane (*79, 83, 84*). Since the vast majority of mitochondrial proteins, including *Afr*LEA3m, are synthesized in the cytoplasm of the cell, it seems plausible that *Afr*LEA3m before its transport into the mitochondrial matrix could aid in protecting the plasma membrane during desiccation. While bioinformatic data suggest that *Afr*LEA3m can form amphipathic α-helices during water stress to integrate into membranes, it remains experimentally undetermined if *Afr*LEA3m can directly or indirectly interact with membranes during water stress (*82*). In contrast, *Afr*LEA6 localizes to the cytoplasm (*85*). While group 3 LEA proteins are commonly found in anhydrobiotic animals, *A. franciscana* is the only known anhydrobiotic animal to express a group 6 LEA protein, making it an interesting target for further study. Furthermore, bioinformatics does not suggest that *Afr*LEA6 can fold into amphipathic α-helices during water stress, making it a good candidate for comparison to *Afr*LEA3m.

AC-electrokinetic based techniques, such as dielectrophoresis, electrorotation (eROT), and electrochemical impedance spectroscopy (EIS) have been used to investigate and analyze the properties of biological systems (*86-96*). DEP measures electrical properties by applying a nonuniform electric field to a liquid media of a known

conductivity containing suspension of cells (*90*). The nonuniform electrical field will induce a dipole within each cell; the induced translation of each cell in the electrical field depends on their phenotype, i.e., permittivity and conductance properties of the membrane and the cytoplasm as well as the conductivity of the solution. In this study, dielectrophoresis was used to gain insights into the molecular mechanisms of cellular protection during water stress conferred by *Afr*LEA3m and *Afr*LEA6, two LEA proteins from the anhydrobiotic brine shrimp, *Artemia franciscana*. Extracted DEP-based characterization data in this study demonstrate that the expression of LEA proteins from *A. franciscana* in desiccation sensitive cells from the fruit fly *D. melanogaster* has a pronounced impact on cytoplasmic conductivity and membrane capacitance. These results show that DEP can offer a novel approach to gain insights into the molecular mechanisms of protections this elusive class of proteins offers during anhydrobiosis.

METHODS

Cells, Culture, and Transfections

Kc167 cells were purchased from the Drosophila Genomics Research Center (DGRC; Bloomington, IN). Cells were cultured on 100 or 60 mm cell culture-treated dishes (Corning Incorporated, Corning NY) in Schneider's media (Caisson, USA) supplemented with 10% heat-inactivated fetal bovine serum (FBS) (Atlanta Biologicals, Lawrenceville, GA). Transfections were performed as previously described with the exception that Schneider's media was used in place of M3+BPYE medium and that 2.0 mg/ml G418 (ultrapure; VWR International) was used to select transfected cells and to generate and maintain stable cell lines (*84*). The *pAc5-STABLE2-neo* vector was acquired from Addgene

(Cambridge, MA). For additional information on the *pAc5-STABLE2-neo* vector, please see the Results and Discussions and Ref. (*97*). Immunoblotting with primary antibodies (Aves Labs Inc., Tigard, OR) raised against *Afr*LEA6 or *Afr*LEA3m was performed on all cell lines to confirm transgenic protein expression (Fig. 2) (*98, 99*). Cell counting and diameter measurements were performed using a Countess II FL Automated Cell Counter (Life Technologies, USA).

Scanning Electron Microscopy

Kc167 cells were plated onto an aluminum SEM stage at a concentration of 2×10^6 cells/ml. The cells were allowed to attach to the stage for 1 h in a humidified chamber at 25 ∘C. Culture media was removed, and cells were then dried overnight at 10% relative humidity. The dried samples were sputter coated with an 18 nm film of gold and palladium and examined using a Zeiss Supra 35 VP scanning electron microscope with an electron high tension voltage of 15–20 kV.

Dielectrophoresis

To collect cells and remove cell-culture medium, Kc167 cells were centrifuged at 400 *g* for 2 min at room temperature. The cellular pellets were resuspended in 10 ml of medium consisting of 85 g/l sucrose plus 3 g/l glucose, 11 mg/l $CaCl_2$, and 24 mg/l $MgCl_2$, ∼360 mOsmol/kg. In experiments using hypertonic media, the osmolarity was brought to ∼560 and ∼760 mOsmol/kg with an additional 200 or 400 mM sucrose, respectively. To ensure complete removal of cell-culture medium, Kc167 cells were pelleted again, and the final resuspension volume was approximately 1 ml. The final conductivity of the medium

was adjusted to 5 mS/m using phosphate buffered saline (PBS) and the desired conductivity was verified with a conductivity meter (HORIBA Ltd., Koyoto, Japan). The number of cells was enumerated using a hemocytometer and adjusted to approximately 5–8×10^6 cells/ml (±10 %) for the DEP measurement. In general, one sample of 5 ml of cells, n_{bio}, in suspension can provide, on average, approximately 10–12 technical repeats, n_{tec}, of data sets with a total number of trials, $n=n_{bio}\times n_{tec}$. The 3DEP (Deptech, Ringmer, UK) platform was used to study the electrical properties of the cell. See (*100*) for information on the 3DEP platform, relevant equations, and modeling.

RESULTS AND DISCUSSION

In this study, a detailed characterization of the electrical properties of Kc167 cells from *D. melanogaster* and the changes that occur in these properties in response to acute osmotic stresses have been achieved. Using ectopic protein-expression models, modulations in the osmotic-stress response could be correlated to molecular mechanisms of cellular protection conferred by two LEA proteins that ameliorate water-stress damage in the anhydrobiotic embryos of *A. franciscana (2)*. Previous studies conducted with artificial liposomes have indicated that *Afr*LEA3m can directly interact with phospholipid bilayers during severe water stress (*79*). Based on these data, it was hypothesized that the specific membrane capacitance of Kc167 cells expressing *Afr*LEA3m will increase during water stress and that the specific membrane conductance be unaltered if *Afr*LEA3m was indeed interacting directly with the plasma membrane during moderate osmotic stress (~760 mOsmol/kg). To test this hypothesis, a dielectrophoresis-based platform was used to characterize the cytoplasmic conductivity, the specific membrane capacitance, and the

specific membrane conductance of cells in isotonic sucrose medium (~360 mOsmol/kg) with a low ionic strength (<6.5 S/m), and hypertonic media of either 560 or 760 mOsmol/kg adjusted by addition of sucrose to reach the desired osmolarity, to mimic water stress (Table 1). The low ionic strength of the media was required to create a significant difference between media conductivity and that of the cytoplasm and membrane, thereby increasing the resolution of DEP measurements (see (*100*), Eq. 2), hence, achieving better resolution. Conversely, relatively high media conductivity (~100 mS/m) will compromise the reliability of the DEP measurements by introducing other electrokinetic effects (e.g., Joule heating). However, these DEP-compatible media may negatively impact cell viability over time, since the cells are deprived of several important components normally found in insect cell-culture media (e.g., monovalent ions, sugars, and amino acids). Not surprisingly, a significant decrease in the values of all three fitted parameters (cytoplasmic conductivity, the specific membrane capacitance, and the specific membrane conductance) was observed for control cells incubated in isotonic sucrose media for ~16 h, where 100% of cells showed a collapse in membrane integrity (Table 1, Vector Control-Dead). Furthermore, the viability of cells in isotonic sucrose media was also significantly reduced after only 60 min of incubation for non-transfected control and vector control cells, indicating the time-sensitivity of the measurements (Fig. 3). However, there was no significant reduction in viability for up to 30 min of incubation for any cell line in all DEP media employed. Based on these data, all other measurements were completed within <18 min to avoid artifacts caused by cell death. There was no significant difference observed in any fitted values between non-transfected control cells and vector control cells demonstrating that the expression of transgenic genes such as the aminoglycoside 3′-phosphotransferase to

confer G418 resistance does not per se change the electrical properties of cells (Table 1).

Interestingly, there was an ~41% and ~51% increase in the cytoplasmic conductivity of cells expressing *Afr*LEA3m and *Afr*LEA6, respectively, over vector controls under isotonic media conditions. The impact on cytoplasmic conductivity was surprising, given that the concentration of cytoplasmic ions is much higher than the concentrations of ectopically expressed proteins. Cytoplasmic conductivity is assumed to be primarily affected by the intracellular [K^+] and, to a lesser amount [Cl^-], given their relatively high concentrations compared to other ions, charged molecules, and macromolecules. The specific membrane capacitance (i.e., the capacitance of the membrane normalized to the unit cell cross section and membrane area), is defined here as the ability of a membrane to hold an electric charge. By treating the membrane as a dielectric slab, with a relative permittivity (ε_r), that is flanked by two parallel plate electrodes that are distance (d) apart, each with an area (A), and a dielectric constant ($\varepsilon 0$), gives rise to the equation $C_{mem} = (\varepsilon_r)(\varepsilon_0)/(d)$ (Farad per unit area). In reference to the cell, changes in the specific membrane capacitance can be affected by the dielectric constant, ε_{mem} (determined by the composition of the membrane), the area of the membrane (i.e., morphology), and the thickness of the plasma membrane (particularly within the insulating hydrophobic tail region) (*101*). The specific membrane conductivity is simply the ability of an electric current to pass through the membrane and was generally thought to be primarily affected by membrane thickness, gating state of ion channels, and area (*102*). However, recent data have shown that an increase in ion efflux or influx can increase the specific membrane conductivity and concurrently decrease cytoplasmic conductivity, while both membrane thickness and area remain unchanged (*103*). In the absence of ion-

channel involvement, any increase in membrane thickness should decrease both the membrane conductance and the capacitance, while an increase in the membrane area should increase both values (*102*). It was hypothesized that *Afr*LEA3m would interact with the inner leaflet of the plasma membrane during acute osmotic stress. Bioinformatic analysis predicts that *Afr*LEA3m folds into amphipathic α-helices during water stress, whereas *Afr*LEA6 does not (*82*). Amphipathic α-helices are often associated with membrane interactions (i.e., a protein would be able to interact with charged phospholipid head groups, as well as their hydrophobic tail region). This may cause a change in its dielectric constant, ε_{mem}, while not significantly impacting the membrane thickness and area (i.e., the specific membrane capacitance increases, while the specific membrane conductance would remain constant). In contrast, *Afr*LEA6 was hypothesized to not interact with the inner leaflet of the plasma membrane, thereby any change (positive or negative) observed in the specific membrane conductance may lead to changes in the specific membrane capacitance.

Data in Table 1 show that the specific membrane conductance and capacitance were unaffected by the ectopic expression of either *Afr*LEA3m or *AfrLEA6.* The effect of both proteins on cytoplasmic conductivity could be mediated by direct or indirect interactions with ion channels causing an influx of monovalent ions (i.e., increasing the concentration of a simple electrolyte such as K^+ or Na^+ will theoretically increase the cytoplasmic conductivity). In the case of red blood cells, however, the specific membrane conductivity and cytoplasmic conductivity move in antiphase with rhythmic efflux of K+ ions (*103*). The lack of K^+ and Na^+ in the employed DEP media and the presence of only minor amounts of divalent ions make a mechanism based on ion influx highly unlikely.

An alternative mechanism might be that, due to the highly hydrophilic and charged nature of *Afr*LEA3m and *Afr*LEA6, the mobility of monovalent ions surrounding *Afr*LEA3m and *Afr*LEA6 is effectively higher than for VC cells, without actually changing ion concentration. This may increase the molar conductivity of the cytoplasm. Molar conductivity (Λ_m) is defined as the relationship between electrolyte concentration (c) and conductivity (κ). In the equation $(\Lambda_m)=(\kappa)/(c)$, any increase in electrolyte concentration will decrease molar conductivity (*101*). This is due to an increase in drag force being placed on a given diffusing ion as the concentration of ions of an opposite charge increases (i.e., Debye-Huckel theory). If the equation is written instead as $\kappa=(\Lambda_m)(c)$, then it becomes clear that an increase in molar conductivity at a constant ion concentration will increase cytoplasmic conductivity. This alternative mechanism is supported by molecular dynamics simulations of polyelectrolytes (highly charged polymers) and simple electrolytes, where increasing the concentration of polyelectrolytes increased the dispersion of ions around the polymers and thereby increased the molar conductivity of the ions (*101*). In addition, the cytoplasmic conductivity of cells expressing *Afr*LEA3m or *Afr*LEA6 progressively decreases as the cells were exposed to hypertonic solutions (Table 1). This is in stark contrast to vector control cells, which displayed a cytoplasmic conductivity that progressively increased when exposed to increasingly hypertonic solutions. In the case where the electrolyte concentrations are increasing, as would be the case when osmotically active water is being pulled out of the cell due to hypertonic stress, conductivity should decrease if molar conductivity decreases. However, the equation $\kappa=(\Lambda_m)(c)$ does demonstrate that increasing ion concentrations in a cell should increase the conductivity of the cytoplasm. However, this assumes that the decrease in molar conductivity is

sufficiently outweighed by the increase in electrolyte concentrations. This can be observed in vector control cells under osmotic stress, where a decrease in cell volume leads to a subsequent increase in intracellular ion concentrations and cytoplasmic conductivity. In the case of cells expressing *Afr*LEA3m and *Afr*LEA6, the observed decrease in cytoplasmic conductivity during hyperosmotic stress may be a result of a decrease in molar conductivity outweighing the increase in electrolyte concentration, leading to a net loss in cytoplasmic conductivity [i.e., in $\kappa=(\Lambda_m)(c)$, the decrease in (Λ) outweighs the increase in (c) and leads to a reduction in (κ)]. These data suggest that, under isotonic conditions, LEA proteins are unentangled and increase the cytoplasmic conductivity by behaving as typical polyelectrolytes, thereby increasing cytoplasmic ion diffusivity (*104*). During osmotic stress, the decrease in cellular volume may be sufficient to concentrate LEA proteins enough to shift their dynamics from a semi-dilute, unentangled state to an entangled state. Under entangled conditions, the effect of LEA proteins on ion diffusivity may be negated (*104, 105*).

When Kc167 cells were challenged with hyperosmotic stress (~570 and 760 mOsmol/kg), cells expressing *Afr*LEA3m experienced a sharp increase in specific membrane capacitance ~56%. However, specific membrane conductance did not significantly change when cells expressing *Afr*LEA3m were challenged with a moderate hypertonic stress of 570 mOsmol/kg. In the case of the osmotically stressed cells, the radius decreases by approximately 11% and, in turn, should increase the specific membrane capacitance by 11%. However, this increase does not sufficiently explain the observed 56% increase in specific membrane capacitance. No apparent differences in cell morphology (aside from reported changes in cell diameter) were observed when cells were subjected to

severe osmotic stress (~760 mOsmol/kg) and imaged with confocal microscopy (data not shown).

Further analysis of these data relies on two assumptions; first, the effective area of the membrane surface is changing, hence changing the capacitance of the membrane ($C_{mem}=\phi\varepsilon_0\varepsilon_r/d$), where ϕ membrane topography parameter that represents the ratio of the actual membrane area of the cell to the membrane area ($4\pi R2$) that would form a perfectly smooth and spherical covering of the cytoplasm and it is proportional to the "roughness" of the membrane surface. Furthermore, cells subjected to the hypertonic media would shrink, causing the membrane to wrinkle leading to an increase in ϕ (≈1.5) and therefore C_{mem} *(102, 106)*. Similar results were observed for salivary gland cells (*Drosophila, Chironomids*, and *Sciarids*), where ϕ ranged from 160 to 830 (*107*). Furthermore, the change in the membrane effective area is further proved by the data reporting a decrease in membrane capacitance of cells suspended in hypotonic media due to cell swelling and the opposite effect when suspended in hypertonic media (*106, 108-110*). However, it is also noted that this increase in C_{mem}, for Kc167 cells expressing either *Afr*LEA3m or *Afr*LEA6 suspended in 760 mOsmol/kg, does not mean the formation of blebs or shriveling of the membrane, as there was no indication of apoptosis or necrosis of the cells (*111, 112*). These data were supplemented with SEM imaging. After complete desiccation for 18–24 h, cells expressing *Afr*LEA3m retained a more circular morphology than vector control cells, which displayed a variety of shapes and sizes (Fig. 4A and B). In addition, cells expressing *Afr*LEA3m often displayed relatively large pore-like structures that were never observed in vector control cells (Fig. 4C and D). These pore-like structures may be stress points where the membrane begun to rip apart, but complete lysis was stopped due to the presence

of *Afr*LEA3m. Indeed, vector control cells can often be seen with large tears that allows for the cytoplasm to leak out while desiccation is still occurring. Data in Table 1 show no significant difference in the membrane conductance of Kc167 cells expressing *Afr*LEA3m, indicating that the cell membrane is intact, and cells did not exhibit either necrosis or apoptosis. Moreover, this increase in the membrane conductance (~16%) for osmotically stressed *Afr*LEA3m can be attributed to the effective area of the membrane surface ($G_{mem}=\phi G_0$, where $\phi\approx1.2$) which is close to the actual increase in G_{mem} (≈1.5). However, the increase in the membrane conductance of the Kc167 vector control could be attributed to the degradation of the plasma membrane (*112*).

The second assumption states that the relative dielectric constant, ε_r, and thickness, d, of the membrane are changing due to the expression of LEA proteins as well as osmotic stress imposed from the hypertonic media, with the relative dielectric constant, ε_r, surprisingly increasing due to the expression of the LEA proteins. The presence of organelles, structures, or polypeptides such as LEA proteins will contribute to the internal dielectric properties of the cell. Several studies reported changes in the dielectric constant which in turn have an influence on the membrane capacitance (*113, 114*). Gentet *et al.* showed a minor decrease in the membrane capacitance (~6%) due to expressing glycine receptors and other membrane proteins in embryonic kidney cells (HEK-293) (*115*). Similarly, Stoneman *et al.* also reported a decrease in the membrane capacitance of yeast cells (~7%) overexpressing a G protein coupled receptor (Ste2p protein) (*116*). In contrast to our work, these two experiments did not induce any osmotic stress on the cells being studied. The C_{mem} value mostly reflects the properties of the hydrophobic layer of the membrane, which is populated by the hydrocarbon tails of the phospholipids and

hydrophobic segments of integral membrane proteins (*117*). Considering that *Afr*LEA3m is expected to only fold into its native structure in response to water stress, the observed increase in the membrane capacitance under osmotic stress is not surprising. Therefore, Kc167 cells expressing *Afr*LEA3m will yield different membrane capacitance (C_{mem}) and conductance (G_{mem}) values when subjected to hyperosmotic stress. It should be noted that the pore-like formations in the SEM images (Fig. 4C and D) only form in the completely dried state. In the case of pore-like formations occurring during an osmotic stress of ~760 mOsmol/kg, the relative dielectric constant of the membrane would decrease by a factor of approximately one-fourth (*118*). This is in contrast to the observed increase in the specific membrane capacitance in cells expressing *Afr*LEA3m. The formation of ~200–300 nm large pores would result in a loss of membrane integrity, but this was not observed during preparation of cells for hyperosmotic stress experiments (data not shown). Furthermore, our data suggest that *Afr*LEA3m is integrating, at least to some capacity, into the plasma membrane which agrees with previously published results that suggests *Afr*LEA3m protects membranes during water stress (*79*).

Lacking any apparent propensity to form amphipathic α-helices, *Afr*LEA6 is an ideal protein to compare to *Afr*LEA3m (*82*). In comparison with *Afr*LEA3m, cells expressing *Afr*LEA6 experienced a significant increase in the membrane conductance, but not specific membrane capacitance, when challenged with moderate hyperosmotic stress (~570 mOsmol/kg). Furthermore, specific membrane capacitance for cells expressing *Afr*LEA6 was not significantly different from what was observed for vector control cells under all conditions. The observed increase in specific membrane conductance for cells expressing *Afr*LEA6, as well as vector control cells, is thought to be due to an efflux of

monovalent ions (likely by gated ion channels) that is ameliorated when *Afr*LEA3m integrates into the membrane as well as the change in the effective area of the membrane surface (i.e., ϕ) which influences both C_{mem} and G_{mem}.

CONCLUSIONS

In summary, a dielectrophoresis-based platform was used to characterize the electrical proprieties of Kc167 cells from *D. melanogaster* expressing late embryogenesis abundant proteins from the anhydrobiotic embryos of *A. franciscana*. The increase in cytoplasmic conductivity observed in Kc167 vector control cells under osmotic stress is related to the reduction in cell volume and the increase in ion concentration. We hypothesize that the increase in cytoplasmic conductivity, for cells ectopically expressing *Afr*LEA3m or *Afr*LEA6, under isotonic conditions, is related to both LEA proteins behaving as typical polyelectrolytes increasing the diffusivity of cytoplasmic ions. Under osmotic-stress conditions, the protein dynamics may shift from an unentangled state to a concentrated one, which leads to a decrease in cytoplasmic conductivity. In the case of *Afr*LEA3m being activated during osmotic stress, then the increases in the specific membrane capacitance during hyperosmotic stress may be due to its direct interactions with the plasma membrane. The increase in specific membrane conductance observed in Kc167 vector control cells was related to changes in plasma membrane morphology during hyperosmotic stress. In contrast, for cells ectopically expressing LEA proteins, the increase in the specific membrane conductance is driven by a change in the effective area of their membrane surfaces in addition to any changes in membrane morphology that may occur during hyperosmotic stress. Altogether, these data support the utility of cellular DEP-based

characterization as a powerful tool to identify protein-membrane interactions *in vivo* when direct observations are challenging.

Tables

Table 1**:** Cellular DEP Values (cytoplasm conductivity, S/m; specific membrane capacitance, mF/m^2; and conductance, S/m^2) of Kc167 cells.

	Isotonic sucrose/glucose medium + $CaCl_2$ and $MgCl_2$ (360 mOsmol/kg)	**Hypertonic sucrose/glucose medium (+200 mM sucrose) (560 mOsmol/kg)**	**Hypertonic sucrose/glucose medium (+400 mM sucrose) (760 mOsmol/kg)**
Cytoplasm conductivity (S/m)			
Kc167 vector control (VC)	0.152 ± 0.016 ($n = 68$)	0.192 ± 0.009^{a} ($n = 62$)	0.189 ± 0.012^{a} ($n = 61$)
Non-transfected control	0.162 ± 0.014 ($n = 18$)		
VC-dead	0.032 ± 0.002^{b} ($n = 7$)		
*Afr*LEA3m	0.215 ± 0.018^{b} ($n = 72$)	$0.172 \pm 0.007^{a,b}$ ($n = 63$)	$0.139 \pm 0.014^{a,b}$ ($n = 58$)
*Afr*LEA6	0.23 ± 0.0186^{b} ($n = 72$)	0.188 ± 0.0163^{a} ($n = 61$)	$0.126 \pm 0.015^{a,b}$ ($n = 57$)
Specific membrane capacitance (mF/m^2)			
Kc167 vector control (VC)	10 ± 1.6 ($n = 68$)	11.4 ± 1.18 ($n = 62$)	12.6 ± 1.3 ($n = 61$)
Non-transfected control	10.5 ± 1.6 ($n = 18$)		
VC-dead	2.7 ± 0.06^{b} ($n = 7$)		
*Afr*LEA3m	9.8 ± 1.2 ($n = 72$)	$14.7 \pm 1.6^{a,b}$ ($n = 63$)	$14.2 \pm 0.8^{a,b}$ ($n = 58$)
*Afr*LEA6	11.8 ± 1.8 ($n = 72$)	12.4 ± 1.53 ($n = 61$)	15.0 ± 3.0 ($n = 57$)
Specific membrane conductance (S/m^2)			
Kc167 vector control (VC)	793 ± 63 ($n = 68$)	1114 ± 80^{a} ($n = 62$)	1129 ± 132^{a} ($n = 61$)
Non-transfected control	812 ± 38 ($n = 18$)		
VC-Dead	503 ± 43^{b} ($n = 7$)		
*Afr*LEA3m	758 ± 75 ($n = 72$)	878 ± 73^{b} ($n = 63$)	$915 \pm 73^{a,b}$ ($n = 58$)
*Afr*LEA6	710 ± 42 ($n = 72$)	$956 \pm 62^{a,b}$ ($n = 61$)	1050 ± 110^{a} ($n = 57$)
Cell diameter (μm)	10 ± 0.23 ($n = 7$)	9.2 ± 0.31 ($n = 10$)	8.9 ± 0.21 ($n = 10$)

[a]Values differ significantly from the corresponding isotonic medium (one-way ANOVA; $P < 0.05$), total number of trials, $n = n_{bio}$ (~ 5–6) × n_{tec}(~ 10–12).

[b]Values differ significantly from the corresponding control (one-way ANOVA; $P < 0.05$), total number of trials, $n = n_{bio}$ (~ 5–6) × n_{tec}(~ 10–12).

Figure Legends

Figure 2. Immunoblots confirming expression of (a) *Afr*LEA3m (~31 kDa) in Kc167 cells. Several possible higher-order structures were also identified (#) as well as breakdown products (∗). Blotting results for vector control cells (VC) stably transfected with the expression vector but lacking inserted LEA proteins are shown for comparison. (b) *Afr*LEA6 expression in Kc167 cells. The apparent Mw was about 8 kDa larger than expected (~27 kDa). The increased apparent Mw might be related to post-translational modification and the known behavior of some LEA proteins to migrate slower during SDS-PAGE than most non-LEA proteins. One higher-order structure was also identified (#). Ladders in both images are in kDa.

Figure 3. Viability of non-transfected controls (NTC), vector controls (VC), and *Afr*LEA3m expressing (LEA3m) of Kc167 cells is significantly reduced when incubated for up to 60 min in low ionic strength (<6.5 S/m) isotonic sucrose medium (~360 mOsmol/kg). White bars represent 0 min incubation, gray bars represent 30 min incubation, and black bars represent 60 min incubation. Letters denote significance (i.e., "A" and "B" are significantly different from one another, but neither are significantly different from "A, B") (±SD; $p<0.05$; one-way ANOVA).

Figure 4. SEM images demonstrating that cells expressing *Afr*LEA3m retain a more circular shape after complete desiccation and have pore-like formations in their plasma membranes. Vector control (VC) cells (A) and cells expressing *Afr*LEA3m (B) and (C)

were completely desiccated prior to imaging. (D) Pores were observed exclusively intact, desiccated *Afr*LEA3m cells. Scale bars for (A-C) represent 5 μm, while the scale bar for (D) represents 100 nm.

Figures

Figure 2

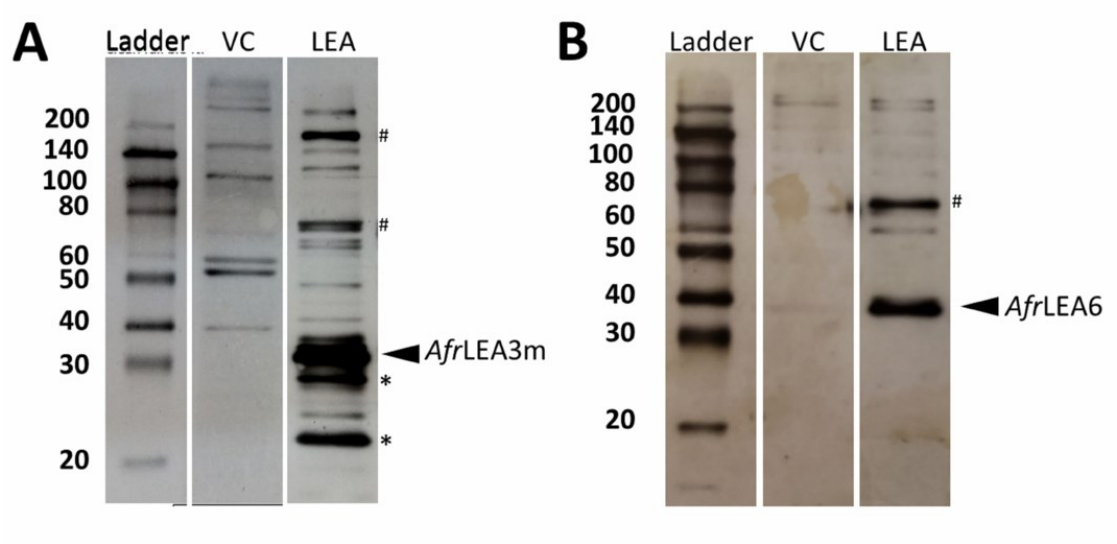

Figure 3

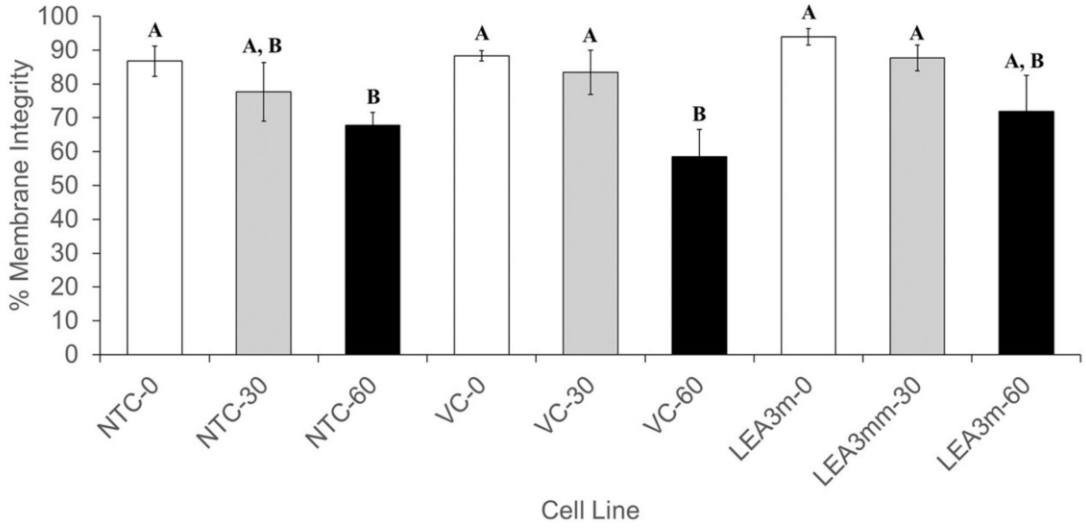
% Membrane Integrity
100
90
80
70
60
50
40
30
20
10
0
A
A, B
B
A
A
B
A
A
A, B
NTC-0
NTC-30
NTC-60
VC-0
VC-30
VC-60
LEA3m-0
LEA3mm-30
LEA3m-60
Cell Line

Figure 4

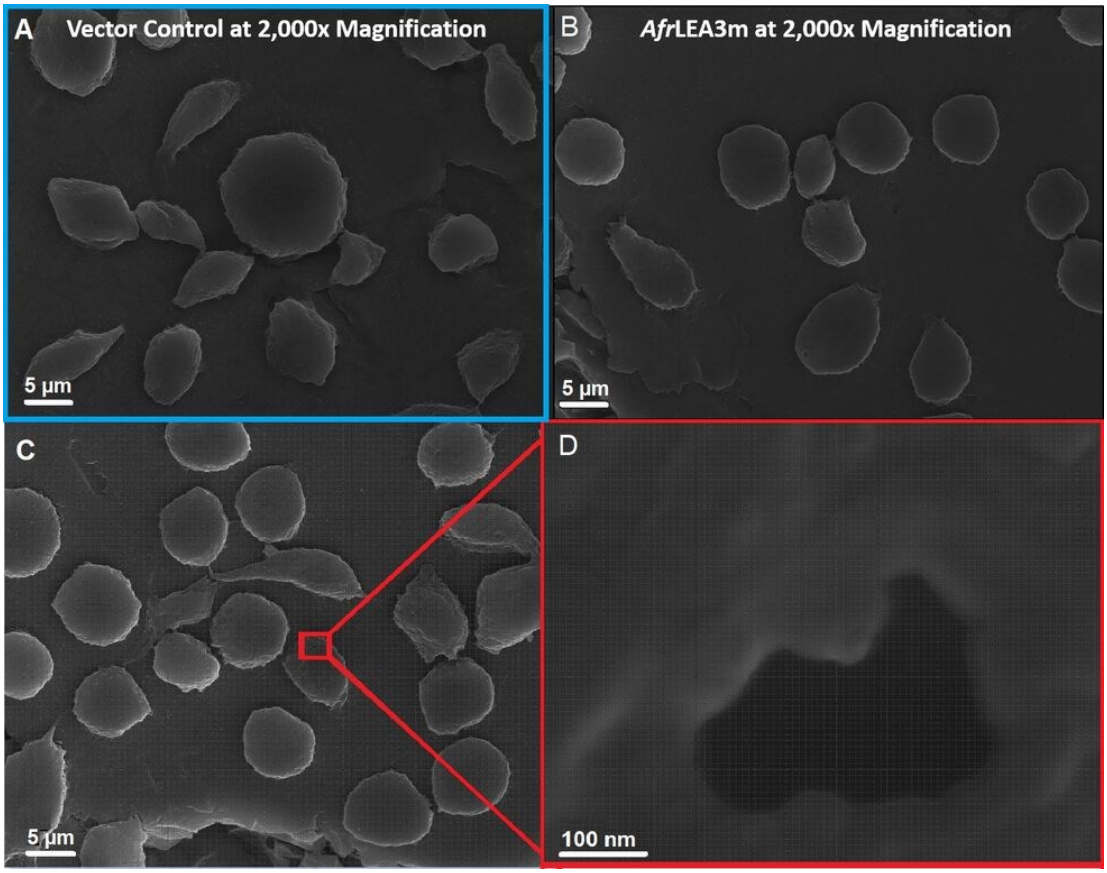
A Vector Control at 2,000x Magnification
5 µm
B AfrLEA3m at 2,000x Magnification
5 µm
C
5 µm
D
100 nm

CHAPTER III

LIQUID-LIQUID PHASE SPEARATION PROMOTES ANIMAL DESICCATION TOLERANCE

SUMMARY

Proteinaceous liquid-liquid phase separation (LLPS) occurs when a polypeptide coalesces into a dense phase to form a liquid droplet (i.e., condensate) in aqueous solution. *In vivo*, functional protein-based condensates are often referred to as 'membraneless organelles,' (MLOs) which have roles in cellular processes ranging from stress responses to the regulation of gene expression. Late Embryogenesis Abundant (LEA) proteins containing seed maturation protein domains (SMP; PF04927) have been linked to storage tolerance of orthodox seeds. The mechanism by which anhydrobiotic longevity is improved is unknown. Interestingly, the brine shrimp *Artemia franciscana* is the only animal known to express such a protein (*Afr*LEA6) in its anhydrobiotic embryos. Ectopic expression of *Afr*LEA6 (AWM11684) in insect cells improves their desiccation tolerance and a fraction of the protein is sequestered into MLOs, while aqueous *Afr*LEA6 raises the viscosity of the cytoplasm. The LLPS of *Afr*LEA6 is driven by the SMP domain while the size of formed MLOs is regulated by a domain predicted to engage in protein binding. *Afr*LEA6 condensates formed *in vitro* selectively incorporate target proteins based on their surface charge, while the cytoplasmic MLOs behave like stress granules *in vivo*. *Afr*LEA6

promotes desiccation tolerance by engaging in two distinct molecular mechanisms: by raising cytoplasmic viscosity at even modest levels of water loss to promote cell integrity during drying and by forming condensates that may act as protective compartments for desiccation-sensitive proteins. Identifying and understanding the molecular mechanisms that govern anhydrobiosis will lead to significant advancements in the way we preserve biological samples.

INTRODUCTION

It is a biological truism that water on Earth appears to be the only solvent suitable for life to occur, although non-aqueous solvents might be available for life to exist elsewhere in the universe (*119-121*). Challenged by variations in water availability, animals have developed a variety of mechanisms to maintain an optimal hydration level, which is considered necessary to maintain organismal homeostasis, ecological competitiveness, and species survival (*122, 123*). In response to the challenge of severe desiccation in terrestrial biotopes, some remarkable organisms have developed mechanisms to survive virtually complete water loss (for review see: (*124*)). Anhydrobiosis is the state of life in which an organism has lost virtually all intracellular water but can resume its biological processes and life cycle upon rehydration. However, the molecular mechanisms governing anhydrobiosis are still largely unknown. Insights gained over several decades of research have demonstrated that there is no singular mechanism that enables anhydrobiosis, but rather that this phenomenon entails a complex array of mechanisms that are carefully orchestrated by certain proteins and osmolytes (*6, 8, 48, 125-127*).

Late embryogenesis abundant (LEA) proteins form a large subgroup of anhydrobiosis-related intrinsically disordered (ARID) proteins and were named for their high expression during late embryogenesis in cotton seeds (*12, 57*). Since their discovery in plants, LEA proteins have also been found in animals belonging to several phyla including Rotifera, Nematoda, and Arthropoda (*6, 54, 58, 62, 128-130*). While classification of LEA proteins *via* bioinformatics has led to multiple organization systems, we will utilize the grouping scheme proposed by Wise et al. (*60*). It is noteworthy that all known animal LEA proteins belong to group 3 with the exception of the brine shrimp *Artemia franciscana*, which also expresses LEA proteins belonging to group 6 (*131*) and group 1 (*132, 133*) in their anhydrobiotic embryos. Interestingly, group 6 LEA proteins have been linked to the prolonged desiccation tolerance of orthodox seeds, but the mechanism(s) by which these proteins confer protection warrants further evaluation (*1, 125, 134*). Here we provide evidence that the seed maturation protein (SMP) domains (PF04927) contained in *Afr*LEA6 (AWM11684) from *A. franciscana* promote liquid-liquid phase separation (LLPS) *in vivo*, and that these condensates can selectively compartmentalize target proteins based on their net surface charge *in vitro*.

Using bioinformatics, *Afr*LEA6 can be organized into three regions: (1) a region of two SMP domains, (2) a proline-glycine spacer, and (3) a domain predicted to engage in protein interactions with unknown targets (*82*). Similar to results obtained on several group 3 LEA proteins from *A. franciscana* (*73*), analysis of circular dichroism data predicts that *Afr*LEA6 compacts into α-helices during desiccation and exists as an intrinsically disordered protein when it is fully hydrated with approximately 90% of its residues involved in random coiling (*98*). A large conformational change and increase in the overall compactness of the protein was also suggested by results obtained *in vivo* by employing

cellular dielectrophoresis, which indicated that ectopically expressed *Afr*LEA6 undergoes a decrease in its hydrodynamic radius in osmotically dehydrated cells (*100*). However, previous bioinformatics analysis of *Afr*LEA6 also identified sequence features associated with proteins known to undergo LLPS to form membraneless organelles (MLOs), which warranted a more thorough evaluation on the role LLPS may play in animal anhydrobiosis (*12, 82, 135, 136*).

MLOs are superstructures formed by driver proteins that undergo LLPS *via* weak multivalent interactions with each other, with scaffolding and client proteins, and/or with nucleic acids (for review see: (*137, 138*)) and form proteinaceous compartments which are not enclosed by a membrane (*139-143*). MLOs may be persistent within the cell or arise in response to some signal and perform a variety of cellular functions including regulating gene expression or partitioning biomolecules. Transient LLPS occurs when the proteins become insoluble in the liquid phase of the cellular milieu or when water becomes unavailable, thereby permitting overall less favorable protein-protein associations. This can occur when the concentration of dissolved ions increases, when other polymers crowd the cellular space, or in response to temperature or pH changes (*144*). Conditions that may promote LLPS of proteins in the cytoplasm of *A. franciscana* are plentiful during the cryptobiotic period when the encysted embryos are released during oviparous reproduction and dehydrate after being washed up at the shoreline of the habitat (*145*). The cytoplasmic concentrations of ions and protein crowding increases during desiccation of the embryo which in turn will promote LLPS of *Afr*LEA6. Consequently, we investigated the behavior of *Afr*LEA6 when ectopically expressed in *Drosophila melanogaster* Kc167 cells under desiccation stress and the behavior of the purified protein in solution. We found that the protein promotes desiccation tolerance *via* two distinct molecular mechanisms: (1) raising

cytoplasmic viscosity at even modest levels of water loss to promote cell integrity during drying and (2) by forming MLOs that may act as protective compartments for desiccation sensitive proteins.

METHODS

Cell Culture and Transgenic Cell Lines

Drosophila melanogaster Kc167 cells were purchased from the Drosophila Genomics Research Center (DGRC; Bloomington, IN). Cells were cultured on 100 mm or 60 mm culture-treated dishes (Corning Incorporated, Corning NY) in Schneider's media (Caisson, USA) supplemented with 10 % heat inactivated fetal bovine serum (FBS) (Atlanta Biologicals, Lawrenceville, GA). Transfections were performed as previously described with the exception that Schneider's media was used in place of M3+BPYE medium (*84*). The pAc5-STABLE2-neo vector was purchased from Addgene (Cambridge, MA). For detailed information on the pAc5-STABLE2-neo vector, please refer to Gonzales et al., 2011 (*97*). Corrected orientation and nucleotide sequence of all genetic constructs were confirmed via sequencing (GenScript, Piscataway, NJ) and immunoblotting was performed as previously described (*100*). The following primers were used to amplify and clone *Afr*LEA6:

1) 5'-CGAGGTACCCAAACATGTCTGAGAATATTGGTCATATTAACATAAATGC-3' and

2) 5'-ATAGCGGCCGCAGTCCATGCGGACATTCCCAATAGTA-3'.

The primers used for a chimeric protein composed of *Afr*LEA6 in frame with GFP were:

1) 5'-CGAGGTACCCAAACATGTCTGAGAATATTGGTCATATTAACATAAATGC-3'

2) 5’-ACTGAGAATTCGTCCATGCGGACATTCCCAATAGTA-3’.

The primers used to amplify a truncated *Afr*LEA6 construct lacking the first SMP domain (Ser2 to Gly56) in frame with mCherry at the c-terminus were:

1) 5’-CGGCGGTACCATGGCCTATGAATCGTGGAATATCAACC-3’ and

2) 5’-ATGTGAATTCGTCCATGCGGACATTCCCAATAGTACTT-3’. The primers used to amplify a truncated *Afr*LEA6 construct lacking both SMP domains (Met1 to Glu140) fused to mCherry at the n-terminus were:

1) 5’-CGGCGCGGCCGCACAGGCCCATTTCAC-3’

2) 5’-ATGTGCGGCCGCAGTCCATGCGGACATTCCCAATAGTA-3’.

The primers used to amplify a truncated *Afr*LEA6 construct lacking the postulated protein-binding domain (Tyr201 to Asp257) in frame with mCherry at the c-terminus were:

1) 5’-CGGCGTACCATGTCTGAGAATATTGGTCAT3’

2) 5’-ATGTGAATTCTGTGGTGATAGAAGGAGGGA-3’.

Confocal Microscopy

All images were taken on a Nikon A1R confocal microscope (Nikon Instruments Inc., Melville, NY) using Kc167 cells plated at approximately 2.0 x 10^6 cells per compartment in a 4-compartment, 35 mm CELLview cell culture dish (Greiner Bio-One, Kremsmünster, Austria). Cells were incubated in 500 µL Schneider’s medium supplemented with 10 % heat inactivated FBS at 25°C for 1 h prior to imaging. In experiments using 1,6-hexanediol (97%; Alfa Aesar, Haverhill, MA) the compound was dissolved in Dulbecco’s PBS (DPBS; VWR, Radnor, PA). Cells were briefly washed with 500 µL DPBS prior to adding 200 µL of hexanediol solution. Cells were imaged for approximately 40 min in presence of the organic compound. Cells were then briefly rinsed

with 500 µL DPBS and an additional 200 µL DPBS was carefully added. After an approximately 40-min recovery period, cells were again subjected to confocal microscopy.

Puromycin (Thermo Fisher Scientific, Waltham, MA) and cycloheximide (VWR, Radnor, PA) stock solutions (100 mg/mL and 2.5 mg/mL, respectively) were prepared fresh in cell culture grade water (VWR, Radnor, PA). The working concentration of puromycin was 25 µg/mL and cycloheximide was 100 µg/mL added to Schneider's media supplemented with 10% heat inactivated FBS. Cells were incubated at 25°C for 2-3 h with the given antibiotic or control media, followed by gentle washing with 200 µL DPBS, and an additional 200 µL of antibiotic-free media was carefully added to keep cells hydrated while imaging. Nile Red, stock solutions were generated by dissolving 1.0 mg/mL of 9-diethylamino-5H-benzo[a]phenoxazin-5-one (Nile Red; TCI America, Portland, OR) in acetone. The working concentration of Nile Red was 0.1 µg/mL dissolved in DPBS. Cells were incubated with 500 µL of dilute Nile Red for 5 min at room temperature. After incubation, the cells were briefly rinsed with 500 µL DPBS and resuspended in a final volume of 200 µL DPBS. To observe Nile Red fluorescence during desiccation in control and *Afr*LEA6 expressing transgenic cells, 150 µL of DPBS was removed and cells were allowed to air-dry while being imaged at varying intervals.

Cell Desiccation and Hyperosmotic Stress Experiments

Desiccation experiments were performed as detailed in Marunde et al., 2013 (*84*). Briefly, Kc167 cells were harvested and washed once with 2-3 mL of Schneider's medium supplemented with 10 % heat inactivated FBS and 200 mM trehalose (Pfanstiehl, Inc., Waukegan, IL) to yield a concentration of 2.0 x 10^7 cells/mL (±2.0 x 10^6 cells/mL) and left on ice for 1 h. Cells suspended in drying medium were placed on 60 mm cell culture dishes

as ten droplets of 15 µL each per plate, and samples were dried over salt isotherms or anhydrous calcium sulfate at 0 %, 35 % ($MgCl_2$), and 75.5% (NaCl) relative humidity (RH). Culture dishes were measured gravimetrically before adding cells, after adding cells, and post-desiccation to calculate gram water per gram dry weight using the dry weight determined after 12 h at 60 °C. After desiccation to various moister contents, samples were hydrated with 3 mL of ice-cold Schneider's media supplemented with 10 % heat inactivated FBS and incubated at 25 °C for 24 h. The number of cells in samples was subsequently enumerated, and percent membrane integrity, relative to non-dried control samples, was determined by trypan blue exclusion. For statistical analysis, significance was set to a p-value ≤ 0.05, and an ANCOVA was performed using XLSTAT (Addinsoft Inc, New York, NY; version 2018.6). Hyperosmotic stress experiments were performed by plating 3-4 x 10^7 cells/mL in Schneider's media supplemented with 10% heat inactivated FBS and either 400 mOsmol/kg of NaCl or sucrose (VWR, Radnor, PA). The osmolarity of culture media was verified by an Osmomat 030 freezing point depression osmometer (Gonotec, Berlin, Germany). Cells were enumerated as described above. For statistical analysis, significance was set to p-value ≤ 0.05, and a one-way ANOVA was performed using XLSTAT (Addinsoft Inc, New York, NY; version 2018.6).

RESULTS

LLPS of *Afr*LEA6 is Governed by the SMP Domains

Kc167 cells concurrently expressing *Afr*LEA6-mCherry and enhanced GFP (eGFP) were imaged using confocal microscopy. The fluorescent proteins eGFP and mCherry both have a mean net surface charge of -5, which is like sGFP-7 used in the *in vitro* experiments above (*146, 147*). *Afr*LEA6 concentrates into spherical structures *in vivo*

which excluded eGFP and ranged in diameter from ~1.0 µm to ~5.0 µm (Fig. 5A, Fig. 10). In addition, *Afr*LEA6 condensates imaged with differential interference contrast (DIC) show a sharp change in the refractive index compared to the surrounding cytosol (Fig. 10, bottom row). A range of 1,6-hexanediol concentrations was used to determine if *Afr*LEA6 undergoes a liquid-liquid phase separation *in vivo* (Fig. 5A). This compound does not interfere with membrane surrounded compartments but is able to interfere with weak intermolecular forces governing LLPS *in vitro* and *in vivo* (*148-152*). Addition of 1,6-hexanediol at 1 % or 2.5 % did not cause significant dispersal of *Afr*LEA6 condensates while immediately after exposure to 5% some cytoplasmic eGFP started to permeate into the *Afr*LEA6 droplets and prolonged exposure to this concentration (≥ 40 min) caused *Afr*LEA6 to fully disperse into the cytosol (Fig. 5A). However, cells exposed to 1,6-hexanediol at 1 % and 2.5 % regain a morphology similar to control cells in 20 min or less after the compound was removed while cells treated with 5% remained intact but lost their ability to attach to the glass-bottom of the culture dish (Fig. 11).

To further investigate the properties of *Afr*LEA6 condensates, puromycin and cycloheximide (CHX) were used to alter the size of the free ribosome pool in the cytoplasm via a decrease or increase in polysome stability, respectively. After a 1 h incubation, the addition of puromycin caused *Afr*LEA6 condensates to become more spherical, larger, and to exclude cytosolic eGFP more effectively compared to untreated controls. In contrast, CHX treatment caused *Afr*LEA6 condensates to become less spherical and more disperse in the cytosol. In the few instances when *Afr*LEA6 droplets were still visible after 2-3 h of exposure to CHX, permeation of eGFP into the MLOs was clearly increased above untreated controls (Fig. 5B).

The overall architecture of *Afr*LEA6 can be bioinformatically described as a composite of three distinct protein regions: two SMP domains, a proline-glycine spacer, and a domain predicted to engage in interactions with other proteins ('protein-binding domain'). In order to characterize the protein domain(s) governing LLPS of *Afr*LEA6 several truncated forms of the protein were expressed in Kc167 cells. A construct lacking both SMP domains did not undergo LLPS, while a construct containing only the protein binding domain formed many smaller MLOs compared to cells expressing the full-length protein (Fig. 6A, B). However, the removal of one SMP domain yielded a construct that was still capable of forming condensates in the cytosol similar to the MLOs observed in cells expressing the full-length protein (Fig. 6C).

_Afr_LEA6 Increases Structural Integrity and Intracellular Viscosity of Kc167 Cells During Desiccation

Kc167 cells expressing *Afr*LEA6 were imaged with DIC confocal microscopy while desiccating on the stage of the microscope (Fig. 7A). There were no apparent morphological differences between cells expressing *Afr*LEA6 and vector control cells (stably transfected with the corresponding vector construct but lacking *Afr*LEA6) when fully hydrated (Fig. 7Aa, Ad). After 30 min of desiccation, control cells flattened out and plasma membranes tended to fuse among neighboring cells. In contrast, cells expressing *Afr*LEA6 retained a height closer to the height observed in fully hydrated cells even after a large amount of bulk water had been removed by evaporation. Surprisingly, fusion of membranes among neighboring cells was not as apparent as in controls (Fig. 7Aa-c). Furthermore, cells that express *Afr*LEA6 and were 'scratched' after 90 min of desiccation

show a sharp contrast in DIC pictures at the points of incisions whereas control cells lack this response (Fig. 7Ac, Af).

To investigate the impact of *Afr*LEA6 on cytoplasmic viscosity during desiccation, control and transgenic Kc167 cells were stained with Nile Red and imaged with confocal microscopy during evaporative water loss (Fig. 7B). Nile Red is a solvatochromatic dye that has been extensively used for staining lipid droplets, but this indicator can also be used to observe viscosity changes in samples (*153-156*). Spherical structures with low Nile Red fluorescence in non-desiccating control cells are likely lipid droplets, while structures exhibiting bright fluorescence in fully hydrated cells expressing *Afr*LEA6 are thought to be MLOs composed of *Afr*LEA6. This assessment was based on the size and distribution of areas with increased fluorescence and the low concentration of Nile Red used, which was about 50-times lower than the concentration that is typically used for staining lipid vesicles *in vivo* (Fig. 7Ba, Bd)(*157*). After 30 minutes of desiccation, there was a robust increase in Nile Red fluorescence throughout cells expressing *Afr*LEA6, and very little change in the fluorescence intensity of control cells (Fig. 7Bb, Be). After 60 minutes of desiccation, there was a steep decline in red fluorescence in cells expressing *Afr*LEA6, while fluorescence intensity for control cells remained unchanged (Fig. 7Bc, Bf).

_Afr_LEA6 Increases Desiccation Tolerance of Kc167 Cells

Kc167 cells expressing *Afr*LEA6 were desiccated at 0 % (Fig. 8A) and 75.5 % RH (Fig 8B) to assess the impact of *Afr*LEA6 on viability post rehydration. Data for non-transfected control cells and cells stably transfected with a vector lacking *Afr*LEA6 were combined, since the response to desiccation was identical for both cell lines. Cells expressing *Afr*LEA6 maintained a higher percent of cells with intact membranes at any

given g H_2O /g dry weight, and faster drying rates observed at 0% RH vs 75.5% RH correlated positively with post-rehydration viability (Fig. 8A, B). For example, the time for control Kc167 cells to reach a moisture content of ~0.5 g H_2O /g dry weight increased from 2.5 h if desiccated at 0 % RH to 8 h if dried at 75.5 % RH and viability dropped by about 25 %. (Fig. 12). In addition to improving desiccation tolerance, expression of *Afr*LEA6 also increased the osmotic-stress tolerance of Kc167 cells to media supplemented with either 400 mOsmol/kg sucrose or NaCl (Fig. 9).

DISCUSSION

This study expands the known functions of proteinaceous condensates to serving a protective role in anhydrobiosis. *In vitro*, *Afr*LEA6 condensates are domain-dependent and selectively exclude eGFP, indicating that the *in vivo* formed structures can be classified as MLOs. *In vivo*, the response of *Afr*LEA6 condensates to chemicals known to effect MLO stability, such as 1,6-hexanediol, cycloheximide, and puromycin, is consistent with the behavior of a stress granule. Furthermore, a fraction of *Afr*LEA6 that remains dissolved in the cytoplasm increases intracellular viscosity significantly above control at modest levels of water loss. A rapid increase in cytoplasmic viscosity during desiccation likely provides physical support to intracellular structures during water loss in anhydrobiotic organisms. *Afr*LEA6 therefore confers protection during desiccation by engaging in two distinct molecular mechanisms in a previously unknown fashion: by forming target selective MLOs that may serve as alternative solvents for desiccation-sensitive proteins and by reinforcing cytoplasmic integrity.

*Afr*LEA6 is the only animal protein known to contain SMP domains and a role of this group 6 LEA protein in anhydrobiosis was previously indicated by bioinformatics and

the observation that the protein is predominantly expressed in desiccation tolerant embryos of *A. franciscana* (*82, 98*). Proteins containing seed maturation domains are common in plants and have been linked to the longevity of orthodox seeds in the desiccated state, but the specific function(s) of the SMP domains remain unclear (*125, 134, 158*). Bioinformatics further indicated that this group 6 protein was capable of undergoing LLPS (*12*) and consequently, we investigated how protein architecture governs the LLPS of *Afr*LEA6 and found that the process was dependent on this domain. This finding may provide further insights into the observation that the group 6 LEA protein Rab28 (At3g22490) from *Arabidopsis thaliana* is selectively incorporated into the nucleolus of transgenic maize roots (*159*). Indeed, it would be highly instructive to know if the SMP domains of other group 6 LEA proteins promote LLPS and how sequence variations within this family of proteins impact the stability of the formed MLOs, their interactions with other preexisting MLOs (e.g. nucleolus, stress granules, p-granules, etc.), and their target selectivity.

Several observations support the hypothesis that the *Afr*LEA6 condensates *in vivo* behave like stress granules. First, a relatively high concentration of 1,6-hexanediol was required to disperse the *Afr*LEA6 condensates or increase their permeability for eGFP. Second, in presence of puromycin the structures formed by *Afr*LEA6 stabilize and become more defined while the MLOs become destabilized in presence of CHX. The compound 1,6-hexanediol dissipates membraneless organelles by interfering with the weak interactions that generally governs LLPS (*141, 148-150, 152*) and a relative high resistance to being dissolved is characteristic for stress granules which may not only be governed by weak interactions (*160*). Furthermore, the results obtained with truncated *Afr*LEA6 constructs suggest that core initiation of the condensate is driven by the SMP domains

while the protein-binding domain may be interacting with client proteins at the periphery of the structure allowing the surrounding shells to fuse similar to stress granules (*160-163*).

A decrease in molar cytoplasmic conductivity in Kc167 cells expressing *Afr*LEA6 during hyperosmotic stress has recently been demonstrated *via* cellular dielectrophoresis (*100*). This observation adds evidence to the assessment that random coil regions of *Afr*LEA6 are folding into defined secondary structures when water levels are reduced, thereby decreasing the hydrodynamic radius of the polypeptide chain and subsequent surface area that can interact with free ions. This interpretation is in line with circular dichroism (CD) data on *Afr*LEA6, where the protein gains substantial amounts of α-helices during desiccation (*98*). However, CD only describes the ratio of secondary structural motifs for a protein that may exist in a wide ensemble of conformations, which may be especially common for intrinsically disordered proteins (IDPs) such as *Afr*LEA6 (*82, 164, 165*). Therefore, it cannot be assumed that all *Afr*LEA6 polypeptides contain the same secondary structure content. For the fraction of *Afr*LEA6 that remains in the dilute phase, folding may allow it to become entangled with other *Afr*LEA6 polypeptides and a wide variety of other proteins, thereby increasing intracellular viscosity by forming weak, cell-wide, promiscuous interactions. A rapid increase in intracellular viscosity via entanglement of *Afr*LEA6 in the diluted phase may act as prelude to entering a glassy state during severe desiccation and counteracts morphological changes early during water loss thereby improving viability (*52, 166*). Structural support conveyed by *Afr*LEA6 may also contribute the increase in the osmotic-stress tolerance observed for Kc167 which agrees with other studies that have suggested a role for group 6 LEA proteins in improving water-stress tolerance (*167, 168*).

CONCLUSIONS

Although we cannot exclude that positively charged proteins may interact with mRNA *in vivo* and allow for mRNA incorporation into *Afr*LEA6 condensates, due to the overall negative charge of *Afr*LEA6 and the negative charge of the ribose-phosphate backbone, the incorporation of nucleic acids into *Afr*LEA6 condensates were not explored here. However, *Afr*LEA6 could significantly hinder cellular development by incorporating various biomolecules, which may explain why the protein is rapidly depleted in the cytoplasm of embryos upon termination of diapause in *A. franciscana* (*98*). Denaturation of globular proteins with hydrophobic cores during desiccation is often irreversible and molecular shielding by LEA proteins is thought to prevent aggregate formation (*68*). LLPS may offer an additional protective mechanism to sterically hindering physical interactions among partially denatured proteins. The physicochemical environment of *Afr*LEA6 condensates might be compatible with the native structure of target proteins, in principle serving as a 'protective solvent' at moderate levels of dehydration and by conformationally locking them through vitrification in the desiccated state. We are just starting to understand the role of LLPS in anhydrobiosis. Furthering our understanding of the mechanisms that govern physiochemical properties of anhydrobiosis-related MLOs offers the exciting possibility to engineer protein-based biomatrices for target-specific biostabilization in the desiccated state.

Figure Legends

Figure 5. *Afr*LEA6 condensates behave like stress granules *in vivo*. A) Cells expressing *Afr*LEA6 tagged with mCherry concurrently with GFP were incubated for 1 h with 0-5 % (w/v) of 1,6-hexanediol in DPBS. B) Cells expressing *Afr*LEA6-mCherry were subjected to either puromycin (25 µg/mL) or cycloheximide (100 µg/mL) for 2-3 h. Lower panels demonstrate the incorporation or exclusion of cytoplasmic eGFP.

Figure 6. *In vitro* liquid-liquid phase separation (LLPS) of *Afr*LEA6 is dependent on the seed maturation (SMP) domain, while condensates fusion is facilitated by the predicted protein binding domain. Kc167 cells expressing truncated versions of *Afr*LEA6 were imaged using confocal microscopy. A) LLPS of *Afr*LEA6 was absent when both SMP domains were removed. B) LLPS of *Afr*LEA6 occurred when the predicted protein binding domain was removed, but condensates fusion was hindered. C) Removing only one of two SMP repeats had no apparent effect on the LLPS of *Afr*LEA6.

Figure 7. *Afr*LEA6 expression increases structural integrity and intracellular viscosity of Kc167 cells during desiccation. A) Kc167 cells expressing *Afr*LEA6 (A, a-c) were desiccated concurrently with vector control cells **(A, d-f)**. Cells expressing *Afr*LEA6 retained more of their native spherical morphology **(A, b)** than vector control cells **(A, e)**. To demonstrate differences in cell height, samples were scratched with a pipette tip **(A, c and f)**. Red arrows indicate areas where the scratch passed through salt deposits, and blue arrows indicate areas where the scratch passed through cells. B) Fresh cells from both lines were incubated with Nile Red at a final concentration of 0.1 µg/mL for 5 min. Increasing red fluorescence is indicative of increasing intracellular viscosity. The decrease in red

fluorescence between **(B, b)** and **(B, c)** may be due to the intracellular environment changing from a viscous gel to a glassy state, where Nile Red starts to precipitate out of solution and become non-fluorescent. Presented images are representative images from one of three separate trials. Scale bars represents 10 μm.

Figure 8. Desiccation tolerance is improved by *Afr*LEA6. Control Kc167 cells (open squares) and cells expressing *Afr*LEA6 (solid circles) were desiccated at a relative humidity of A) 0% and B) 75.5%. Cells expressing *Afr*LEA6 were more desiccation tolerant at either RH (A. ANCOVA: n = 18-28, F-statistic: 68.8 on 2 and 45 DF, p-value < 0.01; B. ANCOVA; n = 26-47; F-statistic: 121.9 on 2 and 72 DF; p-value < 0.01).

Figure 9. *Afr*LEA6 expression increases osmotic stress tolerance towards NaCl and sucrose. Non-transfected control (NTC), vector control (VC), and cells expressing *Afr*LEA6 were cultured for 48 h in culture media supplemented with either +400 mOsmol/kg of NaCl (white bars) or sucrose (gray bars). In both cases, expression of *Afr*LEA6 significantly increased osmotic stress tolerance of Kc167 cells (ANOVA; n = 9-18; p-value < 0.05). Different capital letters denote significant differences between cell lines in response to NaCl, while lower case letters denote significant differences in response to sucrose.

Figure 10: *Afr*LEA6 forms condensates of variable size (~1.0 – 6.0 μm) *in vivo*. Images are representative of several confocal microscopy sessions (top row). Blue arrows indicate faint condensates; fluorescence intensity is lost when using differential interference

contrasting (DIC; what appears to be brightfield; bottom row). Yellow arrows indicate a change in refractive index in the transmitted image.

Figure 11. Kc167 cells morphologically recover after incubation with 1% and 2.5% 1,6-hexanediol, but not 5% 1,6-hexanediol. After imaging, the DPBS supplemented with 1,6-hexanediol was carefully removed, and 200 µL of fresh DBPS was added. After 20 min or less, cells in the 1% and 2.5% 1,6-hexanediol regained control-like morphology (i.e., they lightly attached to the bottom of the plate). The yellow arrow indicates a distortion in the image caused by cells failing to reattach.

Figure 12. The rate of desiccation significantly impacts the desiccation tolerance of Kc167 cells. A) Kc167 cells were desiccated at 0% relative humidity (RH) to gain a baseline understanding of the desiccation tolerance of Kc167 cells. B) Kc167 cells were desiccated at either 0%, 35%, or 75.5% RH. Increasing the RH increased the time it took for Kc167 cells to reach a given gram water per gram dry weight, thereby significantly lowering their viability.

Figures

Figure 5

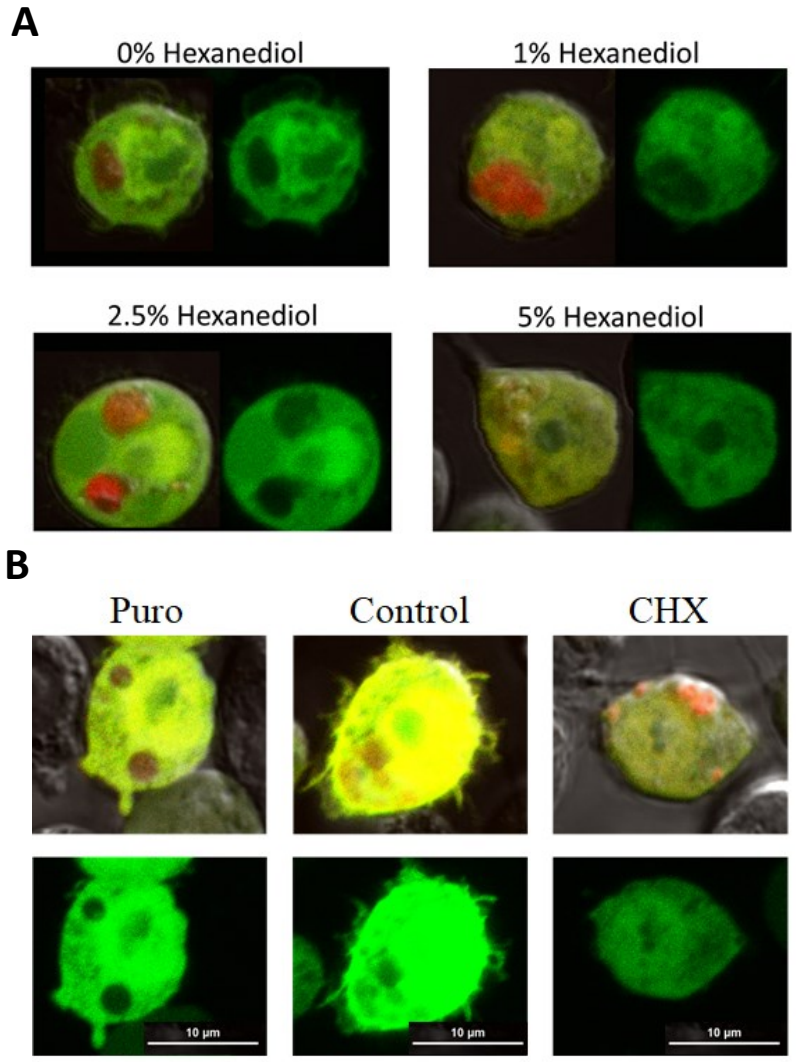

Figure 6

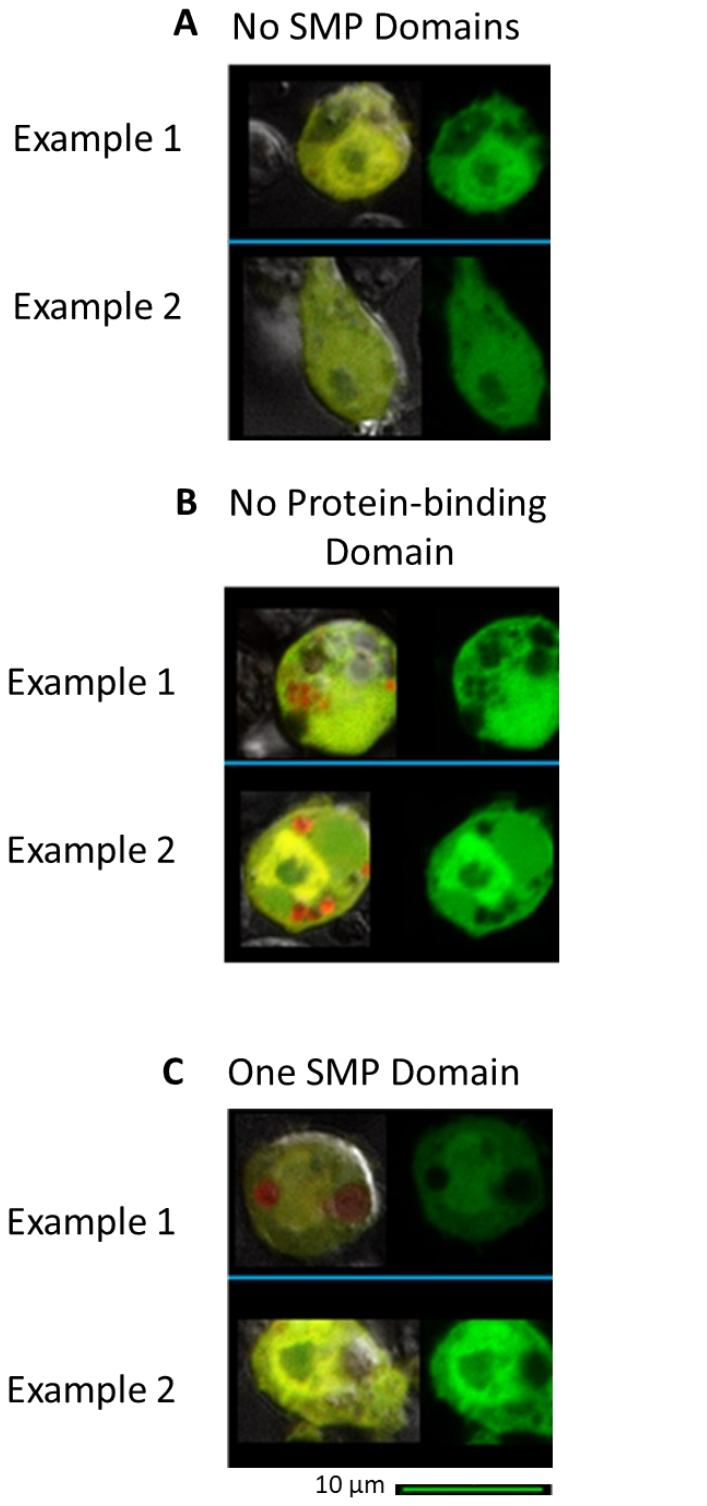
A No SMP Domains
Example 1
Example 2
B No Protein-binding Domain
Example 1
Example 2
C One SMP Domain
Example 1
Example 2
10 µm

Figure 7

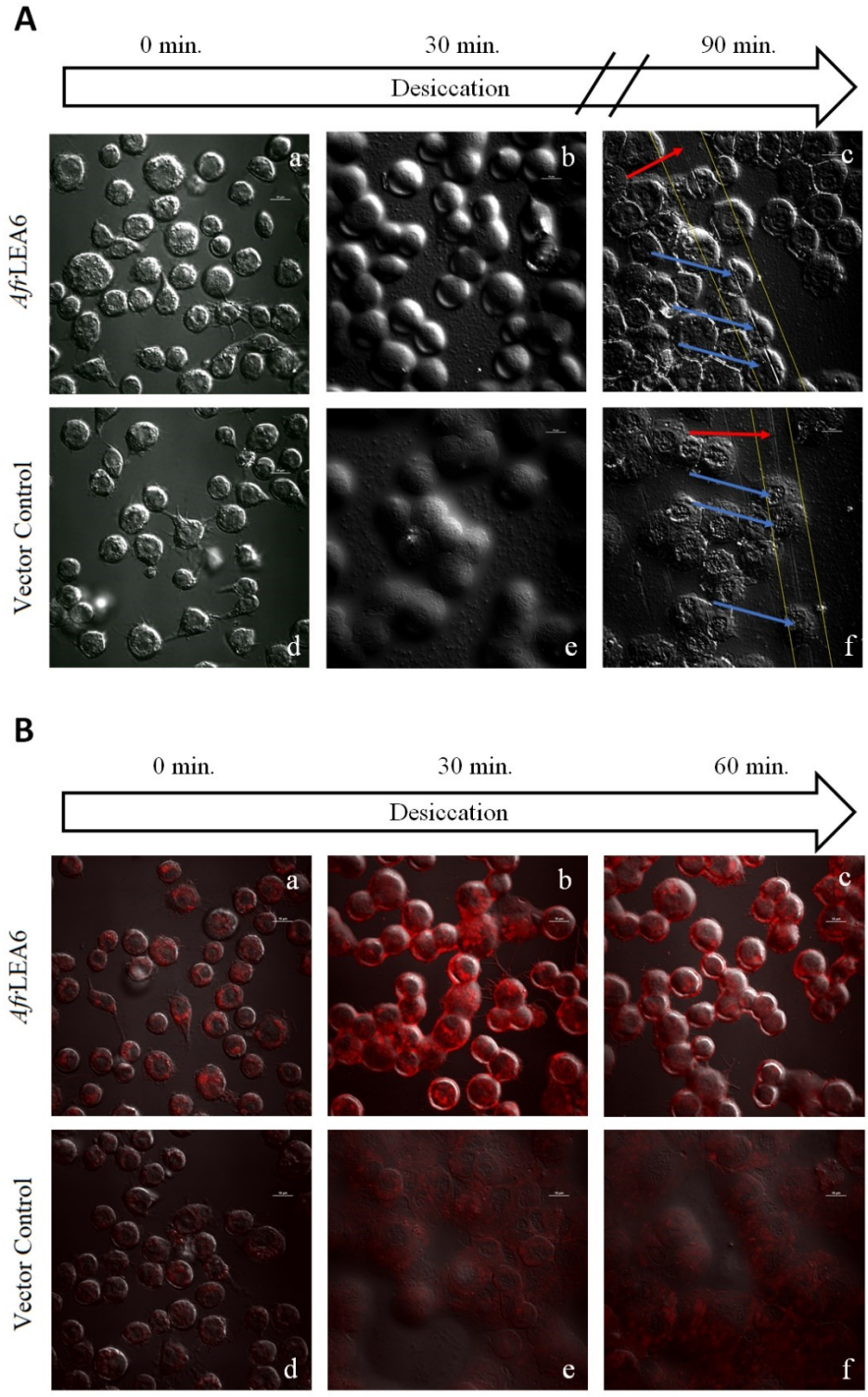

Belott et al. 2020. *PNAS*

Figure 8

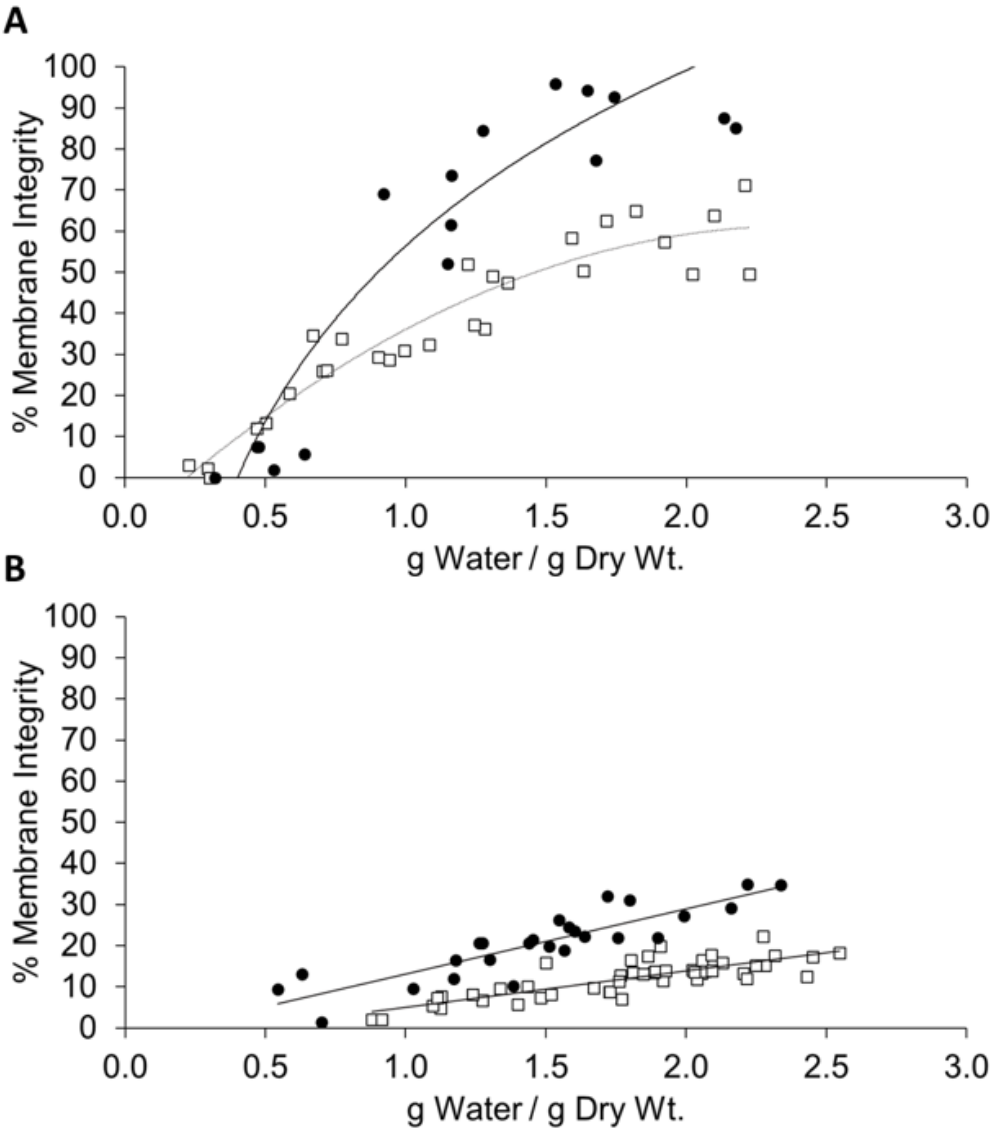
A
% Membrane Integrity
100
90
80
70
60
50
40
30
20
10
0
0.0
0.5
1.0
1.5
2.0
2.5
3.0
g Water / g Dry Wt.
B
% Membrane Integrity
100
90
80
70
60
50
40
30
20
10
0
0.0
0.5
1.0
1.5
2.0
2.5
3.0
g Water / g Dry Wt.

Figure 9

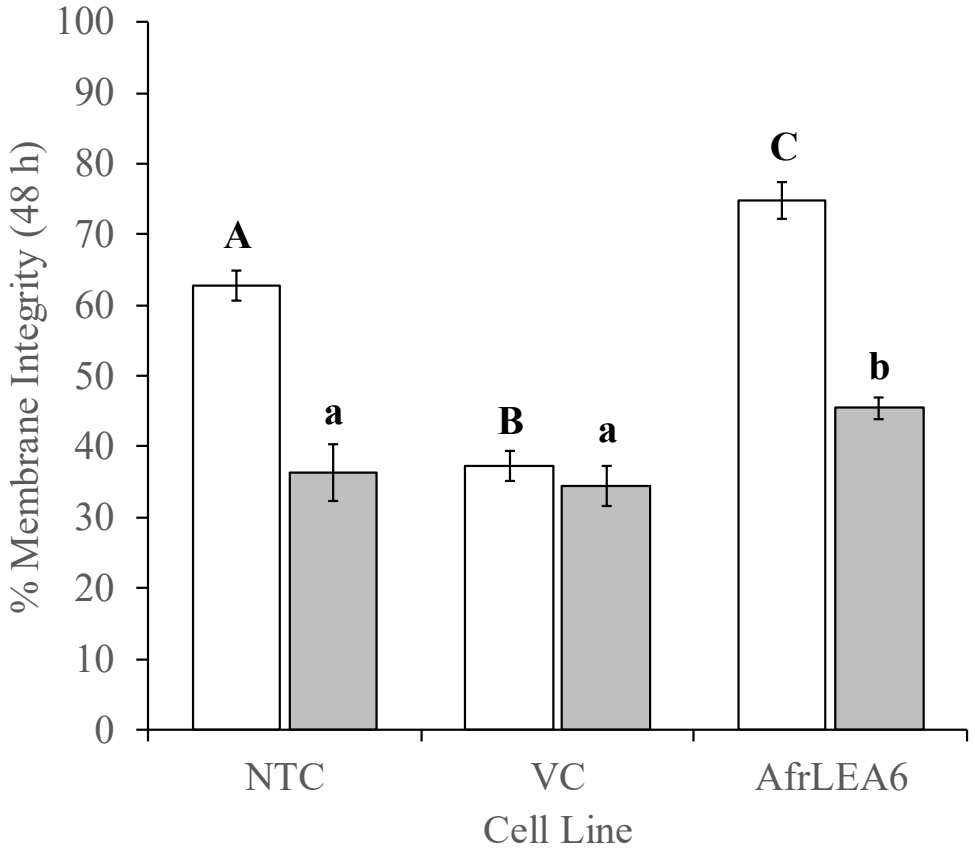
100
90
80
70
60
50
40
30
20
10
0
% Membrane Integrity (48 h)
A
a
B
a
C
b
NTC
VC
AfrLEA6
Cell Line

Figure 10

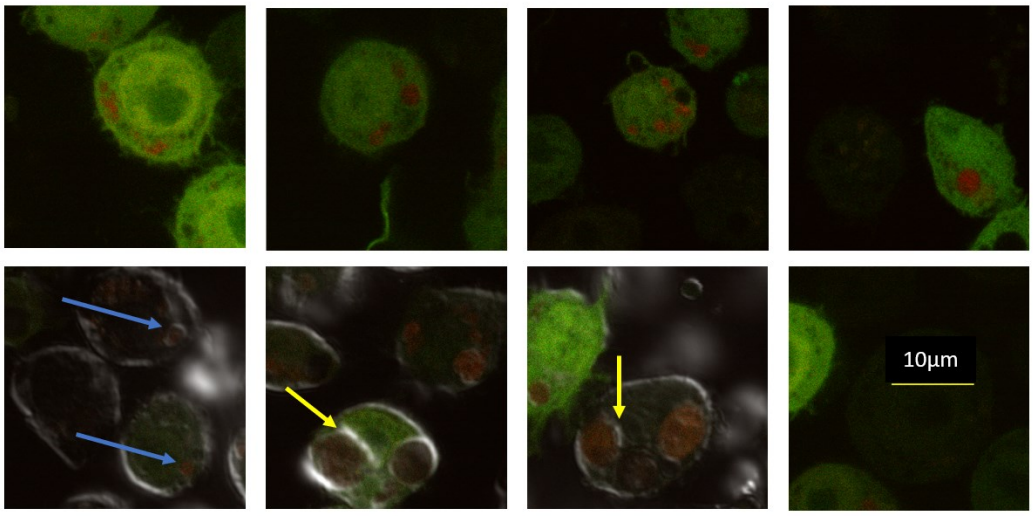

Figure 11

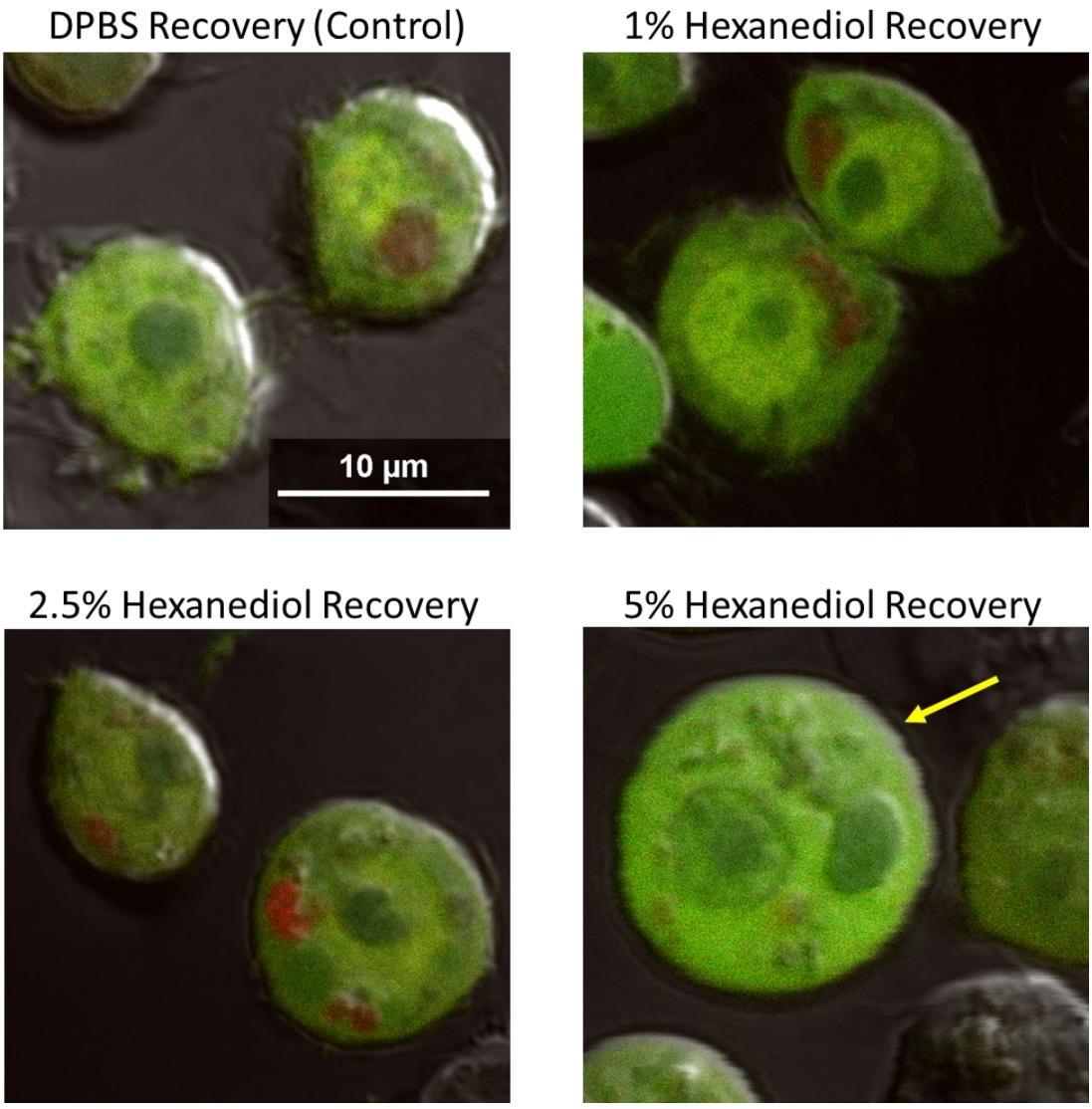
DPBS Recovery (Control)
1% Hexanediol Recovery
10 µm
2.5% Hexanediol Recovery
5% Hexanediol Recovery

Figure 12

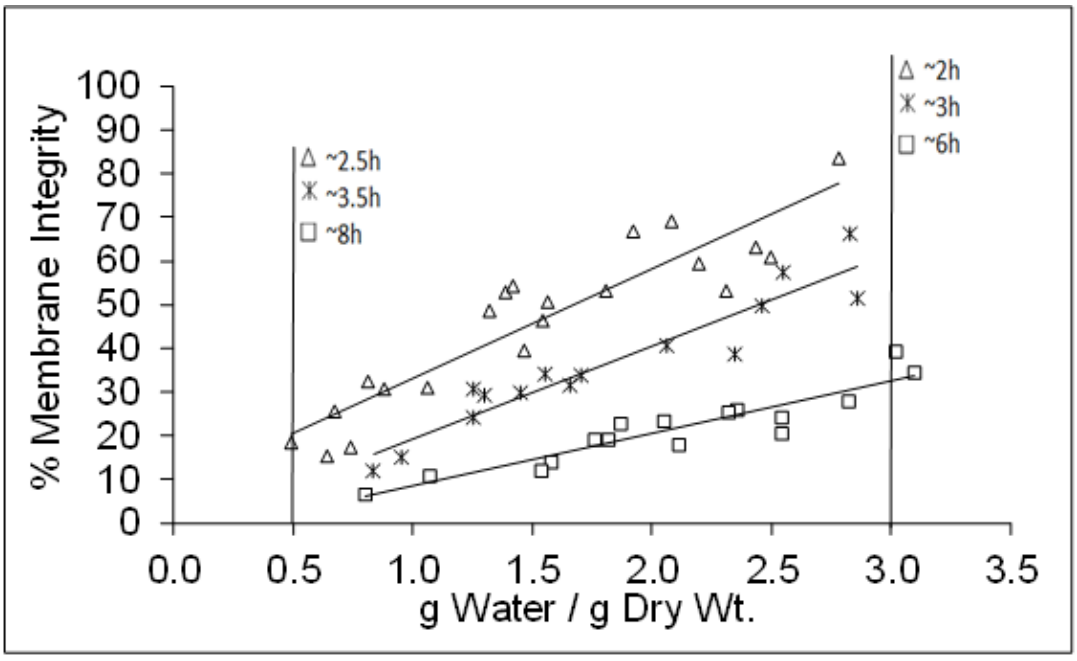

Belott et al. 2020. *PNAS*

CHAPTER IV

CELLULAR REORGANIZATION IN DESICCATION TOLERANT PV11 CELLS

SUMMARY

The larva of *Polypedilum vanderplanki* can enter a desiccation-tolerant, ametabolic state termed anhydrobiosis. Previous studies demonstrated that a preconditioning step with high concentrations of trehalose is crucial to achieving anhydrobiosis in the Pv11 cell line derived from this anhydrobiotic midge, but morphological and physiological changes in membrane-bound and membraneless organelles (MLOs) have remained uncharacterized during preparation for anhydrobiosis, desiccation, and rehydration. Preconditioning consists of culturing cells in a 600 mM trehalose solution supplemented with 10% culture media for 48 h. This low-nutrient, hyperosmotic media causes the formation of large autophagosomes and reduces mitochondrial respiration by 73% compared to not preconditioned controls. Mitochondria in preconditioned cells lose their membrane potential once desiccated but restore a proton motive force upon rehydration. Staining other membrane-bound organelles revealed that the ER and Golgi apparatus fragmented, possibly to reduce shear stress during a water loss. Strikingly, the appearance of the nucleolus immediately upon rehydration and the steady recovery of a previously unknown stress-induced MLO suggests that preconditioned cells have multiple mechanisms to protect physiochemically different MLOs. Lastly, SEM imaging of preconditioned cells revealed increased plasma membrane integrity and resistance to membrane fusion during Belott et al. *Unpublished.*

desiccation. Interestingly, a decrease in the F-actin network observed in preconditioned cells suggests that rearrangements in the cytoskeletal network play an important role in stability during rehydration and desiccation. A better understanding of organelle behavior in anhydrobiotic cells during water loss will foster biotechnological advancements for the long-term storage of biologics at room temperature.

INTRODUCTION

The Pv11 cell line derived from *Polypedilum vanderplanki* is the only anhydrobiotic cell line currently available. Pv11 cells require a 48 h incubation period in 600 mM trehalose solution supplemented with 9% culture media and 1% heat-inactivated FBS (*169*). This media is hyperosmotic and contains very limited nutrients but is required to precondition Pv11 cells for anhydrobiosis. However, the impact this has on membrane-bound and membraneless organelles remains to be unexplored. Elucidating any changes to these compartments will provide additional insights into anhydrobiosis at the cellular level.

Membraneless organelles (MLOs) are proteinaceous liquid-liquid phase separations (LLPSs) that form selective, membraneless compartments that are physiochemically different from their surrounding milieu. *In vivo*, proteinaceous LLPS occurs due to homo- and heterotypic multivalent interactions between an intrinsically disordered protein or region and any wide variety of partners. The resulting entropy favors separation of some fraction of the protein, determined by the critical concentration, from bulk water (for review see: (*137, 138, 170*). It is important to underscore that the physicochemical milieu inside of MLOs can be dramatically different from the properties

of the aqueous cytoplasm, and examples of MLOs behaving more like organic solvents have been reported (*171*).

Recently, the relevance of MLOs in desiccation tolerance was highlighted by the discovery that a group 6 late embryogenesis abundant (LEA) protein, *Afr*LEA6 from *Artemia franciscana,* forms a domain-dependent, stress granule-like MLO when ectopically expressed in *Drosophila melanogaster*, Kc167 cells. Given the wide array of group 3 LEA proteins in *P. vanderplanki*, it is reasonable to hypothesize that one or more of these proteins may also have a role in the formation of stress-induced MLOs, and that one or more play a role in the stabilization of constitutive MLOs (*14, 21, 172*). Therefore, Stabilization of the nucleolus in conjunction with several membrane-bound organelles (i.e. the ER, Golgi, mitochondria, and nucleus) was explored in Pv11 cells during preconditioning, desiccation, and rehydration. Furthermore, the F-actin network and morphology of the plasma membrane was also evaluated. All cellular structures explored underwent significant reorganization during preconditioning, desiccation, and rehydration.

METHODS

Cell Culture and Preconditioning

Pv11 cells were originally derived from embryos of *Polypedilum vanderplanki* from Nigeria and are still being cultured at the National Institute of Agrobiological Sciences, Anhydrobiosis Unit, Tsukuba, Japan (*173*). *Drosophila melanogaster*, Kc167 cells were purchased from the Drosophila Genomics Research Center (DGRC; Bloomington, IN, USA). Both cell lines were cultured in IPL-41 media (Gibco, USA), supplemented with 10% FBS, heat-inactivated at 55°C for 30 min (Atlanta Biologicals,

USA) and 2.6 g/L tryptone phosphate broth (VWR, USA). Pv11 cells were preconditioned by resuspending 3-4 x 10^6 cells/mL in a 600 mM trehalose (Pfanstiehl, Inc., USA) solution supplemented with 10% culture media for 48 h. Kc167 cells did not survive preconditioning.

Confocal Microscopy

Images were taken on either a TCS SP8 Leica confocal microscope (Leica Microsystems, Japan) or a Nikon A1R confocal microscope (Nikon Instruments Inc., Melville, NY). To precondition Pv11 cells for confocal microscopy, 1.5-2 x 10^6 cells/mL were plated in 500 µL/chambers (working volume) of a 4-compartment, 35 mm CELLview cell culture dish (Greiner Bio-One, Austria). All stained samples were exposed to the respective dye for 10 min at room temperature, carefully washed with 200 µL DPBS, and imaged with 200 µL of DPBS to keep the sample hydrated during imaging. Dyes used were Golgi/ER Cytopainter Staining Kit (abcam, USA), MitoView Blue (Biotium, USA), and MitoTracker Deep Red FM (Thermo Fisher Scientific, USA), 9-diethylamino-5H-benzo[a]phenoxazin-5-one (Nile Red; TCI, USA), and CellMask Orange Actin Tracking Stain (Invitrogen, USA). The Golgi/ER Cytopainter Kit and CellMask Orange stains were prepared to their respective manufacturer's instructions. MitoView Blue and MitoTracker Deep Red had final working concentrations of 100 nM and 250 nM in DPBS, respectively. Nile Red was prepared and used as previously described, with a working volume of 0.1 µg/mL (*174*). Sample desiccation was achieved by removing all remaining DPBS and ambiently air drying the samples. Rehydration of samples was achieved in all cases by gently adding 200 µL DPBS into the cell chamber.

Scanning Electron Microscopy (SEM)

A Zeiss Supra 35VP (Zeiss, USA) was used for SEM imaging. Twenty µL of cells at a concentration of 3-4 x 10^6 cells/mL was plated on aluminum stages and allowed to settle for 30 min. Afterwards, excess media was carefully removed, and cells were desiccated at 0% relative humidity in a sealed desiccation chamber over anhydrous calcium sulfate (Drierite, USA) for 2-3 days. Samples were then sputter coated with 19.8 nm gold and immediately imaged.

High Resolution Respirometry

Oxygen flux was measured using an Oxygraph-2k high-resolution respirometer (Oroboros Instruments, Austria). To induce an acute hyperosmotic response, cells were resuspended with culture media supplemented with 200 mM NaCl (VWR, USA). Respiration rates of preconditioned Pv11 cells were measured in preconditioning media. A one-way ANOVA was performed on SigmaPlot (Systat Software Inc.) with significance value of $p < 0.01$.

RESULTS

Preconditioning Causes Substantial Morphological Changes and Inhibits Respiration in Pv11 Cells

Preconditioned Pv11 cells were imaged using confocal microscopy and displayed multiple, large spherical structures (Fig. 13). Despite preconditioning in a low-nutrient media and rehydration in DPBS, viable cells were able to lightly reattach to the plate within 1 h after rehydration. Viable cells can be identified by colocalization of MitoView Blue

(MVB; blue fluorescence) and MitoTracker Deep Red FM (MDR; red fluorescence) in the mitochondria. Both stains localize to the mitochondrion based on membrane potential. MDR staining is well-retained after fixing and the use of detergents, therefore loss of red staining indicates complete loss of mitochondrial inner membrane integrity. MVB is not retained after fixing and loses localization when the mitochondrial membrane potential is lost. However, MVB should accumulate at the mitochondrion if the membrane is reestablished. In control and preconditioned samples, mitochondrial membrane potential is lost upon desiccation, but reestablishes within 30 min post-rehydration in preconditioned cells (Fig. 14). Furthermore, cellular respirometry revealed a striking 73% decrease in cellular respiration of preconditioned Pv11 cells (Fig. 15). To gain further insights if this reduction in respiration of Pv11 cells was regulated or the result of unspecific cellular damage, desiccation sensitive *Drosophila melanogaster* Kc167 cells and Pv11 cells were acutely subjected to culture media supplemented with 200 mM NaCl. The hypertonic media did not decrease respiration of Kc167 significantly (p-value > 0.01). In contrast, hypertonicity significantly decreased respiration in Pv11 cells by 26%. Kc167 cells did not survive preconditioning and could thus not be compared to preconditioned Pv11 cells.

Preconditioning Causes the Nucleolus to Remain Concentrated During Desiccation and Rehydration, while A Stress-induced MLO in the Cytoplasm Reassembles Upon Rehydration

The integrity of the nucleolus, a membraneless organelle within the nucleus, was virtually completely lost in control cells upon desiccation and rehydration in control cells (Fig. 16). However, the nucleolus remained intact (i.e., in the concentrated phase)

Belott et al. *Unpublished.*

throughout desiccation and was immediately visible upon rehydration using differential interference contrasting (DIC). This remained the case in non-viable preconditioned cells, which were identified by their necrotic phenotype. Unexpectedly, a stress-induced MLO was discovered to assemble in preconditioned Pv11 cells (Fig. 17). The MLO displayed red fluorescence, presumably due to off-staining from the ER dye. This structure was confirmed to be a MLO due to its capacity to disassemble during desiccation and quickly reassemble upon rehydration (Fig. 18). The manufacturer of the Cytopainter Kit declined to disclose information about the stains. Therefore, it remains unknown why off-staining occurred in the MLO and the reason behind its red emission.

Preconditioning Causes ER, Golgi, and Nuclear Swelling and ER and Golgi Fragmentation

The ER and Golgi form long networks in Pv11 cells cultured in standard culture media, often spanning long axon-like structures at one or both polar ends of the cell (Fig. 13A and 21). Preconditioned cells have only punctuated ER and Golgi sections (Fig. 17B). Furthermore, the ER, Golgi, nucleus, and cytoplasm swelled during imaging. Swelling of the cell and organelles is almost certainly due to preconditioned cells equilibrating with trehalose in the preconditioning media, and subsequent staining and imaging in relatively hypotonic solutions. Attempts made to stain the cells in culture medium or preconditioning media resulted in necrosis, while adding 300 mM trehalose to the manufacture's solution resulted in poor staining and necrosis in many cells. The manufacture declined to disclose information about the staining solution, so it is unknown why the stains became cytotoxic when resuspended in media or when trehalose was added to the resuspension solution.

Belott et al. *Unpublished.*

Nevertheless, the ER, Golgi, MLO, and nucleus recovered within 60 min after rehydration in preconditioned cells stained with the manufacture's staining solution and imaged in DPBS.

Preconditioning Causes F-actin Reorganization and Increased Plasma Membrane Structural Integrity During Desiccation

The F-actin network was stained in Pv11 cells (Fig. 19). Importantly, the stain used does not stain G-actin (i.e., unpolymerized actin). In control cells, the F-actin network can be seen in the cell body and traveling along the axon-like structures. However, little to no F-actin structures were visible in preconditioned cells. Desiccation increased the visibility of the network in control cells. After 30 min of desiccation, there was a sharp increase in red fluorescence in both samples that was likely due to the stain beginning to precipitate. Scanning electron microscopy (SEM) revealed a rounder morphology in most desiccated preconditioned cells and a substantially reduction of plasma membrane fusion between adjacent cells (Fig. 20). Furthermore, the morphological changes observed during desiccation did not appear to be due to an increase in intracellular viscosity, as indicated by the similar Nile Red fluorescence in control and preconditioned samples (Fig. 22).

DISCUSSION

This study expands our understanding of how membrane-bound and membraneless organelles (MLOs) respond morphologically and physiologically during anhydrobiosis in Pv11 cells derived from the desiccation tolerant midge, *P. vanderplanki*. All cellular structures explored underwent significant reorganization during preconditioning,

desiccation, and rehydration. Preconditioning caused a striking 73% decrease in respiration, the formation of structures that may be autophagosomes, the assembly of a stress-induced MLO, and significant depolymerization of the F-actin network. Desiccation caused loss of mitochondria membrane potential and disassembly of the stress-induced MLO. In addition, SEM revealed an increase in plasma membrane integrity and resistance to fusion with adjacent plasma membranes. Rehydration revealed the reestablishment of the mitochondrial membrane potential, reassembly of the stress-induced MLO, that the nucleolus remains in a concentrated phase (i.e. does not require reassembly), and that the ER, Golgi, and nucleus were able to recover. This complex orchestration of morphological and physiological changes observed in Pv11 cells provided insights into the desiccation tolerance at the cellular level. However, confirmation of these observations in the animal model is essential to fully differentiate if these changes are truly related to anhydrobiosis in *P. vanderplanki*, or if they are a result of the preconditioning technique. Regardless, these results may prove useful for the preservation of biologics at room temperature for extended periods of time.

The Pv11 cell line, which cellular type remained unknown, may be neuronal in origin based on axon-like structures that contain a dense ER network and Golgi outposts (*21, 175*). Pv11 cells require 48 h of preconditioning in a low-nutrient media containing 600 mM trehalose to achieve anhydrobiosis (*169*). Preconditioning caused the formation of multiple large, spherical structures in Pv11 cells. These structures are hypothesized to be autophagosomes, based on their size, numbers, and low nutrient content of the preconditioning media (*176*). Furthermore, the accumulation of trehalose may also have a role in initiating autophagy (*177*). Autophagocytosis, or autophagy is the process by which

Belott et al. *Unpublished.*

cells can recycle damaged or unnecessary cellular components, especially during stress (*178*). As was suggested for yeast and at least one resurrection plant, autophagy may improve desiccation tolerance by removing desiccation-sensitive proteins that are not required during desiccation and recovery after rehydration (*177, 179*).

Considering the nutrient limitations of the preconditioning media, high-resolution mitochondrial respiration was explored. Preconditioned Pv11 cells showed a striking 73% decrease in respiration rates compared to untreated cells, indicating metabolic downregulation. Reducing and detoxifying reactive oxygen species (ROS) is a common strategy employed by *P. vanderplanki* and other anhydrobiotic animals and has been shown to be necessary for tardigrades to maintain an anhydrobiotic state beyond a relatively short period of time (*3, 14, 15, 20, 23-29*). A significant reduction in cellular respiration may contribute to an overall reduction in ROS production in preconditioned Pv11 cells during desiccation and rehydration, although additional experiments directly measuring ROS production are necessary to elaborate on these results. In addition, it was discovered that mitochondria in Pv11 cells rapidly reduce respiration by 26% when acutely challenged with media supplemented with 200 mM NaCl to induce hyperosmotic stress. In contrast, desiccation-sensitive *D. melanogaster* Kc167 cells, showed only a non-significant 8.5% decrease in respiration in response to the increase in osmolarity. These data suggest that inhibition of respiration in Pv11 cells was due to downregulation and not necessarily stress-induced organelle damage. This is in agreement with other studies demonstrating that anhydrobiosis-related genes in *P. vanderplanki* larva can be regulated with hyperosmotic stress (*37, 54, 173, 180*). However, further study is required before a link between respiration inhibition and hyperosmotic stress can be substantiated. Nevertheless, the

integrity of the inner mitochondria membrane of preconditioned Pv11 cells was maintained and, remarkably, mitochondria in viable cells were able to reestablish their membrane potential within 30 minutes following rehydration.

While imaging mitochondria in rehydrated control and preconditioned Pv11 cells, the observation was made that the nucleolus is well-protected in preconditioned Pv11 cells and did not require any detectable time to reassemble after rehydration. The nucleolus is a large RNA and protein-based membraneless organelle within the nucleus and primarily functions as the catalytic center for ribosome biogenesis (*181*). Fascinatingly, the nucleolus is also well-preserved in preconditioned cells that were not viable upon rehydration. In contrast, the nucleolus in non-preconditioned cells was not visible after desiccation and rehydration, suggesting that the physicochemical properties that govern the LLPS of this organelle have changed. Indeed, it would be instructive to know what role, if any, trehalose and LEA proteins have in preserving the nucleolus, and if they have a particular role in allowing the nucleolus to maintain a concentrated phase throughout desiccation and rehydration.

Based on the observation that the inner mitochondrial membrane was protected in preconditioned cells, we sought to explore the fate of other membrane-bound organelles. The swelling observed for the nucleus, ER, and Golgi apparatus suggests that trehalose is being brought into these organelles and may play a role in their stabilization, as well as the stabilization of the sub-organelle components within them (e.g., the nucleolus, proteins, etc.). Swelling of the ER and Golgi apparatus also implies the existence of organelle-specific trehalose transporters since trehalose is membrane impermeant in absence of a carrier protein (*169, 182*). In addition to swelling, the ER and Golgi were observed to be

Belott et al. *Unpublished.*

fragmented. This is hypothesized to reduce sheer stress on these organelles during water loss and will require further exploration.

The concurrent swelling of the nucleus and formation of a more euchromatin-like state suggests that the physicochemical environment inside the nucleus changes post-preconditioning, which concurs with the hypothesis that a change in the nuclear environment aids in protecting the nucleolus during desiccation. However, and in contrast to the nucleolus that remained intact immediately upon rehydration, the stress-induced MLO that forms in response to trehalose preconditioning takes approximately 1 h after rehydration to fully reassemble, suggesting different mechanisms by which Pv11 cells preserve differently structured MLOs. Furthermore, the stress-induced MLO was virtually always singular in number and associated with the nuclear envelope, even after rehydration and reassembly, suggesting organizational importance and perhaps communication with the nucleus (*183*).

Lastly, insights were gained into how the cytoskeletal network and cell morphology are affected during preconditioning, desiccation, and rehydration in Pv11 cells. Filamentous actin (F-actin) transitions heavily into globular actin (G-actin) during preconditioning, suggesting that preconditioned cells relax the rigidity of their cytoskeletal network to accommodate changes in cellular volume associated with desiccation and rehydration. These data were supplemented with SEM data of desiccated Pv11 cell, revealing that many preconditioned cells displayed a round morphology instead of the spindle-like morphology of control cells. Preconditioned cells also exhibited substantially less plasma membrane fusion to adjacent cells. However, changes in cell shape did not appear to be due to intracellular viscosity changes, as both preconditioned and control cells

had similar levels of relative Nile Red fluorescent intensities during desiccation (*153-156, 174*). Endogenous LEA-like proteins in Pv11 cells have been reported to localize to the plasma membrane, which may suggest that Pv11 cells do not require increasing intracellular viscosity to reinforce their cytoskeletal network to maintain plasma membrane integrity, as was hypothesized for Kc167 cells ectopically expressing *Afr*LEA6 (*13, 174*).

CONCLUSION

These data offer an exciting window into the morphological and physiological changes that occur in the only available anhydrobiotic cell line as it undergoes preconditioning, desiccation, and rehydration (*169, 173*). These changes ranged from altered organelle morphology and physiology to the assembly of a stress-induced MLO. However, it is important to note that the observations made in Pv11 cells may not necessarily reflect anhydrobiosis in the animal model and may be a result of stress induced by the preconditioning treatment. Nevertheless, these data may offer guidance for future experiments in the animal model and suggest that MLOs in preconditioned Pv11 cells may be a useful model for engineering artificial LLPS to preserve desiccation-sensitive biological materials.

Belott et al. *Unpublished.*

Figure Legends

Figure 13. Preconditioning in 600 mM trehalose supplemented with only 10% culture media for 48 h is required for Pv11 cells to successfully enter and exit anhydrobiosis. Cells were stained with 1 μM MitoView Blue (MVB) and 0.25 μM Mitotracker Deep Red FM (DR). Both dyes localize to mitochondria based on membrane potential. MVB is released upon loss of membrane potential, while DR becomes fixed inside the mitochondria. Therefore, MVB was used to monitor the loss of mitochondrial membrane potential and DR was an indicator of mitochondria obliteration. Different cells are viewed in each image.

Figure 14. Preconditioning is required for the inner mitochondrial membrane to remain intact after rehydration and to restore a membrane potential. Cells were stained with 1 μM MitoView Blue (MVB) and 0.25 μM Mitotracker Deep Red FM (DR). Both dyes localize to mitochondria based on membrane potential. MVB is released upon loss of membrane potential, while DR becomes membrane-impermeable upon localization. Therefore, MVB was used to monitor changes in mitochondrial membrane potential and DR becomes fixed inside the mitochondria upon localization. Fluorescence intensities are not comparable among images. Different cells are viewed in each image.

Figure 15. Preconditioning significantly reduce mitochondrial respiration in Pv11 cells. Water-stress sensitive Kc167 cells (*D. melanogaster*) were used for comparison to an acute hypertonic (+200 mM NaCl) stress response. Kc167 cells did not survive the preconditioning treatment. *Denotes significance (p-value ≤ 0.01).

Belott et al. *Unpublished.*

Figure 16. The nucleolus, a membraneless organelle, is preserved after preconditioning, desiccation, and rehydration in both viable and necrotic Pv11 cells. The nucleoli in preconditioned cells were visible immediately upon rehydration. Non-preconditioned cells lacked a visible nucleolus or contained a morphologically altered nucleolus compared to viable controls.

Figure 17. Preconditioning causes Golgi (green) and ER (orange) fragmentation and swelling, euchromatin formation (blue) and nuclear swelling, and the formation of a stress-induced MLO. Pv11 cells cultured in routine media displayed vast ER and Golgi networks, but normally not on the same z-plane as the nucleus. The MLO that formed in response to was generally singular and in contact with the nucleus.

Figure 18. Preincubation is required for ER, Golgi, and nuclear envelope recovery after rehydration. ER (orange) and Golgi (green) recovery was visible in Pv11 cells preconditioned with trehalose after 1 h. The lack of a visible ER and Golgi structures prior to 1 h is thought to be caused by desiccation damaging the dyes' targets, as is the case in necrotic cells. The MLO (red) observed in the hydrated state dissociated upon desiccation, but reforms over 1 h after rehydration and retains its proximity to the nucleus. The scale bar represents 10 μM.

Figure 19. Preconditioning causes the F-actin network (red) to disassemble. CellMask Orange Actin Tracking Stain was used to stain the F-actin network in preconditioned and

control Pv11 cells. Importantly, G-actin (monomeric actin) is not targeted. Fluorescence intensities are comparable among all images. The scale bar represents 10 μM.

Figure 20. Scanning electron microscopy (SEM) reveals plasma membrane stabilization in Pv11 cells. Top images offer a broad view of control and preconditioned samples, while bottom images are representative images of membrane fusion and morphological changes. Extracellular trehalose was removed from preconditioned cells by rinsing with DPBS before plating and subsequent desiccation.

Figure 21. Pv11 cells may be neuronal in origin. Pv11 cells in culture exhibit axon-like structures at one or both polar ends of their cell body. These structures contain a long and intricate ER network (orange) that appear to be accompanied by Golgi outposts (green nodes). The scale bar represents 10 μM.

Figure 22. Intracellular viscosity during desiccation is not significantly increased due to preconditioning. Nile Red (red), a salvatochromatic dye, revealed no significant increase in intracellular viscosity between control and preconditioned Pv11 cells during desiccation. The fluorescence is relative among all images. Cells in the rehydrated samples are different cells. The scale bar represents 10 μM.

Belott et al. *Unpublished.*

Figure 13

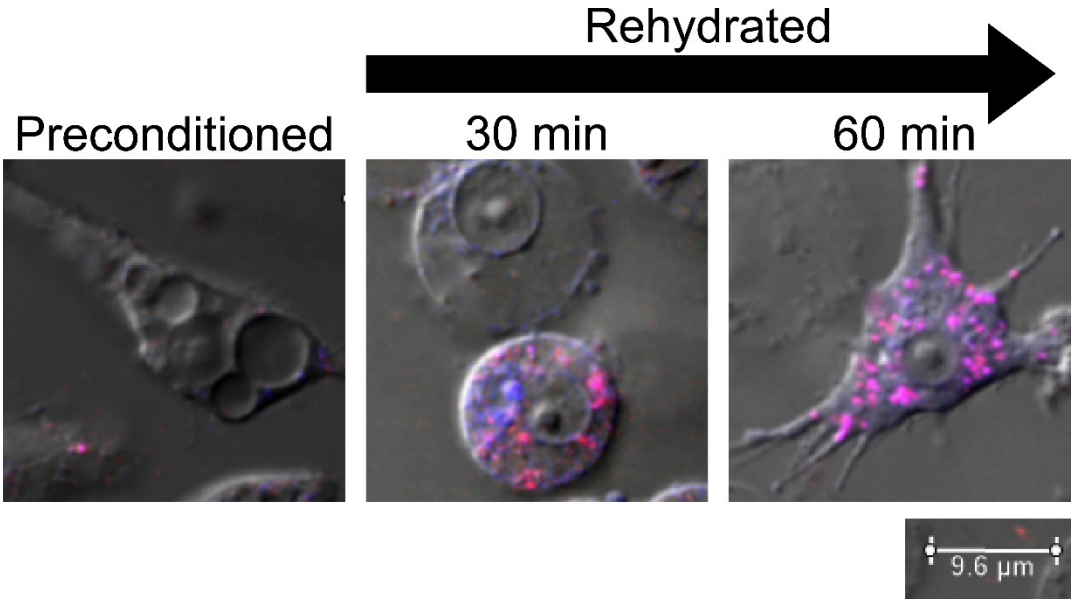

Belott et al. *Unpublished.*

Figure 14

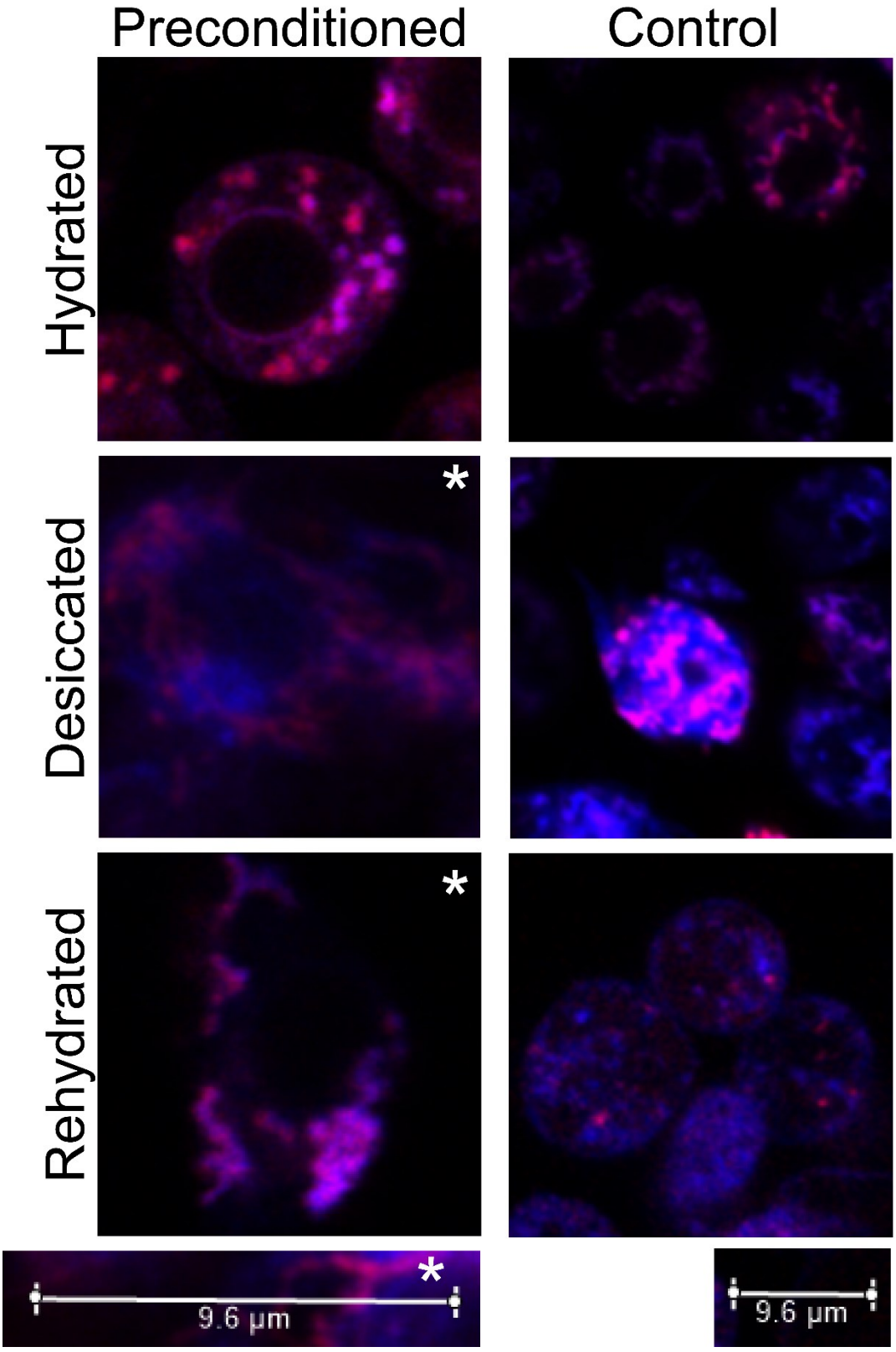

Belott et al. *Unpublished.*

Figure 15

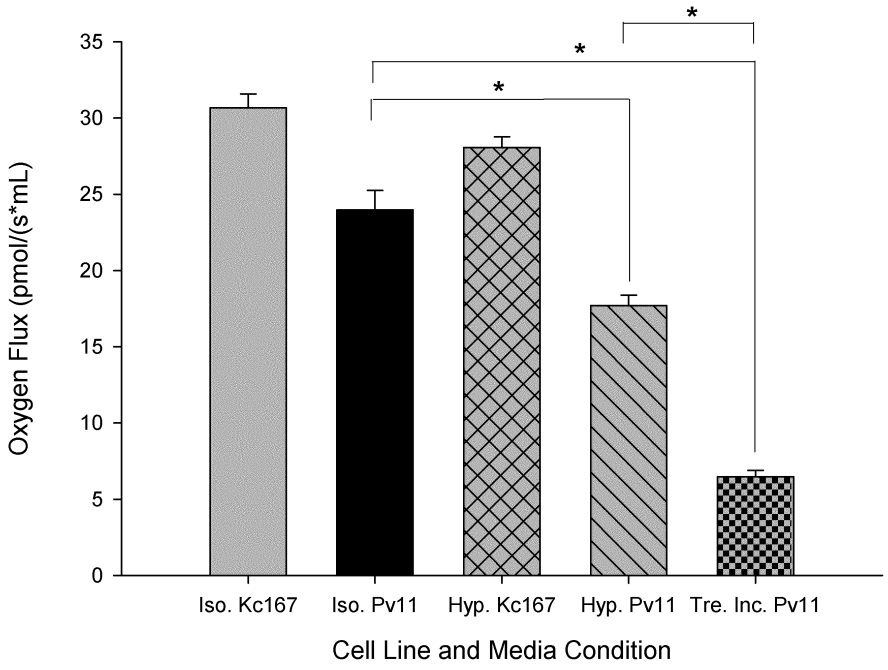

Belott et al. *Unpublished.*

Figure 16

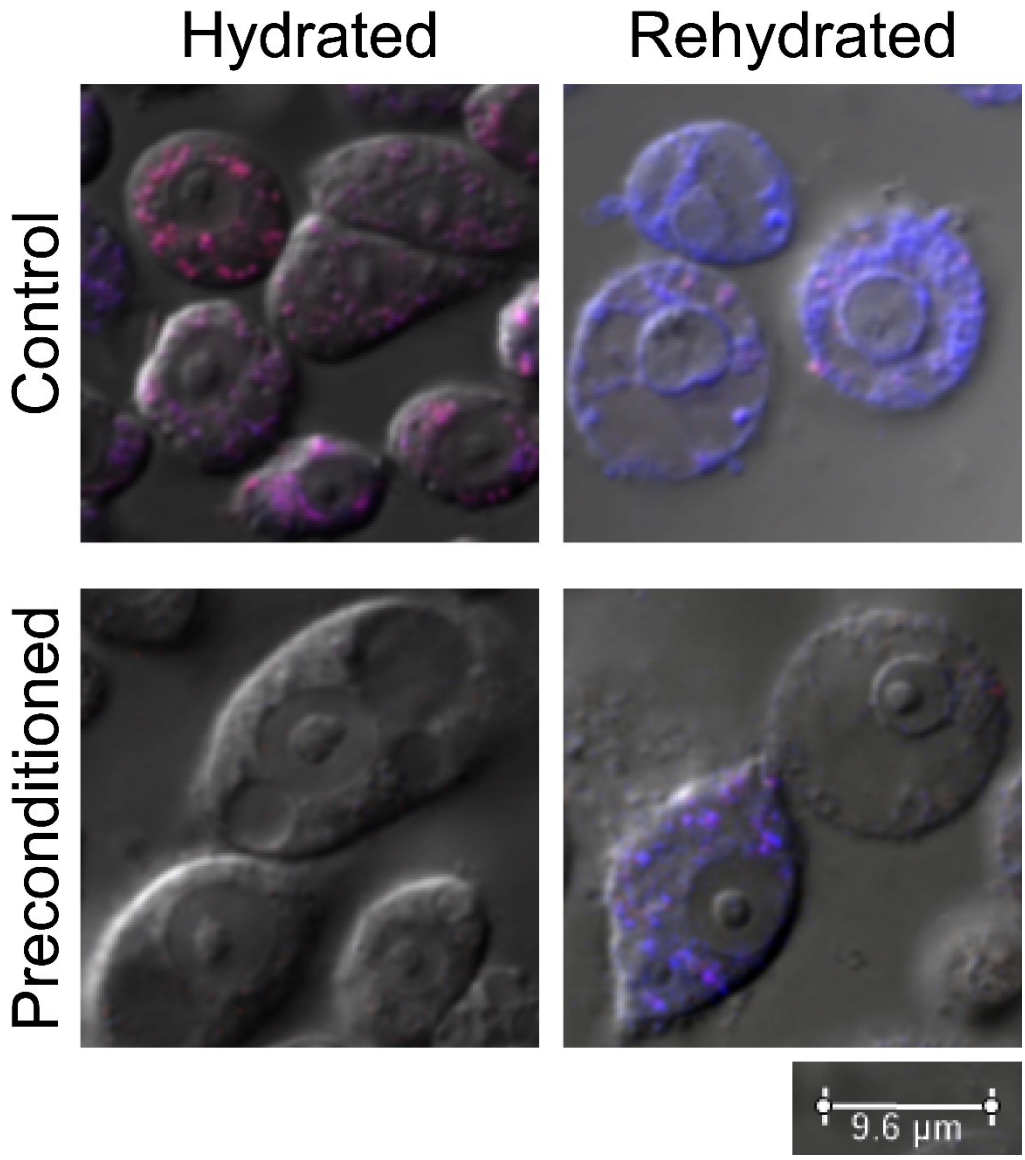

Belott et al. *Unpublished.*

Figure 17

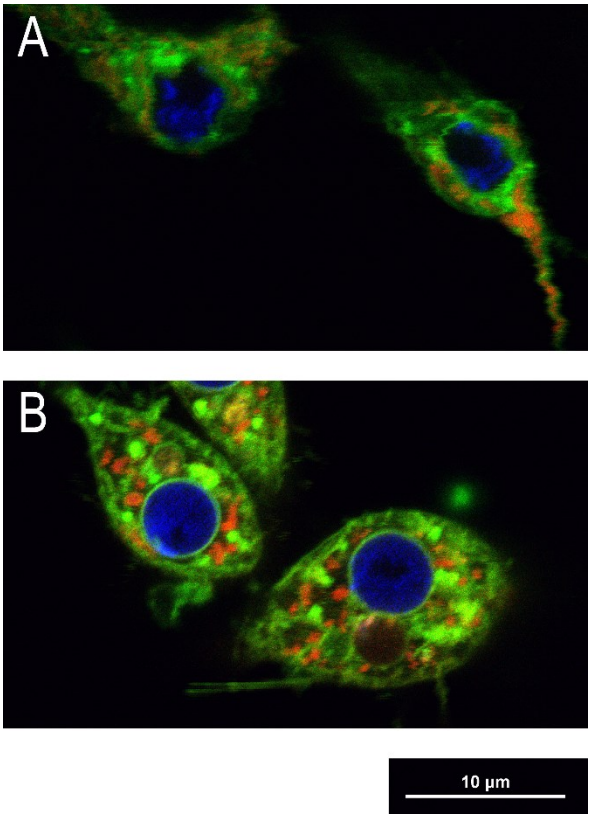

Belott et al. *Unpublished.*

Figure 18

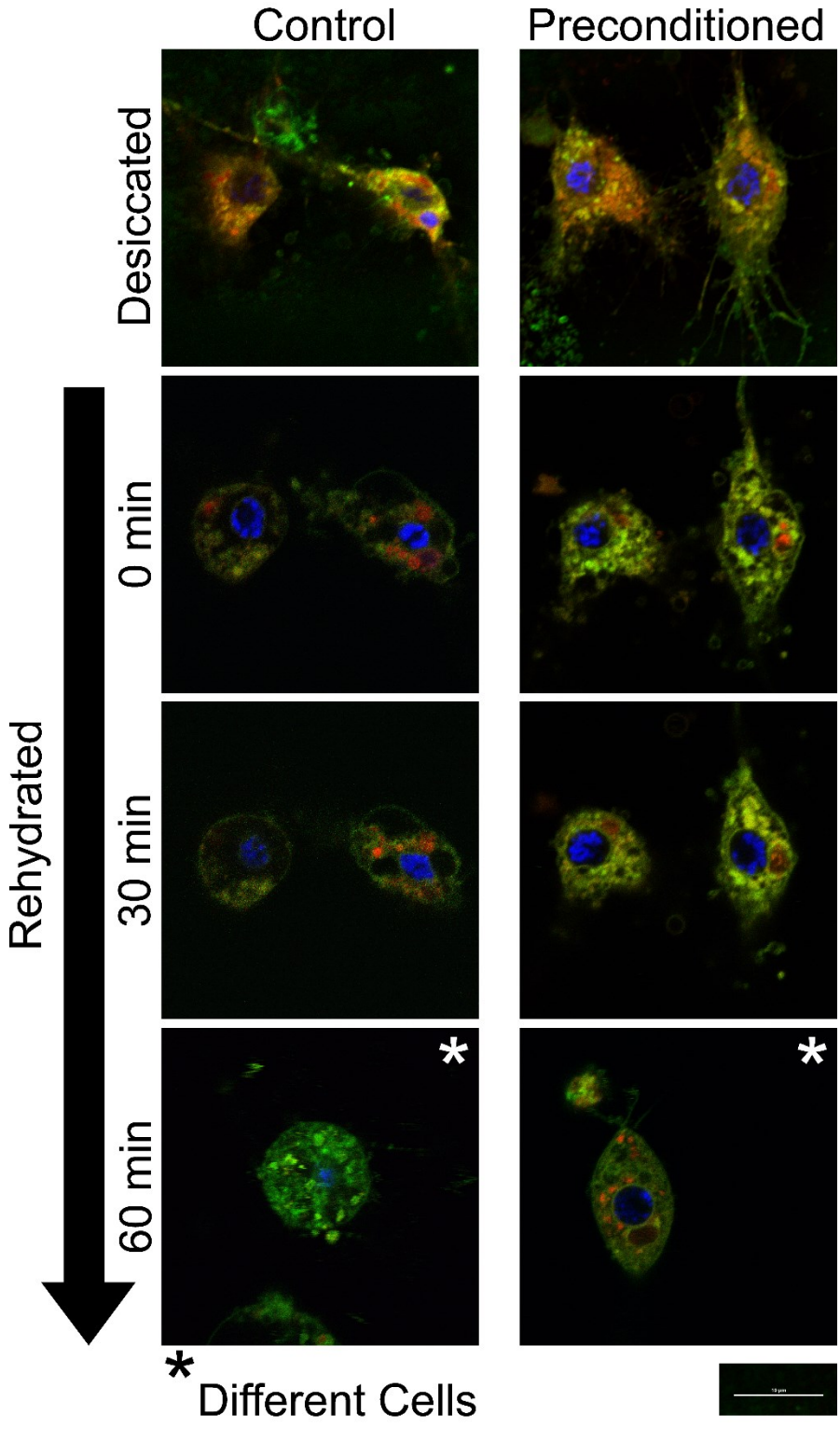

Belott et al. *Unpublished.*

Figure 19

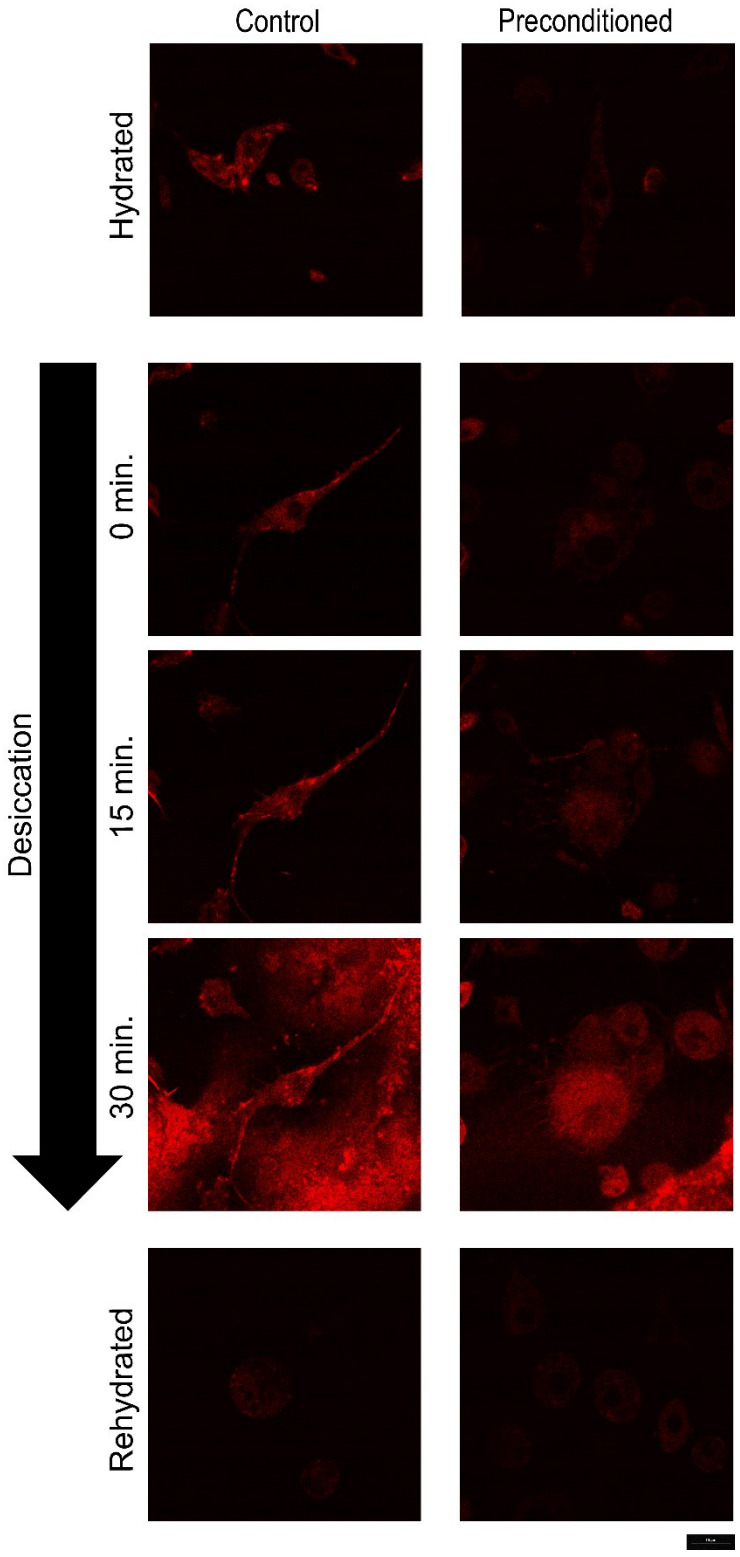

Belott et al. *Unpublished.*

Figure 20

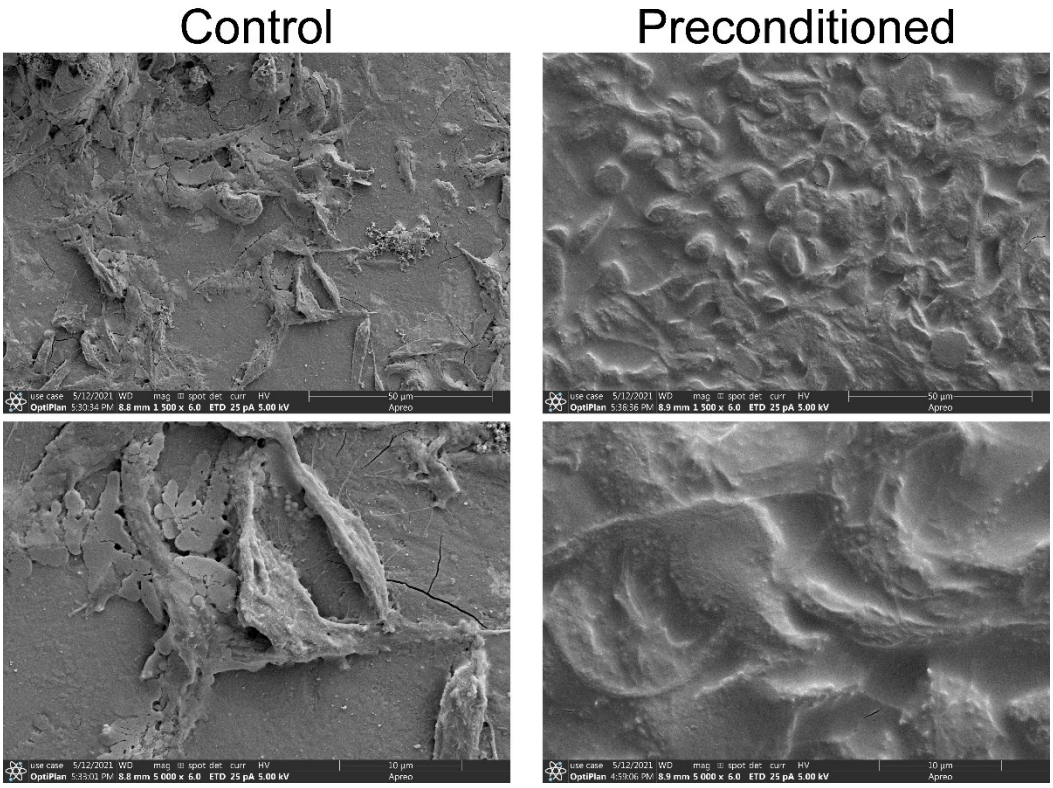

Belott et al. *Unpublished.*

Figure 21

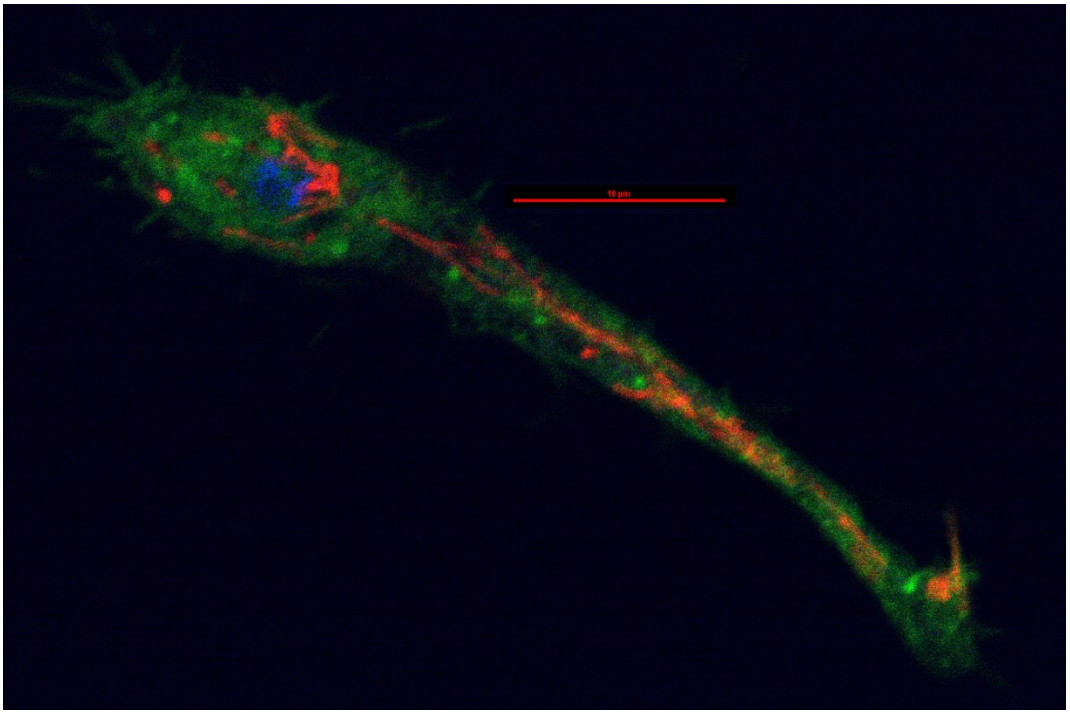

Belott et al. *Unpublished.*

Figure 22

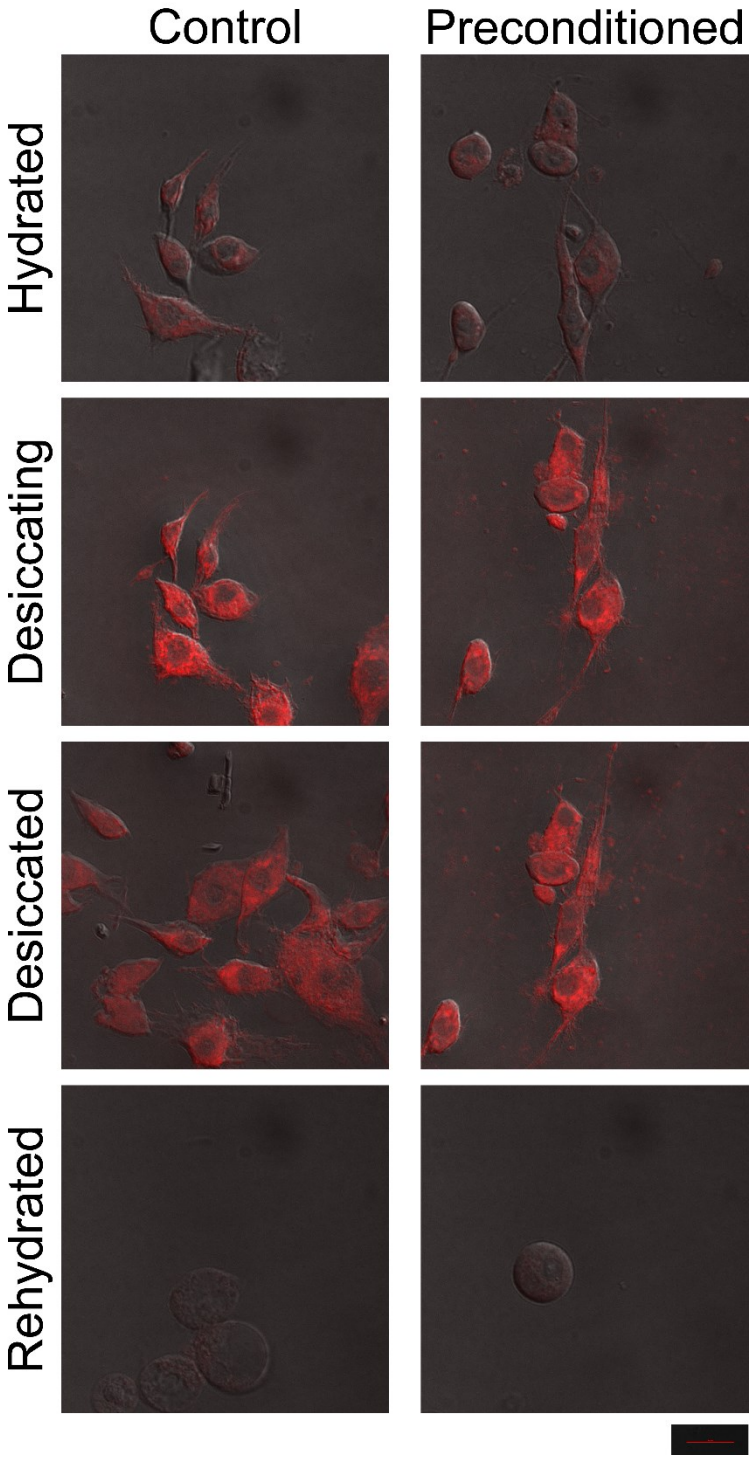

Belott et al. *Unpublished.*

CHAPTER V

SUMMARY AND CONCLUSIONS

This dissertation established that ARID proteins can have robust, cell-wide protective properties that can be sufficiently explained with some fraction of the ARID protein undergoing a liquid-liquid phase separation (LLPS), and the remaining dilute fraction entering an entangled state to increase intracellular viscosity at relatively high water contents. Furthermore, this dissertation established that robust cellular reorganization occurs in Pv11 cells during preconditioning, desiccation, and rehydration. These results may provide guidance for future experiments in *P. vanderplanki* larvae. In addition, MLOs in preconditioned Pv11 cells may be a useful model for engineering artificial LLPS to preserve desiccation-sensitive biological materials.

Cellular dielectrophoresis (DEP) related changing electrical properties of cells to biological processes (*94, 96, 100, 103, 106, 114*). When applied to ectopically expressed LEA proteins in *Drosophila melanogaster* Kc167 cells, ARID protein folding was observed at modest levels of osmotic water loss. Because the DEP measures the transfer of charges throughout a cell, these data demonstrated that the explored ARID proteins were significantly impacting ion diffusivity throughout the cell. Although, there was no evidence to suggest that increasing ion diffusivity plays any significant role in anhydrobiosis. Cellular DEP data on *Afr*LEA3m, but not *Afr*LEA6, also suggested membrane stabilization

was a result of protein folding and direct protein-membrane interaction. SEM imaging of Kc167 cells ectopically expressing *Afr*LEA3m also suggested direct protein-membrane interactions, as indicated by a pore-like formation formed in the plasma membrane of desiccated cells expressing *Afr*LEA3m.

Cellular DEP data also suggested that *Afr*LEA3m and *Afr*LEA6 may be undergoing significant folding at moderate levels of osmotic water loss. This was hypothesized to result in *Afr*LEA3m and *Afr*LEA6 shifting from an untangled state into a tangled one and increasing intracellular viscosity. Further exploration into *Afr*LEA6 using confocal microscopy techniques revealed that *Afr*LEA6 *in vivo* relies on multivalent interactions to undergo a liquid-liquid phase separation (LLPS) to form a selective, stress granule-like membraneless organelle (MLO), while the dilute protein fraction is capable of increasing intracellular viscosity. Furthermore, *Afr*LEA6 was demonstrated to protect the plasma membrane integrity, although not directly as cellular DEP and SEM had suggested for *Afr*LEA3m. The dual-mechanistic function of *Afr*LEA6 provided a framework to explain how a single ARID protein could protect a wide variety of targets without necessarily requiring a high ratio of protective protein to targets, while also aiding in vitrification. The role of MLOs in desiccation tolerance is far from being understood. However, the morphological and physiological changes that occur to organelles in anhydrobiotic cells are also important to consider.

The Pv11 cell line is a desiccation-tolerant cell line derived from the anhydrobiotic midge, *Polypedilum vanderplanki* (*169, 173*). This dissertation utilized the Pv11 cell line as a model to explore organelle-focused morphological and physiological changes during preconditioning, desiccation, and rehydration. During preconditioning, Pv11 cells form

multiple large, spherical structures that are hypothesized to be autophagosomes based on their size, numbers, and low nutrient content of the preconditioning media (*176*). It has been hypothesized that autophagosomes in yeast and at least one resurrection plant are used to remove desiccation-sensitive proteins (*177, 179*). Nevertheless, the role of autophagy in anhydrobiosis, if any, will require further exploration. In addition to this observation, preconditioning decreases cellular respiration by 73%. Reducing and detoxifying reactive oxygen species is a common strategy employed by *P. vanderplanki* and other anhydrobiotic animals and has been shown to be necessary for tardigrades to maintain an anhydrobiotic state beyond a relatively short period of time (*3, 14, 23-27*). Preconditioning also caused swelling in the ER, Golgi, and nucleus, when cells were transferred into relatively hypotonic imaging solutions. Although no ER- and Golgi-specific trehalose transporters have been described, it is reasonable to hypothesize that these organelles are swelling due to equilibration with the 600 mM trehalose in the preconditioning media. Furthermore, the ER and Golgi networks fragmented, which may reduce sheer stress during desiccation and rehydration. All organelles observed were able to recover within 1 h following rehydration, with mitochondria able being to restore their membrane potential within 30 min.

Perhaps the most striking change caused by preconditioning was the assembly of a stress-induced membraneless organelle. While the liquid nature and reassembly of the MLO after desiccation was determined, the functionality and composition of the MLO remains to be elucidated. However, it is possible that LEA proteins play a role in its assembly and stability in the desiccated state, considering their increased expression during preconditioning and the propensity of intrinsically disordered proteins to undergo LLPS (*21, 183, 184*). Likewise, it is suspected that LEA proteins and nuclear trehalose

equilibration play a role in the stabilization of the nucleolus during desiccation and rehydration. Interestingly, the nucleolus did not require time to reform like the stress-induced MLO, suggesting that these two MLOs are protected by different mechanisms. From a biotechnological standpoint, identifying organelle-specific trehalose transporters may be useful for engineering desiccation tolerant cell-based products, and MLOs in preconditioned Pv11 cells may provide a useful model for engineering artificial LLPS to preserve desiccation-sensitive biological materials.

Unlike observations in Kc167 cells ectopically expressing *Afr*LEA6, desiccation of preconditioned Pv11 cells did not reveal an increase in intracellular viscosity. It is unknown if this was due to the constitutive expression of some LEA proteins in Pv11 cells, or if Pv11 cells require a less viscous intracellular milieu at higher water contents during desiccation (*21*). Evidence of Pv11 cells requiring a less rigid morphology was supported by the lack of F-actin networking in preconditioned cells. Nevertheless, SEM imaging revealed increased plasma membrane structural integrity and resistance to membrane fusion during desiccation in preconditioned cells.

In conclusion, much of the complex molecular orchestra that governs anhydrobiosis remains to be elucidated. This dissertation contributed to our understanding of anhydrobiosis by describing how an ARID protein could protect a wide variety of targets without necessarily requiring a high ratio of protective protein to targets. Furthermore, this dissertation described the complex cellular reorganization that occurs in Pv11 during preconditioning, desiccation, and rehydration, which may help guide future experiments in the animal model. From LLPS to cellular reorganization, the complexity of 'life without water' is stunning.

REFERENCES

1. O. Leprince, J. Buitink, Introduction to desiccation biology: from old borders to new frontiers. *Planta* **242**, 369-378 (2015).
2. S. C. Hand, M. A. Menze, Molecular approaches for improving desiccation tolerance: insights from the brine shrimp Artemia franciscana. *Planta* **242**, 379-388 (2015).
3. W. Welnicz, M. A. Grohme, L. Kaczmarek, R. O. Schill, M. Frohme, Anhydrobiosis in tardigrades--the last decade. *J Insect Physiol* **57**, 577-583 (2011).
4. F. A. Hoekstra, E. A. Golovina, J. Buitink, Mechanisms of plant desiccation tolerance. *Trends Plant Sci* **6**, 431-438 (2001).
5. J. H. Crowe, F. A. Hoekstra, L. M. Crowe, Anhydrobiosis. *Annu Rev Physiol* **54**, 579-599 (1992).
6. A. Tunnacliffe, J. Lapinski, Resurrecting Van Leeuwenhoek's rotifers: a reappraisal of the role of disaccharides in anhydrobiosis. *Philos T Roy Soc B* **358**, 1755-1771 (2003).
7. A. Van Leeuwenhoek. (dated 9 February 1702).
8. S. C. Hand, M. A. Menze, M. Toner, L. Boswell, D. Moore, LEA proteins during water stress: not just for plants anymore. *Annu Rev Physiol* **73**, 115-134 (2011).
9. P. Alpert, Constraints of tolerance: why are desiccation-tolerant organisms so small or rare? *J Exp Biol* **209**, 1575-1584 (2006).
10. R. Guidetti, K. I. Jonsson, Long-term anhydrobiotic survival in semi-terrestrial micrometazoans. *J Zool* **257**, 181-187 (2002).
11. J. H. Crowe, Anhydrobiosis: An Unsolved Problem with Applications in Human Welfare. *Subcell Biochem* **71**, 263-280 (2015).
12. B. Janis, C. Belott, M. A. Menze, Role of Intrinsic Disorder in Animal Desiccation Tolerance. *Proteomics* **18**, e1800067 (2018).
13. T. A. Voronina *et al.*, New group of transmembrane proteins associated with desiccation tolerance in the anhydrobiotic midge Polypedilum vanderplanki. *Sci Rep* **10**, 11633 (2020).
14. O. Gusev *et al.*, Comparative genome sequencing reveals genomic signature of extreme desiccation tolerance in the anhydrobiotic midge. *Nat Commun* **5**, 4784 (2014).
15. C. Erkut *et al.*, Molecular strategies of the Caenorhabditis elegans dauer larva to survive extreme desiccation. *PLoS One* **8**, e82473 (2013).
16. R. Cornette, T. Kikawada, The Induction of Anhydrobiosis in the Sleeping Chironomid: Current Status of Our Knowledge. *Iubmb Life* **63**, 419-429 (2011).
17. A. Tunnacliffe, M. J. Wise, The continuing conundrum of the LEA proteins. *Naturwissenschaften* **94**, 791-812 (2007).
18. T. C. Boothby, G. J. Pielak, Intrinsically Disordered Proteins and Desiccation Tolerance: Elucidating Functional and Mechanistic Underpinnings of Anhydrobiosis. *Bioessays* **39**, (2017).
19. A. Reuner *et al.*, Stress response in tardigrades: differential gene expression of molecular chaperones. *Cell Stress Chaperon* **15**, 423-430 (2010).
20.

A. M. Rizzo *et al.*, Antioxidant defences in hydrated and desiccated states of the tardigrade Paramacrobiotus richtersi. *Comp Biochem Physiol B Biochem Mol Biol* **156**, 115-121 (2010).
21. T. G. Yamada *et al.*, Transcriptome analysis of the anhydrobiotic cell line Pv11 infers the mechanism of desiccation tolerance and recovery. *Sci Rep* **8**, 17941 (2018).
22. C. C. S. Evangelista *et al.*, Multiple genes contribute to anhydrobiosis (tolerance to extreme desiccation) in the nematode Panagrolaimus superbus. *Genet Mol Biol* **40**, 790-802 (2017).
23. S. Tokumoto *et al.*, Genome-Wide Role of HSF1 in Transcriptional Regulation of Desiccation Tolerance in the Anhydrobiotic Cell Line, Pv11. *Int J Mol Sci* **22**, (2021).
24. A. Nesmelov, R. Cornette, O. Gusev, T. Kikawada, The Antioxidant System in the Anhydrobiotic Midge as an Essential, Adaptive Mechanism for Desiccation Survival. *Adv Exp Med Biol* **1081**, 259-270 (2018).
25. D. Wojciechowska *et al.*, Mitochondrial alternative oxidase contributes to successful tardigrade anhydrobiosis. *Frontiers in Zoology* **18**, 15 (2021).
26. R. Cornette *et al.*, Identification of anhydrobiosis-related genes from an expressed sequence tag database in the cryptobiotic midge Polypedilum vanderplanki (Diptera; Chironomidae). *J Biol Chem* **285**, 35889-35899 (2010).
27. J. E. Podrabsky, S. C. Hand, Physiological strategies during animal diapause: lessons from brine shrimp and annual killifish. *J Exp Biol* **218**, 1897-1906 (2015).
28. O. Gusev *et al.*, Anhydrobiosis-associated nuclear DNA damage and repair in the sleeping chironomid: linkage with radioresistance. *PLoS One* **5**, e14008 (2010).
29. C. Boschetti, N. Pouchkina-Stantcheva, P. Hoffmann, A. Tunnacliffe, Foreign genes and novel hydrophilic protein genes participate in the desiccation response of the bdelloid rotifer Adineta ricciae. *J Exp Biol* **214**, 59-68 (2011).
30. M. B. Franca, A. D. Panek, E. C. Eleutherio, Oxidative stress and its effects during dehydration. *Comp Biochem Physiol A Mol Integr Physiol* **146**, 621-631 (2007).
31. A. M. King, T. H. MacRae, Insect heat shock proteins during stress and diapause. *Annu Rev Entomol* **60**, 59-75 (2015).
32. Y. Sun, T. H. MacRae, Small heat shock proteins: molecular structure and chaperone function. *Cell Mol Life Sci* **62**, 2460-2476 (2005).
33. A. M. King, J. Toxopeus, T. H. MacRae, Functional differentiation of small heat shock proteins in diapause-destined Artemia embryos. *Febs j* **280**, 4761-4772 (2013).
34. P. V. Mazin *et al.*, Cooption of heat shock regulatory system for anhydrobiosis in the sleeping chironomid Polypedilum vanderplanki. *Proceedings of the National Academy of Sciences of the United States of America* **115**, E2477-e2486 (2018).
35. E. Schokraie *et al.*, Investigating heat shock proteins of tardigrades in active versus anhydrobiotic state using shotgun proteomics. *J Zool Syst Evol Res* **49**, 111-119 (2011).
36. F. Narberhaus, Alpha-crystallin-type heat shock proteins: socializing minichaperones in the context of a multichaperone network. *Microbiol Mol Biol Rev* **66**, 64-93; table of contents (2002).
37. T. Kikawada *et al.*, Dehydration-inducible changes in expression of two aquaporins in the sleeping chironomid, Polypedilum vanderplanki. *Biochim Biophys Acta* **1778**, 514-520 (2008).
38. M. A. Grohme *et al.*, The Aquaporin Channel Repertoire of the Tardigrade Milnesium tardigradum. *Bioinform Biol Insights* **7**, 153-165 (2013).

39. B. Mali *et al.*, Transcriptome survey of the anhydrobiotic tardigrade Milnesium tardigradum in comparison with Hypsibius dujardini and Richtersius coronifer. *Bmc Genomics* **11**, 168 (2010).
40. N. Y. Denekamp, Reinhardt, R., Albrecht, M. W., Drungowski, M., Kube, M., and Lubzens, E., The expression pattern of dormancy-associated genes in multiple life-history stages in the rotifer Brachionus plicatilis. *Hydrobiologia* **662**, 51-63 (2011).
41. J. Lapinski, A. Tunnacliffe, Anhydrobiosis without trehalose in bdelloid rotifers. *Febs Lett* **553**, 387-390 (2003).
42. J. H. Crowe, J. F. Carpenter, L. M. Crowe, The role of vitrification in anhydrobiosis. *Annu Rev Physiol* **60**, 73-103 (1998).
43. J. H. Crowe, Trehalose as a "chemical chaperone": fact and fantasy. *Advances in experimental medicine and biology* **594**, 143-158 (2007).
44. S. N. Timasheff, S. G.N., O. C.B., B. C.L., Eds. (Springer, Springer, Berlin, Heidelberg, 1992), pp. 70-84.
45. S. N. Timasheff, The control of protein stability and association by weak interactions with water: how do solvents affect these processes? *Annu Rev Biophys Biomol Struct* **22**, 67-97 (1993).
46. J. S. Clegg, The Origin of Trehalose and Its Significance during the Formation of Encysted Dormant Embryos of Artemia Salina. *Comp Biochem Physiol* **14**, 135-143 (1965).
47. K. Madin, J. Crowe, Anhydrobiosis in Nematodes - Carbohydrate and Lipid Metabolism During Dehydration. *Journal of Experimental Biology* **193**, 335-342 (1975).
48. J. H. Crowe *et al.*, The trehalose myth revisited: introduction to a symposium on stabilization of cells in the dry state. *Cryobiology* **43**, 89-105 (2001).
49. M. Caprioli *et al.*, Trehalose in desiccated rotifers: a comparison between a bdelloid and a monogonont species. *Comp Biochem Physiol A Mol Integr Physiol* **139**, 527-532 (2004).
50. S. A. Watts, Lee K. J., and Cline G. B., Elevated ornithine decarboxylase activity and polyamine levels during early development in the brine shrimp Artemia franciscana. *J Exp Biol* **270**, 426-431 (1994).
51. T. H. MacRae, Stress tolerance during diapause and quiescence of the brine shrimp, Artemia. *Cell Stress Chaperon* **21**, 9-18 (2016).
52. T. C. Boothby *et al.*, Tardigrades Use Intrinsically Disordered Proteins to Survive Desiccation. *Mol Cell* **65**, 975-984 e975 (2017).
53. K. Goyal, L. J. Walton, A. Tunnacliffe, LEA proteins prevent protein aggregation due to water stress. *Biochem J* **388**, 151-157 (2005).
54. T. Kikawada *et al.*, Dehydration-induced expression of LEA proteins in an anhydrobiotic chironomid. *Biochem Biophys Res Commun* **348**, 56-61 (2006).
55. S. Tanaka *et al.*, Novel mitochondria-targeted heat-soluble proteins identified in the anhydrobiotic Tardigrade improve osmotic tolerance of human cells. *PLoS One* **10**, e0118272 (2015).
56. A. Yamaguchi *et al.*, Two novel heat-soluble protein families abundantly expressed in an anhydrobiotic tardigrade. *PLoS One* **7**, e44209 (2012).
57. L. Dure, C. Chlan, Developmental Biochemistry of Cottonseed Embryogenesis and Germination : XII. PURIFICATION AND PROPERTIES OF PRINCIPAL STORAGE PROTEINS. *Plant Physiol* **68**, 180-186 (1981).
58. A. Solomon, R. Salomon, I. Paperna, I. Glazer, Desiccation stress of entomopathogenic nematodes induces the accumulation of a novel heat-stable protein. *Parasitology* **121 (Pt 4)**, 409-416 (2000).

59. L. Dure, 3rd *et al.*, Common amino acid sequence domains among the LEA proteins of higher plants. *Plant Mol Biol* **12**, 475-486 (1989).
60. M. J. Wise, A. Tunnacliffe, POPP the question: what do LEA proteins do? *Trends in plant science* **9**, 13-17 (2004).
61. E. Jaspard, D. Macherel, G. Hunault, Computational and Statistical Analyses of Amino Acid Usage and Physico-Chemical Properties of the Twelve Late Embryogenesis Abundant Protein Classes. *PLOS ONE* **7**, e36968 (2012).
62. S. C. Hand, D. Jones, M. A. Menze, T. L. Witt, Life without water: expression of plant LEA genes by an anhydrobiotic arthropod. *J Exp Zool A Ecol Genet Physiol* **307**, 62-66 (2007).
63. A. C. Cuming, in *Seed Proteins,* P. R. Shewry, R. Casey, Eds. (Springer Netherlands, Dordrecht, 1999), pp. 753-780.
64. M.-D. Shih, F. A. Hoekstra, Y.-I. C. Hsing, in *Advances in Botanical Research,* K. Jean-Claude, D. Michel, Eds. (Academic Press, 2008), vol. Volume 48, pp. 211-255.
65. M. Battaglia, A. Covarrubias, Late Embryogenesis Abundant (LEA) proteins in legumes. *Frontiers in Plant Science* **4**, (2013).
66. S. Hengherr, A. G. Heyer, F. Brummer, R. O. Schill, Trehalose and vitreous states: desiccation tolerance of dormant stages of the crustaceans Triops and Daphnia. *Physiol Biochem Zool* **84**, 147-153 (2011).
67. J. H. Crowe, J. F. Carpenter, L. M. Crowe, The role of vitrification in anhydrobiosis. *Annu. Rev. Physiol.* **60**, 73-103 (1998).
68. S. Chakrabortee *et al.*, Intrinsically disordered proteins as molecular shields. *Mol Biosyst* **8**, 210-219 (2012).
69. J. M. Mouillon, P. Gustafsson, P. Harryson, Structural investigation of disordered stress proteins. Comparison of full-length dehydrins with isolated peptides of their conserved segments. *Plant Physiol* **141**, 638-650 (2006).
70. M. Hara, M. Fujinaga, T. Kuboi, Metal binding by citrus dehydrin with histidine-rich domains. *J Exp Bot* **56**, 2695-2703 (2005).
71. J. Svensson, E. T. Palva, B. Welin, Purification of recombinant Arabidopsis thaliana dehydrins by metal ion affinity chromatography. *Protein Expr Purif* **20**, 169-178 (2000).
72. W. F. Wolkers, S. McCready, W. F. Brandt, G. G. Lindsey, F. A. Hoekstra, Isolation and characterization of a D-7 LEA protein from pollen that stabilizes glasses in vitro. *Biochim Biophys Acta* **1544**, 196-206 (2001).
73. L. C. Boswell, M. A. Menze, S. C. Hand, Group 3 Late Embryogenesis Abundant Proteins from Embryos of Artemia franciscana: Structural Properties and Protective Abilities during Desiccation. *Physiol Biochem Zool* **87**, 640-651 (2014).
74. P. Tompa, P. Csermely, The role of structural disorder in the function of RNA and protein chaperones. *FASEB J* **18**, 1169-1175 (2004).
75. P. Tompa, D. Kovacs, Intrinsically disordered chaperones in plants and animals. *Biochem Cell Biol* **88**, 167-174 (2010).
76. R. Hatanaka *et al.*, An abundant LEA protein in the anhydrobiotic midge, PvLEA4, acts as a molecular shield by limiting growth of aggregating protein particles. *Insect Biochem Mol Biol* **43**, 1055-1067 (2013).
77. T. Shimizu *et al.*, Desiccation-induced structuralization and glass formation of group 3 late embryogenesis abundant protein model peptides. *Biochemistry* **49**, 1093-1104 (2010).
78. A. Bremer, M. Wolff, A. Thalhammer, D. K. Hincha, Folding of intrinsically disordered plant LEA proteins is driven by glycerol-induced crowding and the presence of membranes. *FEBS J* **284**, 919-936 (2017).

79. D. S. Moore, R. Hansen, S. C. Hand, Liposomes with diverse compositions are protected during desiccation by LEA proteins from Artemia franciscana and trehalose. *Biochim Biophys Acta* **1858**, 104-115 (2016).
80. B. M. LeBlanc, S. C. Hand, Target enzymes are stabilized by AfrLEA6 and a gain of alpha-helix coincides with protection by a group 3 LEA protein during incremental drying. *Biochimica et biophysica acta. Proteins and proteomics* **1869**, 140642 (2021).
81. L. French-Pacheco, C. L. Cuevas-Velazquez, L. Rivillas-Acevedo, A. A. Covarrubias, C. Amero, Metal-binding polymorphism in late embryogenesis abundant protein AtLEA4-5, an intrinsically disordered protein. *PeerJ* **6**, e4930 (2018).
82. B. Janis, V. N. Uversky, M. A. Menze, Potential functions of LEA proteins from the brine shrimp Artemia franciscana - anhydrobiosis meets bioinformatics. *J Biomol Struct Dyn*, 1-19 (2017).
83. M. A. Menze, L. Boswell, M. Toner, S. C. Hand, Occurrence of mitochondria-targeted Late Embryogenesis Abundant (LEA) gene in animals increases organelle resistance to water stress. *J Biol Chem* **284**, 10714-10719 (2009).
84. M. R. Marunde *et al.*, Improved tolerance to salt and water stress in Drosophila melanogaster cells conferred by late embryogenesis abundant protein. *J Insect Physiol* **59**, 377-386 (2013).
85. B. M. LeBlanc, S. C. Hand, A novel group 6 LEA protein from diapause embryos of Artemia franciscana is cytoplasmically localized. *Tissue Cell* **67**, 101410 (2020).
86. L. M. Broche, F. H. Labeed, M. P. Hughes, Extraction of dielectric properties of multiple populations from dielectrophoretic collection spectrum data. *Phys Med Biol* **50**, 2267-2274 (2005).
87. J. Chen *et al.*, A microfluidic device for simultaneous electrical and mechanical measurements on single cells. *Biomicrofluidics* **5**, 14113 (2011).
88. G. Fuhr, R. Glaser, R. Hagedorn, Rotation of dielectrics in a rotating electric high-frequency field. Model experiments and theoretical explanation of the rotation effect of living cells. *Biophys J* **49**, 395-402 (1986).
89. L. Huang, P. Zhao, W. Wang, 3D cell electrorotation and imaging for measuring multiple cellular biophysical properties. *Lab Chip* **18**, 2359-2368 (2018).
90. L. S. Jang, M. H. Wang, Microfluidic device for cell capture and impedance measurement. *Biomed Microdevices* **9**, 737-743 (2007).
91. K. Keim *et al.*, On-chip technology for single-cell arraying, electrorotation-based analysis and selective release. *Electrophoresis* **40**, 1830-1838 (2019).
92. F. H. Labeed, H. M. Coley, M. P. Hughes, Differences in the biophysical properties of membrane and cytoplasm of apoptotic cells revealed using dielectrophoresis. *Biochim Biophys Acta* **1760**, 922-929 (2006).
93. U. Lei, P. H. Sun, R. Pethig, Refinement of the theory for extracting cell dielectric properties from dielectrophoresis and electrorotation experiments. *Biomicrofluidics* **5**, 44109-4410916 (2011).
94. A. Nakano, A. Ros, Protein dielectrophoresis: advances, challenges, and applications. *Electrophoresis* **34**, 1085-1096 (2013).
95. V. Velasco *et al.*, An orbital shear platform for real-time, in vitro endothelium characterization. *Biotechnol Bioeng* **113**, 1336-1344 (2016).
96. L. Zheng, J. P. Brody, P. J. Burke, Electronic manipulation of DNA, proteins, and nanoparticles for potential circuit assembly. *Biosens Bioelectron* **20**, 606-619 (2004).
97. M. Gonzalez *et al.*, Generation of stable Drosophila cell lines using multicistronic vectors. *Sci Rep* **1**, 75 (2011).

98. B. M. LeBlanc, M. T. Le, B. Janis, M. A. Menze, S. C. Hand, Structural properties and cellular expression of AfrLEA6, a group 6 late embryogenesis abundant protein from embryos of Artemia franciscana. *Cell Stress Chaperones*, (2019).
99. L. C. Boswell, S. C. Hand, Intracellular localization of group 3 LEA proteins in embryos of Artemia franciscana. *Tissue & Cell* **46**, 514-519 (2014).
100. M. Z. Rashed, C. J. Belott, B. R. Janis, M. A. Menze, S. J. Williams, New insights into anhydrobiosis using cellular dielectrophoresis-based characterization. *Biomicrofluidics* **13**, 064113 (2019).
101. W. Liang *et al.*, Determination of Cell Membrane Capacitance and Conductance via Optically Induced Electrokinetics. *Biophys J* **113**, 1531-1539 (2017).
102. R. Pethig *et al.*, Electrokinetic measurements of membrane capacitance and conductance for pancreatic beta-cells. *IEE Proc Nanobiotechnol* **152**, 189-193 (2005).
103. E. A. Henslee *et al.*, Rhythmic potassium transport regulates the circadian clock in human red blood cells. *Nat Commun* **8**, 1978 (2017).
104. C. J. Lee *et al.*, Ionic Conductivity of Polyelectrolyte Hydrogels. *ACS Appl Mater Interfaces* **10**, 5845-5852 (2018).
105. F. Bordi, R. H. Colby, C. Cametti, L. De Lorenzo, T. Gili, Electrical Conductivity of Polyelectrolyte Solutions in the Semidilute and Concentrated Regime: The Role of Counterion Condensation. *The Journal of Physical Chemistry B* **106**, 6887-6893 (2002).
106. K. Asami, Dielectric properties of microvillous cells simulated by the three-dimensional finite-element method. *Bioelectrochemistry* **81**, 28-33 (2011).
107. W. R. Loewenstein, Y. Kanno, Some Electrical Properties of the Membrane of a Cell Nucleus. *Nature* **195**, 462-464 (1962).
108. A. Irimajiri, K. Asami, T. Ichinowatari, Y. Kinoshita, Passive electrical properties of the membrane and cytoplasm of cultured rat basophil leukemia cells. I. Dielectric behavior of cell suspensions in 0.01-500 MHz and its simulation with a single-shell model. *Biochim Biophys Acta* **896**, 203-213 (1987).
109. V. L. Sukhorukov, W. M. Arnold, U. Zimmermann, Hypotonically induced changes in the plasma membrane of cultured mammalian cells. *J Membr Biol* **132**, 27-40 (1993).
110. X. B. Wang *et al.*, Changes in Friend murine erythroleukaemia cell membranes during induced differentiation determined by electrorotation. *Biochim Biophys Acta* **1193**, 330-344 (1994).
111. X. F. Zhou, G. H. Markx, R. Pethig, I. M. Eastwood, Differentiation of viable and non-viable bacterial biofilms using electrorotation. *Biochim Biophys Acta* **1245**, 85-93 (1995).
112. K. F. Hoettges, J. W. Dale, M. P. Hughes, Rapid determination of antibiotic resistance in E. coli using dielectrophoresis. *Phys Med Biol* **52**, 6001-6009 (2007).
113. H. Pauly, Electrical conductance and dielectric constant of the interior of erythrocytes. *Nature* **183**, 333-334 (1959).
114. R. Pethig, D. B. Kell, The passive electrical properties of biological systems: their significance in physiology, biophysics and biotechnology. *Phys Med Biol* **32**, 933-970 (1987).
115. L. J. Gentet, G. J. Stuart, J. D. Clements, Direct measurement of specific membrane capacitance in neurons. *Biophys J* **79**, 314-320 (2000).
116. M. Stoneman *et al.*, Protein influence on the plasma membrane dielectric properties: in vivo study utilizing dielectric spectroscopy and fluorescence microscopy. *Bioelectrochemistry* **70**, 542-550 (2007).

117. M. Muratore, V. Srsen, M. Waterfall, A. Downes, R. Pethig, Biomarker-free dielectrophoretic sorting of differentiating myoblast multipotent progenitor cells and their membrane analysis by Raman spectroscopy. *Biomicrofluidics* **6**, 34113 (2012).
118. R. Pethig, Review article-dielectrophoresis: status of the theory, technology, and applications. *Biomicrofluidics* **4**, (2010).
119. P. Ball, Water is an active matrix of life for cell and molecular biology. *Proc Natl Acad Sci U S A* **114**, 13327-13335 (2017).
120. S. A. Benner, A. Ricardo, M. A. Carrigan, Is there a common chemical model for life in the universe? *Curr Opin Chem Biol* **8**, 672-689 (2004).
121. J. L. Finney, Water? What's so special about it? *Philos Trans R Soc Lond B Biol Sci* **359**, 1145-1163; discussion 1163-1145, 1323-1148 (2004).
122. P. H. Yancey, Organic osmolytes as compatible, metabolic and counteracting cytoprotectants in high osmolarity and other stresses. *J Exp Biol* **208**, 2819-2830 (2005).
123. K. E. McCluney *et al.*, Shifting species interactions in terrestrial dryland ecosystems under altered water availability and climate change. *Biol Rev Camb Philos Soc* **87**, 563-582 (2012).
124. P. Alpert, The constraints of tolerance: Why are desiccation-tolerant organisms small and rare? *Integr Comp Biol* **44**, 515-515 (2004).
125. O. Leprince, A. Pellizzaro, S. Berriri, J. Buitink, Late seed maturation: drying without dying. *Journal of Experimental Botany* **68**, 827-841 (2017).
126. J. S. Clegg, P. Seitz, W. Seitz, C. F. Hazlewood, Cellular responses to extreme water loss: the water-replacement hypothesis. *Cryobiology* **19**, 306-316 (1982).
127. J. Grelet *et al.*, Identification in pea seed mitochondria of a late-embryogenesis abundant protein able to protect enzymes from drying. *Plant Physiol* **137**, 157-167 (2005).
128. J. Browne, A. Tunnacliffe, A. Burnell, Anhydrobiosis: plant desiccation gene found in a nematode. *Nature* **416**, 38 (2002).
129. M. S. Clark *et al.*, Surviving extreme polar winters by desiccation: clues from Arctic springtail (Onychiurus arcticus) EST libraries. *Bmc Genomics* **8**, 475 (2007).
130. N. N. Pouchkina-Stantcheva *et al.*, Functional divergence of former alleles in an ancient asexual invertebrate. *Science* **318**, 268-271 (2007).
131. G. Wu *et al.*, Diverse LEA (late embryogenesis abundant) and LEA-like genes and their responses to hypersaline stress in post-diapause embryonic development of Artemia franciscana. *Comp Biochem Physiol B Biochem Mol Biol* **160**, 32-39 (2011).
132. M. A. Sharon, A. Kozarova, J. S. Clegg, P. O. Vacratsis, A. H. Warner, Characterization of a group 1 late embryogenesis abundant protein in encysted embryos of the brine shrimp Artemia franciscana. *Biochem Cell Biol* **87**, 415-430 (2009).
133. A. H. Warner *et al.*, Evidence for multiple group 1 late embryogenesis abundant proteins in encysted embryos of Artemia and their organelles. *Journal of biochemistry* **148**, 581-592 (2010).
134. E. Chatelain *et al.*, Temporal profiling of the heat-stable proteome during late maturation of Medicago truncatula seeds identifies a restricted subset of late embryogenesis abundant proteins associated with longevity. *Plant Cell Environ* **35**, 1440-1455 (2012).
135. L. M. A. Dirk *et al.*, Late Embryogenesis Abundant Protein-Client Protein Interactions. *Plants (Basel)* **9**, (2020).
136. C. L. Cuevas-Velazquez, J. R. Dinneny, Organization out of disorder: liquid-liquid phase separation in plants. *Curr Opin Plant Biol* **45**, 68-74 (2018).

137. E. Gomes, J. Shorter, The molecular language of membraneless organelles. *J Biol Chem* **294**, 7115-7127 (2019).
138. W. van Leeuwen, C. Rabouille, Cellular stress leads to the formation of membraneless stress assemblies in eukaryotic animal cells. *Traffic*, (2019).
139. T. J. Nott *et al.*, Phase transition of a disordered nuage protein generates environmentally responsive membraneless organelles. *Mol Cell* **57**, 936-947 (2015).
140. H. B. Schmidt, D. Gorlich, Transport Selectivity of Nuclear Pores, Phase Separation, and Membraneless Organelles. *Trends Biochem Sci* **41**, 46-61 (2016).
141. P. B. Sehgal, J. Westley, K. M. Lerea, S. DiSenso-Browne, J. D. Etlinger, Biomolecular condensates in cell biology and virology: phase-separated membraneless organelles (MLOs). *Anal Biochem*, 113691 (2020).
142. Y. Shin, C. P. Brangwynne, Liquid phase condensation in cell physiology and disease. *Science* **357**, (2017).
143. V. N. Uversky, Intrinsically disordered proteins in overcrowded milieu: Membrane-less organelles, phase separation, and intrinsic disorder. *Curr Opin Struct Biol* **44**, 18-30 (2017).
144. C. P. Brangwynne, Phase transitions and size scaling of membrane-less organelles. *J Cell Biol* **203**, 875-881 (2013).
145. T. J. Abatzopoulos, J. Beardmore, J. S. Clegg, P. Sorgeloos, *Artemia: Basic and Applied Biology*. Biology of Aquatic Organisms (Springer Netherlands, ed. 1, 2002), vol. 1, pp. 286.
146. B. Kim, C. N. Lam, B. D. Olsen, Nanopatterned Protein Films Directed by Ionic Complexation with Water-Soluble Diblock Copolymers. *Macromolecules* **45**, 4572-4580 (2012).
147. D. M. Norris *et al.*, An improved Akt reporter reveals intra- and inter-cellular heterogeneity and oscillations in signal transduction. *J Cell Sci* **130**, 2757-2766 (2017).
148. D. L. Updike, S. J. Hachey, J. Kreher, S. Strome, P granules extend the nuclear pore complex environment in the C. elegans germ line. *J Cell Biol* **192**, 939-948 (2011).
149. S. Kroschwald *et al.*, Promiscuous interactions and protein disaggregases determine the material state of stress-inducible RNP granules. *Elife* **4**, e06807 (2015).
150. A. Molliex *et al.*, Phase separation by low complexity domains promotes stress granule assembly and drives pathological fibrillization. *Cell* **163**, 123-133 (2015).
151. S. S. Patel, B. J. Belmont, J. M. Sante, M. F. Rexach, Natively unfolded nucleoporins gate protein diffusion across the nuclear pore complex. *Cell* **129**, 83-96 (2007).
152. K. Ribbeck, D. Gorlich, The permeability barrier of nuclear pore complexes appears to operate via hydrophobic exclusion. *Embo J* **21**, 2664-2671 (2002).
153. M. A. Haidekker, E. A. Theodorakis, Environment-sensitive behavior of fluorescent molecular rotors. *J Biol Eng* **4**, 11 (2010).
154. J. A. Levitt, P. H. Chung, K. Suhling, Spectrally resolved fluorescence lifetime imaging of Nile red for measurements of intracellular polarity. *J Biomed Opt* **20**, 096002 (2015).
155. J. Swain, A. K. Mishra, Nile red fluorescence for quantitative monitoring of micropolarity and microviscosity of pluronic F127 in aqueous media. *Photochem Photobiol Sci* **15**, 1400-1407 (2016).
156. D. G. Yablon, A. M. Schilowitz, Solvatochromism of Nile Red in nonpolar solvents. *Appl Spectrosc* **58**, 843-847 (2004).
157. P. Greenspan, E. P. Mayer, S. D. Fowler, Nile red: a selective fluorescent stain for intracellular lipid droplets. *J Cell Biol* **100**, 965-973 (1985).

158. J. Verdier *et al.*, A regulatory network-based approach dissects late maturation processes related to the acquisition of desiccation tolerance and longevity of Medicago truncatula seeds. *Plant Physiol* **163**, 757-774 (2013).
159. I. Amara, M. Capellades, M. D. Ludevid, M. Pages, A. Goday, Enhanced water stress tolerance of transgenic maize plants over-expressing LEA Rab28 gene. *J Plant Physiol* **170**, 864-873 (2013).
160. J. R. Wheeler, T. Matheny, S. Jain, R. Abrisch, R. Parker, Distinct stages in stress granule assembly and disassembly. *Elife* **5**, (2016).
161. S. Jain *et al.*, ATPase-Modulated Stress Granules Contain a Diverse Proteome and Substructure. *Cell* **164**, 487-498 (2016).
162. D. Davis *et al.*, Human Antiviral Protein MxA Forms Novel Metastable Membraneless Cytoplasmic Condensates Exhibiting Rapid Reversible Tonicity-Driven Phase Transitions. *J Virol* **93**, (2019).
163. N. Shiina, Liquid- and solid-like RNA granules form through specific scaffold proteins and combine into biphasic granules. *J Biol Chem* **294**, 3532-3548 (2019).
164. V. N. Uversky, Natively unfolded proteins: a point where biology waits for physics. *Protein Sci* **11**, 739-756 (2002).
165. C. J. Oldfield, A. K. Dunker, Intrinsically disordered proteins and intrinsically disordered protein regions. *Annu Rev Biochem* **83**, 553-584 (2014).
166. N. Chakraborty *et al.*, A Spin-Drying Technique for Lyopreservation of Mammalian Cells. *Ann Biomed Eng* **39**, 1582-1591 (2011).
167. J. Boudet *et al.*, Comparative analysis of the heat stable proteome of radicles of Medicago truncatula seeds during germination identifies late embryogenesis abundant proteins associated with desiccation tolerance. *Plant Physiol* **140**, 1418-1436 (2006).
168. A. Borrell *et al.*, Arabidopsis thaliana atrab28: a nuclear targeted protein related to germination and toxic cation tolerance. *Plant Mol Biol* **50**, 249-259 (2002).
169. K. Watanabe, S. Imanishi, G. Akiduki, R. Cornette, T. Okuda, Air-dried cells from the anhydrobiotic insect, Polypedilum vanderplanki, can survive long term preservation at room temperature and retain proliferation potential after rehydration. *Cryobiology* **73**, 93-98 (2016).
170. S. Park *et al.*, Dehydration entropy drives liquid-liquid phase separation by molecular crowding. *Communications Chemistry* **3**, 83 (2020).
171. T. J. Nott, T. D. Craggs, A. J. Baldwin, Membraneless organelles can melt nucleic acid duplexes and act as biomolecular filters. *Nature chemistry* **8**, 569-575 (2016).
172. R. Hatanaka *et al.*, Diversity of the expression profiles of late embryogenesis abundant (LEA) protein encoding genes in the anhydrobiotic midge Polypedilum vanderplanki. *Planta* **242**, 451-459 (2015).
173. Y. Nakahara *et al.*, Cells from an anhydrobiotic chironomid survive almost complete desiccation. *Cryobiology* **60**, 138-146 (2010).
174. C. Belott, B. Janis, M. A. Menze, Liquid-liquid phase separation promotes animal desiccation tolerance. *Proc Natl Acad Sci U S A* **117**, 27676-27684 (2020).
175. Z. Öztürk, C. J. O'Kane, J. J. Pérez-Moreno, Axonal Endoplasmic Reticulum Dynamics and Its Roles in Neurodegeneration. *Frontiers in Neuroscience* **14**, (2020).
176. N. Mizushima, Y. Ohsumi, T. Yoshimori, Autophagosome formation in mammalian cells. *Cell Struct Funct* **27**, 421-429 (2002).
177. B. Williams *et al.*, Trehalose Accumulation Triggers Autophagy during Plant Desiccation. *PLoS Genet* **11**, e1005705 (2015).

178. C. A. Lamb, T. Yoshimori, S. A. Tooze, The autophagosome: origins unknown, biogenesis complex. *Nat Rev Mol Cell Biol* **14**, 759-774 (2013).
179. S. Ratnakumar *et al.*, Phenomic and transcriptomic analyses reveal that autophagy plays a major role in desiccation tolerance in Saccharomyces cerevisiae. *Mol Biosyst* **7**, 139-149 (2011).
180. M. Watanabe, T. Kikawada, T. Okuda, Increase of internal ion concentration triggers trehalose synthesis associated with cryptobiosis in larvae of Polypedilum vanderplanki. *J Exp Biol* **206**, 2281-2286 (2003).
181. I. A. Sawyer, D. Sturgill, M. Dundr, Membraneless nuclear organelles and the search for phases within phases. *Wiley Interdiscip Rev RNA* **10**, e1514 (2019).
182. T. Kikawada *et al.*, Trehalose transporter 1, a facilitated and high-capacity trehalose transporter, allows exogenous trehalose uptake into cells. *Proceedings of the National Academy of Sciences* **104**, 11585-11590 (2007).
183. S. V. Nesterov, N. S. Ilyinsky, V. N. Uversky, Liquid-liquid phase separation as a common organizing principle of intracellular space and biomembranes providing dynamic adaptive responses. *Biochim Biophys Acta Mol Cell Res* **1868**, 119102 (2021).
184. A. Majumdar, P. Dogra, S. Maity, S. Mukhopadhyay, Liquid–Liquid Phase Separation Is Driven by Large-Scale Conformational Unwinding and Fluctuations of Intrinsically Disordered Protein Molecules. *The Journal of Physical Chemistry Letters* **10**, 3929-3936 (2019).

APPENDIX 1

PERMISSION FROM JOHN WILEY AND SONS TO RESUSE ‘ROLE OF INTRINSIC DISORDER IN ANIMAL DESICCATION TOLERANCE’

JOHN WILEY AND SONS LICENSE
TERMS AND CONDITIONS
Oct 25, 2021

This Agreement between University of Louisville -- Clinton Belott ("You") and John Wiley and Sons ("John Wiley and Sons") consists of your license details and the terms and conditions provided by John Wiley and Sons and Copyright Clearance Center.

License Number	5174380842071
License date	Oct 22, 2021
Licensed Content Publisher	John Wiley and Sons
Licensed Content Publication	Proteomics
Licensed Content Title	Role of Intrinsic Disorder in Animal Desiccation Tolerance
Licensed Content Author	Brett Janis, Clinton Belott, Michael A. Menze
Licensed Content Date	Sep 20, 2018
Licensed Content Volume	18
Licensed Content Issue	21-22
Licensed Content Pages	15
Type of use	Dissertation/Thesis
Requestor type	Author of this Wiley article

Format	Print and electronic
Portion	Full article
Will you be translating?	No
Title	VISUALIZING ANHYDROBIOSIS: LIQUID-LIQUID PHASE SEPARATION, MEMBRANELESS ORGANELLES, AND CELLULAR REORGANIZATION
Institution name	University of Louisville
Expected presentation date	Dec 2021
Requestor Location	University of Louisville 2555 Glenmary Ave., Apt. 4 LOUISVILLE, KY 40204 United States Attn: University of Louisville
Publisher Tax ID	EU826007151
Total	0.00 USD

Terms and Conditions

TERMS AND CONDITIONS

This copyrighted material is owned by or exclusively licensed to John Wiley & Sons, Inc. or one of its group companies (each a"Wiley Company") or handled on behalf of a society with which a Wiley Company has exclusive publishing rights in relation to a particular work (collectively "WILEY"). By clicking "accept" in connection with completing this licensing transaction, you agree that the following terms and conditions apply to this transaction (along with the billing and payment terms and conditions established by the Copyright Clearance Center Inc., ("CCC's Billing and Payment terms and conditions"), at the time that you opened your RightsLink account (these are available at any time at http://myaccount.copyright.com).

Terms and Conditions

- The materials you have requested permission to reproduce or reuse (the "Wiley Materials") are protected by copyright.

- You are hereby granted a personal, non-exclusive, non-sub licensable (on a stand-alone basis), non-transferable, worldwide, limited license to reproduce the Wiley Materials for the purpose specified in the licensing process. This license, **and any CONTENT (PDF or image file) purchased as part of your order,** is for a one-time use only and limited to any maximum distribution number specified in the license. The first instance of republication or reuse granted by this license must be completed within two years of the date of the grant of this license (although copies prepared before the end date may be distributed thereafter). The Wiley Materials shall not be used in any other manner or for any other purpose, beyond what is granted in the license. Permission is granted subject to an appropriate acknowledgement given to the author, title of the material/book/journal and the publisher. You shall also duplicate the copyright notice that appears in the Wiley publication in your use of the Wiley Material. Permission is also granted on the understanding that nowhere in the text is a previously published source acknowledged for all or part of this Wiley Material. Any third party content is expressly excluded from this permission.

- With respect to the Wiley Materials, all rights are reserved. Except as expressly granted by the terms of the license, no part of the Wiley Materials may be copied, modified, adapted (except for minor reformatting required by the new Publication), translated, reproduced, transferred or distributed, in any form or by any means, and

no derivative works may be made based on the Wiley Materials without the prior permission of the respective copyright owner.**For STM Signatory Publishers clearing permission under the terms of the STM Permissions Guidelines only, the terms of the license are extended to include subsequent editions and for editions in other languages, provided such editions are for the work as a whole in situ and does not involve the separate exploitation of the permitted figures or extracts,** You may not alter, remove or suppress in any manner any copyright, trademark or other notices displayed by the Wiley Materials. You may not license, rent, sell, loan, lease, pledge, offer as security, transfer or assign the Wiley Materials on a stand-alone basis, or any of the rights granted to you hereunder to any other person.

- The Wiley Materials and all of the intellectual property rights therein shall at all times remain the exclusive property of John Wiley & Sons Inc, the Wiley Companies, or their respective licensors, and your interest therein is only that of having possession of and the right to reproduce the Wiley Materials pursuant to Section 2 herein during the continuance of this Agreement. You agree that you own no right, title or interest in or to the Wiley Materials or any of the intellectual property rights therein. You shall have no rights hereunder other than the license as provided for above in Section 2. No right, license or interest to any trademark, trade name, service mark or other branding ("Marks") of WILEY or its licensors is granted hereunder, and you agree that you shall not assert any such right, license or interest with respect thereto

- NEITHER WILEY NOR ITS LICENSORS MAKES ANY WARRANTY OR REPRESENTATION OF ANY KIND TO YOU OR ANY THIRD PARTY, EXPRESS, IMPLIED OR STATUTORY, WITH RESPECT TO THE MATERIALS OR THE ACCURACY OF ANY INFORMATION CONTAINED IN THE MATERIALS, INCLUDING, WITHOUT LIMITATION, ANY IMPLIED WARRANTY OF MERCHANTABILITY, ACCURACY, SATISFACTORY QUALITY, FITNESS FOR A PARTICULAR PURPOSE, USABILITY, INTEGRATION OR NON-INFRINGEMENT AND ALL SUCH WARRANTIES ARE HEREBY EXCLUDED BY WILEY AND ITS LICENSORS AND WAIVED BY YOU.

- WILEY shall have the right to terminate this Agreement immediately upon breach of this Agreement by you.

- You shall indemnify, defend and hold harmless WILEY, its Licensors and their respective directors, officers, agents and employees, from and against any actual or threatened claims, demands, causes of action or proceedings arising from any breach of this Agreement by you.

- IN NO EVENT SHALL WILEY OR ITS LICENSORS BE LIABLE TO YOU OR ANY OTHER PARTY OR ANY OTHER PERSON OR ENTITY FOR ANY SPECIAL, CONSEQUENTIAL, INCIDENTAL, INDIRECT, EXEMPLARY OR PUNITIVE DAMAGES, HOWEVER CAUSED, ARISING OUT OF OR IN CONNECTION WITH THE DOWNLOADING, PROVISIONING, VIEWING OR USE OF THE MATERIALS REGARDLESS OF THE FORM OF ACTION,

WHETHER FOR BREACH OF CONTRACT, BREACH OF WARRANTY, TORT, NEGLIGENCE, INFRINGEMENT OR OTHERWISE (INCLUDING, WITHOUT LIMITATION, DAMAGES BASED ON LOSS OF PROFITS, DATA, FILES, USE, BUSINESS OPPORTUNITY OR CLAIMS OF THIRD PARTIES), AND WHETHER OR NOT THE PARTY HAS BEEN ADVISED OF THE POSSIBILITY OF SUCH DAMAGES. THIS LIMITATION SHALL APPLY NOTWITHSTANDING ANY FAILURE OF ESSENTIAL PURPOSE OF ANY LIMITED REMEDY PROVIDED HEREIN.

- Should any provision of this Agreement be held by a court of competent jurisdiction to be illegal, invalid, or unenforceable, that provision shall be deemed amended to achieve as nearly as possible the same economic effect as the original provision, and the legality, validity and enforceability of the remaining provisions of this Agreement shall not be affected or impaired thereby.

- The failure of either party to enforce any term or condition of this Agreement shall not constitute a waiver of either party's right to enforce each and every term and condition of this Agreement. No breach under this agreement shall be deemed waived or excused by either party unless such waiver or consent is in writing signed by the party granting such waiver or consent. The waiver by or consent of a party to a breach of any provision of this Agreement shall not operate or be construed as a waiver of or consent to any other or subsequent breach by such other party.

- This Agreement may not be assigned (including by operation of law or otherwise) by you without WILEY's prior written consent.

- Any fee required for this permission shall be non-refundable after thirty (30) days from receipt by the CCC.

- These terms and conditions together with CCC's Billing and Payment terms and conditions (which are incorporated herein) form the entire agreement between you and WILEY concerning this licensing transaction and (in the absence of fraud) supersedes all prior agreements and representations of the parties, oral or written. This Agreement may not be amended except in writing signed by both parties. This Agreement shall be binding upon and inure to the benefit of the parties' successors, legal representatives, and authorized assigns.

- In the event of any conflict between your obligations established by these terms and conditions and those established by CCC's Billing and Payment terms and conditions, these terms and conditions shall prevail.

- WILEY expressly reserves all rights not specifically granted in the combination of (i) the license details provided by you and accepted in the course of this licensing transaction, (ii) these terms and conditions and (iii) CCC's Billing and Payment terms and conditions.

- This Agreement will be void if the Type of Use, Format, Circulation, or Requestor Type was misrepresented during the licensing process.

- This Agreement shall be governed by and construed in accordance with the laws of the State of New York, USA, without regards to such state's conflict of law rules. Any legal action, suit or proceeding arising out of or relating to these Terms and Conditions or the breach thereof shall be instituted in a court of competent jurisdiction in New York County in the State of New York in the United States of America and each party hereby consents and submits to the personal jurisdiction of such court, waives any objection to venue in such court and consents to service of process by registered or certified mail, return receipt requested, at the last known address of such party.

WILEY OPEN ACCESS TERMS AND CONDITIONS

Wiley Publishes Open Access Articles in fully Open Access Journals and in Subscription journals offering Online Open. Although most of the fully Open Access journals publish open access articles under the terms of the Creative Commons Attribution (CC BY) License only, the subscription journals and a few of the Open Access Journals offer a choice of Creative Commons Licenses. The license type is clearly identified on the article.

The Creative Commons Attribution License

The Creative Commons Attribution License (CC-BY) allows users to copy, distribute and transmit an article, adapt the article and make commercial use of the article. The CC-BY license permits commercial and non-

Creative Commons Attribution Non-Commercial License

The Creative Commons Attribution Non-Commercial (CC-BY-NC)License permits use, distribution and reproduction in any medium, provided the original work is properly cited and is not used for commercial purposes.(see below)

Creative Commons Attribution-Non-Commercial-NoDerivs License

The Creative Commons Attribution Non-Commercial-NoDerivs License (CC-BY-NC-ND) permits use, distribution and reproduction in any medium, provided the original work is properly cited, is not used for commercial purposes and no modifications or adaptations are made. (see below)

Use by commercial "for-profit" organizations

Use of Wiley Open Access articles for commercial, promotional, or marketing purposes requires further explicit permission from Wiley and will be subject to a fee.

Further details can be found on Wiley Online Library
http://olabout.wiley.com/WileyCDA/Section/id-410895.html

Other Terms and Conditions:

v1.10 Last updated September 2015

APPENDIX 2

PERMISSION FROM AIP PUBLISHING TO REUSE NEW INSIGHTS INTO ANHYDROBIOSIS USING CELLULAR DIELECTROPHORESIS-BASED CHARACTERIZATION

AIP PUBLISHING LICENSE
TERMS AND CONDITIONS
Oct 26, 2021

This Agreement between University of Louisville -- Clinton Belott ("You") and AIP Publishing ("AIP Publishing") consists of your license details and the terms and conditions provided by AIP Publishing and Copyright Clearance Center.

License Number	5174380754161
License date	Oct 22, 2021
Licensed Content Publisher	AIP Publishing
Licensed Content Publication	Biomicrofluidics
Licensed Content Title	New insights into anhydrobiosis using cellular dielectrophoresis-based characterization
Licensed Content Author	Mohamed Z. Rashed, Clinton J. Belott, Brett R. Janis, et al
Licensed Content Date	Nov 1, 2019
Licensed Content Volume	13
Licensed Content Issue	6
Type of Use	Thesis/Dissertation
Requestor type	Author (original article)
Format	Print and electronic
Portion	Excerpt (> 800 words)
Will you be translating?	No

Title	VISUALIZING ANHYDROBIOSIS: LIQUID-LIQUID PHASE SEPARATION, MEMBRANELESS ORGANELLES, AND CELLULAR REORGANIZATION
Institution name	University of Louisville
Expected presentation date	Dec 2021
Portions	All text, figures, and tables.
Requestor Location	University of Louisville 2555 Glenmary Ave., Apt. 4 LOUISVILLE, KY 40204 United States Attn: University of Louisville
Total	0.00 USD

Terms and Conditions

AIP Publishing -- Terms and Conditions: Permissions Uses

AIP Publishing hereby grants to you the non-exclusive right and license to use and/or distribute the Material according to the use specified in your order, on a one-time basis, for the specified term, with a maximum distribution equal to the number that you have ordered. Any links or other content accompanying the Material are not the subject of this license.

1. You agree to include the following copyright and permission notice with the reproduction of the Material:"Reprinted from [FULL CITATION], with the permission of AIP Publishing." For an article, the credit line and permission notice must be printed on the first page of the article or book chapter. For photographs, covers, or tables, the notice may appear with the Material, in a footnote, or in the reference list.
2. If you have licensed reuse of a figure, photograph, cover, or table, it is your responsibility to ensure that the material is original to AIP Publishing and does not

contain the copyright of another entity, and that the copyright notice of the figure, photograph, cover, or table does not indicate that it was reprinted by AIP Publishing, with permission, from another source. Under no circumstances does AIP Publishing purport or intend to grant permission to reuse material to which it does not hold appropriate rights.

You may not alter or modify the Material in any manner. You may translate the Material into another language only if you have licensed translation rights. You may not use the Material for promotional purposes.

3. The foregoing license shall not take effect unless and until AIP Publishing or its agent, Copyright Clearance Center, receives the Payment in accordance with Copyright Clearance Center Billing and Payment Terms and Conditions, which are incorporated herein by reference.
4. AIP Publishing or Copyright Clearance Center may, within two business days of granting this license, revoke the license for any reason whatsoever, with a full refund payable to you. Should you violate the terms of this license at any time, AIP Publishing, or Copyright Clearance Center may revoke the license with no refund to you. Notice of such revocation will be made using the contact information provided by you. Failure to receive such notice will not nullify the revocation.
5. AIP Publishing makes no representations or warranties with respect to the Material. You agree to indemnify and hold harmless AIP Publishing, and their officers, directors, employees or agents from and against any and all claims arising out of your use of the Material other than as specifically authorized herein.

6. The permission granted herein is personal to you and is not transferable or assignable without the prior written permission of AIP Publishing. This license may not be amended except in a writing signed by the party to be charged.
7. If purchase orders, acknowledgments or check endorsements are issued on any forms containing terms and conditions which are inconsistent with these provisions, such inconsistent terms and conditions shall be of no force and effect. This document, including the CCC Billing and Payment Terms and Conditions, shall be the entire agreement between the parties relating to the subject matter hereof.

This Agreement shall be governed by and construed in accordance with the laws of the State of New York. Both parties hereby submit to the jurisdiction of the courts of New York County for purposes of resolving any disputes that may arise hereunder.

V1.2

APPENDIX 3

PERMISSION FROM THE PROCEEDINGS OF THE NATIONAL ACADEMY OF SCIENCES TO REUSE 'LIQUID-LIQUID PHASE SEPARATION PROMOTES ANIMAL DESICCATION TOLERANCE

Rights and Permissions

The author(s) retains copyright to individual PNAS articles, and the National Academy of Sciences of the United States of America (NAS) holds copyright to the collective work and retains an exclusive License to Publish these articles, except for open access articles submitted beginning September 2017. For such open access articles, NAS retains a nonexclusive License to Publish, and these articles are distributed under either a CC BY-NC-ND or CC BY license.

For volumes 106–114 (2009–September 2017), the author(s) retains copyright to individual articles, and NAS retains an exclusive License to Publish these articles and holds copyright to the collective work. Volumes 90–105 (1993–2008) are copyright National Academy of Sciences. For volumes 1–89 (1915–1992), the author(s) retains copyright to individual articles, and NAS holds copyright to the collective work.

Authors whose work will be reused should be notified. Use of PNAS material must not imply any endorsement by PNAS or NAS. The full journal reference must be cited and,

for articles published in Volumes 90–105 (1993–2008), "Copyright (copyright year) National Academy of Sciences" must be included as a copyright note.

Please visit the Permissions FAQ for detailed information about PNAS copyright and self-archiving guidelines. The PNAS listing on the Sherpa RoMEO publisher policies pages can be found here.

Additional information and answers to frequently asked questions about author rights and permissions are available on our FAQ page.

PNAS authors need not obtain permission for the following cases:

1. to use their original figures or tables in their future works;
2. to make copies of their articles for their own personal use, including classroom use, or for the personal use of colleagues, provided those copies are not for sale and are not distributed in a systematic way;
3. to include their articles as part of their dissertations; or
4. to use all or part of their articles in printed compilations of their own works.

The full journal reference must be cited and, for articles published in volumes 90–105 (1993–2008), "Copyright (copyright year) National Academy of Sciences" must be included as a copyright note.

CURRICULUM VITAE

Clinton James Belott

Doctorate Candidate, Nation Science Foundation and JSPS Fellow Alumnus

University of Louisville, Department of Biology

139 Life Sciences Bldg., Louisville, KY, 40292

217-607-6322, cjbelo01@louisville.edu; cjbelott@gmail.com

Education:

Current	Ph.D. Candidate	University of Louisville, Louisville, KY, USA Program: Molecular and Cellular Biology
2016	Mast. Student	Eastern Illinois University, Charleston, IL, USA Program: Molecular and Cellular Biology Transferred into Doctoral Program Cumulative GPA: 4.00
2015	Bach. Sci.	Eastern Illinois University, Charleston, IL, USA Major: Biology, Minor: Chemistry Cumulative GPA: 3.94

2013	Assc. Sci.	Parkland College, Champaign, IL, USA Major: Biology
2010	HS Dipl.	Cissna Park High School, Cissna Park IL, USA

Professional Experience:

2020 – Current;	Teaching Assistant, Anatomy and Physiology Laboratory. Supervising Professor: Dr. Jennifer Mansfield-Jones. Department of Biological Sciences, University of Louisville, Louisville, KY, USA.
2019 – 2020	Japanese Society for the Propagation of Science (JSPS) Doctoral Fellow. Mentor: Dr. Michael A. Menze. Department of Biological Sciences, University of Louisville, Louisville KY, USA; Sponsor: Dr. Oleg Gusev, Unit Leader, KFU-RIKEN, Translation Genomics Unit, Yokohama, Kanagawa Prefecture, Japan.
2017 – 2020	National Science Foundation Doctoral Fellow. Mentor: Dr. Michael A. Menze. Department of Biological Sciences, University of Louisville, Louisville, KY, USA.

2016 – 2017 Teaching Assistant, Anatomy and Physiology Laboratory. Supervising Professor: Dr. Jennifer Mansfield-Jones. Department of Biological Sciences, University of Louisville, Louisville, KY, USA.

2015 – 2016 Assistant Researcher. Mentor: Dr. Michael A. Menze. Department of Biological Sciences, Eastern Illinois University, Charleston, IL, USA.

2013 – 2015 Undergraduate Researcher. Mentor: Dr. Michael A. Menze, Department of Biological Sciences, Eastern Illinois University, Charleston, IL, USA.

Research Experience:

- Extensive Laboratory Management Training
    - Ordering/Organization of Consumables, Micropipette Maintenance, Hazardous Chemical Usage Protocols, Hazardous Waste Management, Research Leadership, and Community Involvement
- Cell Culture (Insect and Mammalian)
- Cell Line Development (Insect)
- Desiccation Assays (Convection Oven and Salt Isotherms)

- Genetic Engineering (Primer Designing, Restriction Digests, PCR, Transformation, and Transfection)
- Advanced Genetic Engineering (Polycistronic mRNA Expression in Eukaryotes and Tag-less Protein Expression and Purification)
- Western Blotting and SDS-PAGE
- Oxygraph-2k, High-resolution Respirometry
- Advanced Confocal Microscopy
- Scanning Electron Microscopy
- Transcriptomics
- Cellular Dielectrophoresis
- Bioinformatics

Publications:

- **Belott, C**., T. Kikawada, O. Gusev, and M.A. Menze. (2021) Desiccation Tolerant Pv11 Cells Maintain Organelle Organization During Drying and Rehydration. *In Preperation.* Submission to *PNAS* in September 2021 is anticipated.
- **Belott, C**.*, B. Janis*, and M.A. Menze. (2020) Liquid-liquid Phase Separation Promotes Animal Desiccation Tolerance. *Proceeding of the National Academy of Sciences (PNAS)* **117**.
- Rashed, M.*, **C. Belott***, M.A. Menze, and S.J. Williams. (2019) New Insights into Anhydrobiosis using Cellular Dielectrophoresis-based Characterization. *Biomicrofluidics* **13**.

- Janis, B.*, **C. Belott**.*, and M.A. Menze. (2018) Role of Intrinsic Disorder in Animal Desiccation Tolerance. *Proteomics* **18**.

*Equally contributing authors.

Grants and Awards:

- University of Louisville, Louisville, KY, USA

  – Intramural Research Grants and Awards

    - Biology Graduate Student Publication Award. Awarded for publishing in the highest impact journal among biology department graduate students (2018). Amount awarded: $100

  – Extramural Research Grants and Awards:

    - **American Physiology Society Cell Section Research Recognition Award.** "Desiccation Tolerant Pv11 Cells Maintain Organelle Organization During Drying and Rehydration." Annual Experimental Biology (EB) Conference, Virtual Meeting (2021). Mentor: Dr. Michael Menze. Amount awarded: $570.
    - **NSF Graduate Research Opportunities Worldwide (GROW) / Japan Society for the Promotion of Science (JSPS) Postdoctoral Fellowship for Overseas Researchers (Strategic Program)**, "Characterization of Mitochondrial Morphology and Membrane Potential During Anhydrobiosis: A Comparison Between Desiccation Sensitivity and

Tolerance" (2019). Mentor: Dr. Michael Menze; Sponsor in Japan: Dr. Oleg Gusev, Unit Leader, KFU-RIKEN, Yokohama, Kanagawa Prefecture, Japan. Amount awarded: $40,200 total. Term: 6.5 months.

- **National Science Foundation Graduate Research Fellowship (GRFP)**, "Importance of Protein-based Desiccation Tolerance in the Anhydrobiotic Brine Shrimp, *Artemia franciscana*, and the Potential to Achieve Dry-state Storage of Insect Cells" (2017). Mentor: Dr. Michael Menze. Amount awarded: $138,000 total. Term: 3 years.

- Eastern Illinois University, Charleston, IL, USA

  – Intramural Research Grants and Awards

  - Betty Wright Downing Award. Awarded for excellence in graduate research and academic achievement (2016). Amount awarded: $500
  - Scholars in Undergraduate Research at Eastern (SURE) Award. "Dichloroacetate Toxicity to Hepatocellular Carcinoma Cells is Ameliorated in Galactose Based Medium" (2015). Mentor: Dr. Michael Menze. Amount awarded: $500.
  - Student Advisory Board Student Assistance Award. Awarded for high academic achievements despite low income (2015). Amount awarded: $500.
  - Errett and Maizie Warner Award in Zoology (2015). Amount awarded: $1,800.
  - G. B. Dudley Memorial Scholarship. (2014). Amount awarded: $1,200.

- Undergraduate Research, Scholarship, and Creative Activities (URSCA) Award. “Synergistic Cancer Treatment” (2014). Mentor: Dr. Michael Menze. Amount awarded: $500.

– Extramural Research Grants and Awards

- National Science Foundation Graduate Research Fellowship (GRFP). “Improving Desiccation Tolerance in *Drosophila melanogaster* Cells by Applying Common Biochemical Strategies Found in Anhydrobiotic Animals” (2016). Honorable Mention. Mentor: Dr. Michael Menze.

Presentations:

- Oral Presentations
  - Centner, C., M. Vinseiro-Figueira, Z. Long, J.T. Moore, M. E. Baxter, **C. J. Belott**, M. A. Menze, K. Yaddanapudi, P. J. Bates, J. A. Kopechek. “Modulation of Acoustofluidic Parameters to Assess Effect on Molecular Loading in Human T cells”. Acoustical Society of America (ASA). Seattle, WA, USA. 2021.
  - **Belott, C**. “Membraneless Organelles in Desiccation Tolerance: A New Phase in Anhydrobiosis”. Invited speaker. University of Louisville, Louisville, KY, USA (Presented 9-10-2021)
  - **Belott, C**.*, M. Rashed*, S.J. Williams and M.A. Menze “New Insights into Anhydrobiosis using Cellular Dielectrophoresis-based Characterization”. Invited speaker. National Agriculture and Food

Research Organization (NARO) HQ, Tsukuba, Ibaraki Prefecture, Japan (Presented 10-1-2019)

- **Belott, C.** and M.A. Menze. "Membraneless Organelles in Desiccation Tolerance: A New Phase in Physiology". Annual Society for Integrative & Comparative Biology (SICB) Conference. Tampa, FL. 2019. (Presented 1-4-2019)

- Poster Presentations
  - Centner, C., **C. J. Belott**, M. A. Menze, K. Yaddanapudi, P. J. Bates, J. A. Kopechek. Biomodulatory Effect of Acustofluidic-induced Molecular Delivery to Human T-cells. Research!Louisville Conference. University of Louisville, Louisville, KY, USA. 2021.
  - **Belott, C**., T. Kikawada, O. Gusev, and M.A. Menze. "Desiccation Tolerant Pv11 Cells Maintain Organelle Organization During Drying and Rehydration". Annual Experimental Biology (EB) Conference. Virtual Meeting. 2021. Abstract published in *The Federation of American Societies for Experimental Biology (FASEB) Journal* **35**. **American Physiology Society Cell Section Research Recognition Award.**
  - **Belott, C**.,* B. Janis*, T. Sithu, and M.A. Menze. "Membraneless Organelles and Viscosity Changes during Desiccation: A New Phase in Anhydrobiosis". Annual Experimental Biology (EB) Conference, San Diego, CA, USA. 2020. Abstract published in *The Federation of American Societies for Experimental Biology (FASEB) Journal* **34**.

- **Belott, C.**, R. Skolik, and M.A. Menze. "LEA proteins protect *Drosophila melanogaster* cells during prolonged periods of desiccation and osmotic stress". Annual Society for Integrative & Comparative Biology (SICB) Conference. New Orleans, LA, USA. 2017. (Abstract number: 481-61255)
- **Belott, C.**, D. Webster, and M.A. Menze. "Dichloroacetate Toxicity to Hepatocellular Carcinoma Cells is Ameliorated in Galactose Based Medium". Annual National Council on Undergraduate Research, Spokane, WA, USA. 2015.

*Equally contributing authors.

Service and Outreach:

- Eastern Illinois University, Charleston, IL, USA

  - Graduate Student Advisory Council Representative, Biological Sciences (2015-2016).
  - Graduate Student Advisory Council Vice President of Programming, Biological Science, Eastern Illinois University (2016). As V.P of Programming, **created a campus-wide graduate research symposium** for all fields of research to prepare graduate students to present their research and to attract potential undergraduate and graduate students from local high schools, community colleges, and universities, Eastern Illinois University (2016).

- **Created an outreach opportunity for students in rural communities** (Cissna Park High School, Cissna Park IL, United States) to experience hands-on and inquiry-based science experiments otherwise unavailable to them and to work with science teachers to design affordable experiments for their future classes (2015 - 2016).

- University of Louisville, Louisville, KY, USA
  - Confocal Training Specialist for Biological Sciences – Nikon A1R Confocal Microscope
  - **Student testimonials on mentorship:**
    - **2018: Olivia Hawkins** – High school student
      - **"I learned more in my time in the lab [this summer] than I had in my years of high school, and it motivated me to further pursue a career in the sciences."** Quoted with Permission.
    - **2017-Current: Tryphena Sithu** – Graduated from high school in 2018 and is currently under my mentorship as an undergraduate student at the University of Louisville, KY, USA.
      - "Over the course of my research experience, I've become very appreciative of the way Clinton challenges me to think critically - about WHY I perform each step in each procedure and HOW it applies to the bigger picture. From the beginning, he taught me each lab technique with such precision, and he

pushes me outside of my comfort zone by encouraging me to perform experiments on my own, even when I feel incapable. When I mess up, his gentle correction points out my mistakes and helps me avoid repeating them. **He is a teacher I look up to but also a friend I can trust.**" Quoted with Permission.

- **2019-Current: David Grimm** – Graduate student
  - "Clinton's mentorship has no doubt had a life-long impact on me. Two things that standout to me are his patience and attention to detail. Clinton continually made time for me and offered his input whether it was about biological systems, experimental design, or navigating the challenges of graduate school. His meticulous nature inspired personal growth that has transformed my approach to problem solving. **Clinton is an outstanding mentor, and I am grateful to have received his guidance during my first 2 years as a PhD student.**" Quoted with Permission.

Professional Development:

- Completed Principles of Fluorescence Techniques course. Fluorescence Foundation and ISS. Urbana-Champaign, IL, USA (2015)

References:

Dr. Michael A. Menze, Associate Professor

University of Louisville

Dept. of Biology

Louisville KY, 40292 USA

Phone: 502-852-8816

Cell Phone: 225-281-7503

Email: michael.menze@louisville.edu

Dr. Steven C. Hand, Professor

Louisiana State University

Dept. of Biology

Baton Rouge, LA, 70803 USA

Phone: 225-578-5144

Cell Phone: 225-938-5184

Email: shand@lsu.edu

Dr. Jennifer Mansfield-Jones, Associate Professor

University of Louisville

Dept. of Biology

Louisville KY, 40292 USA

Phone: 502-489-2246

Email: jennifer.mansfieldjones@louisville.edu